Investigation of the functional architecture of the human thermoregulatory system through biochemical indices

by

Angelica Valente

Submitted in partial fulfilment of the requirements
for the degree of Doctor of Philosophy

at

University of Thessaly
Volos, Greece
October 2015

UNIVERSITY OF THESSALY

DATE: 22 October 2015

AUTHOR: Angelica Valente

TITLE: Investigation of the functional architecture of the human thermoregulatory system through biochemical indices

DEPARTMENT OR SCHOOL: School of Physical Education and Sport Science

DEGREE: Doctor of Philosophy CONVOCATION: October YEAR: 2015

Permission is herewith granted to University of Thessaly to circulate and to have copied for non-commercial purposes, at its discretion, the above title upon the request of individuals or institutions.

_____

Signature of Author

UNIVERSITY OF THESSALY

SCHOOL OF PHYSICAL EDUCATION AND SPORT SCIENCE

The undersigned hereby certify that they have read and recommend to the Programme of Postgraduate Studies for acceptance a thesis entitled “Investigation of the functional architecture of the human thermoregulatory system through biochemical indices” by Angelica Valente in partial fulfillment of the requirements for the degree of Doctor of Philosophy.

Dated: _____

Supervisor: _____

Committee: _____

_____

_____

_____

_____

_____

Academic Advisor: _____

ACKNOWLEDGMENTS

First, I would like to thank Dr. Andreas Flouris for his guidance in this research project, his friendship and infinite patience in teaching me life and science as well. My special gratitude goes to Prof. Thanasis Jamurtas, Prof. Yiannis Koutedakis, Dr. Giorgos Sakkas, and Prof. Christina Karatzaferi for their supervision and precious advises during the all research period and my stay in Greece. It was my great pleasure to work with all the FAMElab members in Dr. Andreas Flouris' laboratory, especially with Dr. Andres Carrillo, Petros Dinas and Gina Dinas, who have provided me plenty of personal support and working assistance during my stay in Greece. I would like also thank all faculty and staff in Department of Exercise Sciences of the University of Thessaly.

My sincere gratitude goes to all my friends in Italy, Greece, Belgium and United States. My special gratitude goes to my parents Nicola and Maria, my sister Rossella, and my husband Bogdan: without their support I could not have become who I am today. Finally, infinite thanks to life itself for preparing me a big surprise: Adrian & Giulia, born March 2015.

Table of Contents

ABSTRACT

Uncoupling protein-1, a mitochondrial inner membrane protein, is the main player in non-shivering thermogenesis and is expressed in brown and brown-like adipocytes. Uncoupling protein 1-mediated thermogenesis leads to excess energy expenditure as the fat energy storage is used for body heat production and thus, is one of the most rapidly advancing areas in obesity research. The present PhD project aims to identify factors to treat human adipose excess through uncoupling protein-1 activation. Our systematic analysis identified L-menthol as one of the molecules that can activate rodent UCP1 in brown and brown-like adipocytes through transient receptor potential melastatin 8 ion channel (TRPM8) stimulation, leading to increase rodent metabolism and decrease adiposity. In humans, a single L-menthol skin administration increased thermogenesis and metabolic rate but these showed a minor increase following oral L-menthol administration. However, 1-month of daily L-menthol cream application did not increase human metabolism or white adipose tissue plasticity and did not affect body composition. Future analysis on the activity of proteins involved in metabolism and white adipose tissue plasticity following daily L-menthol administration and also on human TRPM8 cold-sensitive gating are essential to clarify the observed results and thus, to confirm L-menthol as promising candidate treatment for human cardio-metabolic diseases.

List of Tables

List of Figures

control and L-menthol treatments within the same group for the same time-point (Wilcoxon Signed-Rank tests, p<0.05); Ṣ = significant differences between SKIN vs. ORAL group for the same treatment and time-point (Mann-Whitney U tests, p<0.05).

Figure 3. Results (mean ± SEM) and comparisons for heat storage (S), metabolic rate (M) and respiratory exchange ratio (RER) at baseline (Base) and for 7 hours after oral and skin treatments. Note: * = significant differences from baseline within the same treatment (Wilcoxon Signed-Rank tests; p<0.05); ǂ = significant differences from the previous time-point within the same treatment (Wilcoxon Signed-Rank tests; p<0.05); † = significant differences between control and L-menthol treatments within the same group for the same time-point (Wilcoxon Signed-Rank tests; p<0.05); Ṣ = significant differences between SKIN vs. ORAL group for the same treatment and time-point (Mann-Whitney U tests; p<0.05).

Figure 4. Results (mean ± SEM) and comparisons for thermal comfort and sensation at baseline (Base) and for 7 hours after oral and skin treatments. Note: * = significant differences from baseline within the same treatment (Wilcoxon Signed-Rank tests; p<0.05); ǂ = significant differences from the previous time-point within the same treatment (Wilcoxon Signed-Rank tests; p<0.05); † = significant differences between control and L-menthol treatments within the same group for the same time-point (Wilcoxon Signed-Rank tests; p<0.05); Ṣ = significant differences between SKIN vs. ORAL group for the same treatment and time-point (Mann-Whitney U tests; p<0.05).

Chapter 4 - Daily L-menthol skin administration effects on metabolism, body composition and white adipose tissue plasticity

Figure 1. Results (mean ± SD) of Steps number (A), Kilocalories (B), Total fat (C), Protein (D), Carbohydrate (E), Maltose (F), Galactose (G), Sodium (H), Vitamin D (I), and Vitamin E (L), at baseline and the following week 1, 2, 3, and 4 of the cream application period in CON (0 mg·kg-1 body weight of L-menthol crystals), LM (10 mg·kg-1 body weight of L-menthol crystals), and HM (20 mg·kg-1 body weight of L-menthol crystals) groups. Note: * = significant differences from baseline within the same group; ǂ = significant differences from the previous week within the same group; $ = significant differences versus CON for the same week; # = significant differences HM vs LM for the same week; —— = average of cream application period (from week 1 to week 4).

Figure 2. Results (mean ± SD) of dermis relative mRNA expression of TRPM8-L (full-length functional isoform) and TRPM8-S (short non-functional TRPM8α and TRPM8β isoforms) at baseline and the day after the last cream application (day 30) in LM (10 mg·kg-1 body weight of L-menthol crystals) and HM (20 mg·kg-1 body weight of L-menthol crystals) groups. Note: # = significant differences for TRPM8-S versus TRPM8-L within the same group for the same time-point.

Figure 3. Results (mean ± SD) of white adipose tissue relative mRNA expression of UCP1, RALD, PLAC8, NPRA, PGC1α, COX IV, PPARγ, Leptin, Adiponectin, PPARα, PGK1, FABP3, Glut4, TRPM8-L, and TRPM8-S, at baseline and the day after the last

cream application (day 30) in CON (0 mg·kg-1 body weight of L-menthol crystals), LM (10 mg·kg-1 body weight of L-menthol crystals) and HM (20 mg·kg-1 body weight of L-menthol crystals) groups. Note: * = significant differences from baseline within the same group.

Figure 4. Results (mean ± SD) of thermal comfort and sensation of arms, legs, and chest-belly at week 1, 2, 3, and 4 of the cream application period in CON (0 mg·kg-1 body weight of L-menthol crystals), LM (10 mg·kg-1 body weight of L-menthol crystals), and HM (20 mg·kg-1 body weight of L-menthol crystals) groups. Note: $ = significant differences versus CON for the same week.

Acronyms

NST = non-shivering thermogenesis

UCP1 = uncoupling protein 1

BAT = brown adipose tissue

WAT = white adipose tissue

EE = energy expenditure

M = metabolic rate

BMR = basal metabolic rate

RER = respiratory exchange ratio

HRV = heart rate variability

S = heat storage

T_{sk} = skin temperature

T_{re} = rectal temperature

SkBF = skin blood flow

RMR = resting metabolic rate

BMI = body mass index

BW = body weight

TRPM8 = transient receptor potential cation channel subfamily M member 8

CHAPTER 1

GENERAL INTRODUCTION

Obesity and its related disorders represent a major global health concern. Recent studies reported that during the last thirty-five years worldwide mean body mass index has been increasing by 0.45 kg/m² per decade, while rates of overweightness and obesity are projected to increase in almost all countries (World Health Organization 2010; World Health Organization 2010; Finucane et al. 2011). The countermeasure often proposed against overweightness and obesity is a reduction of energy intake and/or an increase in physical activity (Flouris et al. 2008; Bischoff et al. 2012; Carrillo et al. 2013; Golubovic et al. 2013). However, increasing basal metabolic rate (BMR) through frequent stimulation of non-shivering thermogenesis (NST) is also a viable alternative that can be beneficial (Feldmann et al. 2009; Shabalina et al. 2010; Carrillo and Flouris 2011). This is because up to 20% of average daily metabolic rate may consist of cold-induced NST (van Marken Lichtenbelt and Schrauwen 2011).

NST which is a heat production process not associated with the muscle shivering, takes place in mammal brown adipose tissue (BAT) and human skeletal muscle (Wijers et al. 2008; Mattson 2010; Mitchell et al. 2010; van Marken Lichtenbelt and Schrauwen 2011). Uncoupling protein 1 (UCP1), a mitochondrial inner membrane protein, is the main player in NST process and is expressed in mammal brown and brown-like (beige or brite) adipocytes (Mattson 2010; Petrovic et al. 2010; Walden et al. 2012). Frequent stimulation of UCP1 results in an increase of basal metabolic rate and a reduction of adiposity levels in rodents as the fat energy storage is used for body heat production (Inokuma et al. 2006; Yamashita et al. 2008; Feldmann et al. 2009; Yoneshiro et al. 2013; Valente et al. 2014). Briefly, the expression of UCP1 in brown and brown-like adipocytes provides an alternative biochemical pathway compared to the rest of eukaryotic cells which results in the production of heat instead of ATP. Normally, the protons that are pumped across the

mitochondrial inner membrane due to the oxidation of NADH and FADH2 by the electron transport chain generate an electrochemical gradient which is dissipated as they enter the mitochondrial matrix through ATP synthase resulting in ATP production. However, the activation of UCP1 in brown and brown-like adipocytes allows protons to bypass the ATP synthase entry and return to the mitochondrial matrix. Through this process, the energy of the electrochemical gradient is dissipated as heat (Rousset et al. 2004; Ducharme and Bickel 2008; Mattson 2010). Thus, adipose tissue biology pertaining to UCP1-mediated thermogenesis is one of the most rapidly advancing areas in obesity research, with an ever-increasing number of molecular, physiological, pharmacological and dietary factors implicated in increasing metabolism and decreasing adiposity being therefore potential targets for obesity management.

Given the above, the present PhD project aims to identify factors that increase human metabolism and treat adipose excess through UCP1 activation. The following three studies are included: 1) a systematic review to analyse all published evidence from 2006 to 2013 regarding the molecular pathways linking NST and obesity in mammals, focusing on mechanisms involved in BAT development; 2) absorption and metabolism of a single L-menthol oral versus skin administration and the effects on human thermogenesis and metabolic rate; 3) effect of daily L-menthol skin administration on metabolism, body composition and white adipose tissue plasticity.

THESIS OBJECTIVES

The thesis objectives are:

1) Evaluate the available recent evidence on the molecular pathways linking NST and obesity in mammals, focusing on the mechanisms involved in BAT development.
2) Assess the effects of one of the identified factors on increase human metabolism and treat adipose excess through UCP1 activation.

HYPOTHESES

The research hypotheses are:

1) Both L-menthol oral and skin L-menthol administration would increase thermogenesis and metabolic rate in humans.
2) L-menthol skin administration would be more potent in increasing thermogenesis and metabolic rate in humans.
3) 1-month daily L-menthol cream administration (lower and higher L-menthol concentration cream) would increase human metabolism, decrease body weight and adiposity.
4) 1-month daily L-menthol cream administration (lower and higher L-menthol concentration cream) would stimulate subcutaneous adipose tissue plasticity with UCP1 expression increased in subcutaneous white adipocytes.
5) The daily administration of the higher L-menthol cream concentration would be more potent in increasing human metabolism, decreasing body weight and adiposity as well as stimulating subcutaneous adipose tissue plasticity.

The research null hypotheses are:

1) Oral or skin L-menthol administration would not increase thermogenesis and metabolic rate in humans.

2) Skin administration would have a similar effect as oral administration on thermogenesis and metabolic rate in humans.
3) 1-month daily L-menthol cream administration (lower or higher L-menthol concentration cream) would not increase human metabolism, decrease body weight and adiposity.
4) 1-month daily L-menthol cream administration would not stimulate subcutaneous adipose tissue plasticity with UCP1 expression increased in subcutaneous white adipocytes.
5) The daily administration of the higher L-menthol cream concentration would have a similar effect on human metabolism, body weight and subcutaneous adipose tissue plasticity.

CHAPTER 2

Published as:

Valente A, Jamurtas AZ, Koutedakis Y, Flouris AD. Molecular pathways linking non-shivering thermogenesis and obesity: focusing on brown adipose tissue development. Biol Rev Camb Philos Soc. 2015 Feb;90(1):77-88.

Literature Review - Molecular pathways linking non-shivering thermogenesis and obesity: focusing on brown adipose tissue development

Angelica Valente[1,2], Athanasios Z. Jamurtas[2], Yiannis Koutedakis[2,3] and Andreas D. Flouris[1,*]

[1]FAME Laboratory, Centre for Research and Technology Hellas, Karies, Trikala 42100, Greece

[2]Department of Exercise Sciences, University of Thessaly, Trikala 42100, Greece

[3]School of Sport, Performing Arts and Leisure, University of Wolverhampton, Walsall, WS13BD, UK

[*]Author for correspondence (Tel.: +30 2431 500 601; Fax: +30 2431 063 191; E-mail: aflouris@ireteth.cereteth.gr).

ABSTRACT

An increase in energy intake and/or a decrease in energy expenditure lead to fat storage, causing overweight and obesity phenotypes. The objective of this review was to analyse, for the first time using a systematic approach, all published evidence from the past eight years regarding the molecular pathways linking non-shivering thermogenesis and obesity in mammals, focusing on mechanisms involved in brown adipose tissue development. Two major databases were scanned from 2006 to 2013 using “brown adipose tissue” AND “uncoupling protein-1” AND “mammalian thermoregulation” AND “obesity” as key words. A total of 61 articles were retrieved using the search criteria. The available research used knockout methodologies, various substances, molecules and agonist treatments, or different temperature and diet conditions, to assess the molecular pathways linking non-shivering thermogenesis and obesity. By integrating the results of the evaluated animal and human studies, our analysis identified specific molecules that enhance non-shivering thermogenesis and metabolism by: (*i*) stimulating “brite” (brown-like) cell development in white adipose tissue; (*ii*) increasing uncoupling protein-1 expression in brite adipocytes; and (*iii*) augmenting brown and/or brite adipose tissue mass. The latter can be also increased through low temperature, hibernation and/or molecules involved in brown adipocyte differentiation. Cold stimuli and/or certain molecules activate uncoupling protein-1 in the existing brown adipocytes, thus increasing total energy expenditure by a magnitude proportional to the number of available brown adipocytes. Future research should address the interplay between body mass, brown adipose tissue mass, as well as the main molecules involved in brite cell development.

Key words: brite cells, metabolism, energy expenditure, white adipose tissue, retinaldehyde dehydrogenase 1, tri-iodothyronine, uncoupling protein-1.

INTRODUCTION

Since 1980, worldwide mean body mass index has been increasing by 0.45 kg/m^2 per decade (Finucane et al. 2011). By the end of 2010, around 43 million children under the age of five were overweight, while rates of overweightness and obesity are projected to increase in almost all countries, leading to 1.5 billion overweight individuals by 2015 (World Health Organization 2010). The countermeasure often proposed against overweightness and obesity is a reduction of energy intake (Golubovic et al. 2013) and/or an increase in physical activity (Flouris et al. 2008; Bischoff et al. 2012; Carrillo et al. 2013). However, increasing basal metabolic rate (BMR) through frequent stimulation of non-shivering thermogenesis (NST) – *via* changes in the thyroid hormones – is also a viable alternative that can be beneficial (Koutedakis et al. 2005; Feldmann et al. 2009; Shabalina et al. 2010; Carrillo and Flouris 2011). This is because human data summarized in a recent review showed that up to 20% of average daily metabolic rate may consist of cold-induced NST (van Marken Lichtenbelt and Schrauwen 2011). In rodents, NST takes place exclusively in brown adipose tissue (BAT) by uncoupling protein-1 (UCP1) (Mattson 2010), a mitochondrial inner membrane protein, while in humans NST can also occur in skeletal muscle (Wijers et al. 2008; Mitchell et al. 2010; van Marken Lichtenbelt and Schrauwen 2011). The prevailing hypothesis to date is that the function of BAT in mammals is to maintain body temperature during exposure to cold which, as a consequence, leads to excess energy expenditure (EE) (Kozak 2010). Indeed, frequent stimulation of NST irrevocably increases BMR, resulting in decreased body mass and stored fat (Feldmann et al. 2009; Shabalina et al. 2010).

Adipose tissue biology pertaining to UCP1-mediated thermogenesis is one of the most rapidly advancing areas in obesity research, with an ever-increasing number of molecular, physiological, pharmacological and dietary factors being implicated in the transdifferentiation of white adipocytes to “brite” (i.e. brown-like)

adipocytes and potential targets for obesity management. In rodents, brite cells in white adipose tissue express UCP1 and may play an important role in NST and metabolism when UCP1 is activated through pathways similar to those of brown adipocytes. Nevertheless, brite cells possess a different gene expression pattern (e.g. transcription factors) than classic brown adipocytes (Petrovic et al. 2010; Walden et al. 2012).

BMR is reduced with ageing in humans (Carrillo and Flouris 2011), while an ageing effect on NST has been also observed in rodents (Feldmann et al. 2009; Shabalina et al. 2010), leading to overweightness or obesity. Moreover, a recent human study reported that obese individuals demonstrate low BAT activity and EE in response to cold compared with lean controls, suggesting that BAT is either reduced or absent in obese individuals (Vijgen et al. 2011). Therefore, it is crucial to intensify research efforts aimed at the prevention of BAT loss and/or BAT regeneration to treat human adipose excess.

The importance of systematic analyses is based on reducing the likelihood of bias on the effects of certain phenomena across a wide range of settings and empirical methods (Wieseler and McGauran 2010). However, recent research findings concerning BAT biology and its role in obesity have not yet been reviewed using a systematic methodology. Thus, the purpose of this review is to summarise critically– for the first time using a systematic approach – all the recent evidence on the molecular pathways linking NST and obesity in mammals, focusing on the mechanisms involved in BAT development.

METHODS

This systematic review was performed according to published guidelines (Wieseler and McGauran 2010). The databases PubMed and Scopus were searched for

articles published from the beginning of 2006 to the end of October 2013, using the key words “brown adipose tissue” AND “uncoupling protein-1” AND “mammalian thermoregulation” AND “obesity”. We used 2006 as a start year for this systematic search because, in that year, UCP1 was established as the only mediator of NST in mammalian BAT (Barger et al. 2006). The limitation “research articles” was applied to the search parameters in order to exclude reviews and conference proceedings. Only English-language literature was considered eligible. Titles and abstracts were screened independently by two reviewers (A.V. and A.D.F.) to identify relevant articles.

Due to the methodology outlined above, our searching and selection procedure eliminated bias since the inclusion (or not) of a study was based on content (i.e. investigating molecular pathways linking NST and obesity with a focus on the mechanisms involved in mammalian BAT development), and not on quality, journal, or other factors. A total of 56 articles were retrieved during the search and all were identified as relevant (Fig. 1).

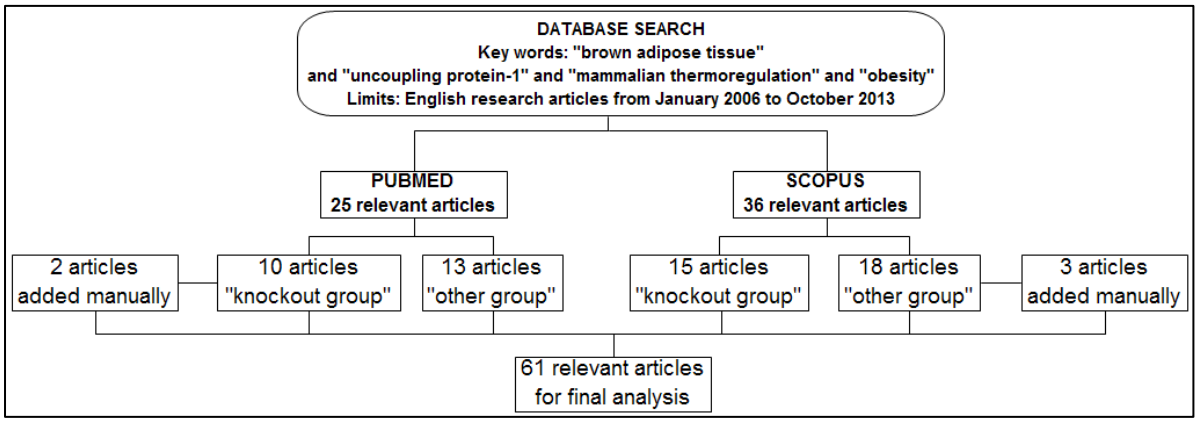

Figure 1. *Systematic selection process used to identify relevant studies within the adopted criteria.*

Five additional articles were included manually. These five articles met all the set criteria but were excluded erroneously from the 56 articles when the search limits were applied. Therefore, 61 articles meeting all the established criteria were considered for subsequent analysis. To enable a systematic synthesis of the

presented evidence, the articles were separated into two categories based on research methodology: “knockout studies” in which gene-function analysis was performed using knockout animals lacking the gene under study (Table 1), and “other studies” in which the analysis was carried out using various substances, molecules/agonist treatments, as well as different temperature and diet conditions (Table 2).

Table 1. The "Knockout studies" articles identified by our search criteria and their main results.

Group	Article	Main results
UCP1-KO	Yamashita *et al.* (2008)	FABP3 affects free fatty acid flux and ↑UCP1 thermogenesis.
	Feldmann *et al.* (2009)	UCP1 activity affects obesity development in mice and humans.
	Inokuma *et al.* (2006)	Anti-obesity effect of β3-adrenergic stimulation is largely attributable to UCP1 in BAT.
	Oelkrug *et al.* (2011)	Functional BAT is essential for rapid arousal from torpor.
	Shabalina *et al.* (2010)	↑shivering muscle and ↓heat loss induces cold adaptations in UCP1-KO mice.
	Anunciado-Koza *et al.* (2011)	SLC25A25 induces alternative thermogenesis.
	Meyer *et al.* (2010)	↓heat loss by ↑vasoconstriction and ↓thermal conductance in UCP1-KO mice.
	Adjeitey *et al.* (2013)	UCP1 expression in muscles ↑ EE, ↓ body mass, and ↓ reactive oxygen species production.
Brain	Streijger *et al.* (2009)	Inefficient neuronal transmission induces dysfunction in NST.
	Chao *et al.* (2011)	Deficiency of NPY induces ↑both WAT lipogenesis and BAT thermogenesis.
	De Jonghe *et al.* (2011)	Deficiency of PTP1B in POMC induces ↑ cold-induced thermogenesis through thyroid axis.
Receptors, enzymes, and transcription factors	Korach-Andréa *et al.* (2011)	Deficiency of LXRα and LXRβ induces ↑ EE, ↑ UCP1 expression and ↓ body mass loss.
	Vila-Bedmar *et al*. (2012)	GRK2 hemizygous (+/-) induces ↑ NST, ↑ EE and ↓ body mass.
	Pelletier *et al*. (2008)	Chronic muscle shivering in mice with dysfunctional NST.
	Hudson-Davies *et al.* (2009)	Deficiency of RIP140 ↓ metabolism and ↓ thermoregulatory adaptations.
	Gray *et al.* (2006)	PPAR-γ is required for full activation and recruitment of brown adipocytes.
	Giralt *et al.* (2011)	Sirt3 is essential for the differentiation of fully thermogenic-competent brown adipocytes.
	Bordicchia *et al.* (2012)	Cardiac NPs induce ↑ BAT thermogenesis, ↑ PGC-1α and ↑ UCP1 and ↓ WAT mass *via* p38 MAPK.
	Tseng *et al.* (2008)	BMP-7 induces brown adipocyte differentiation and NST.
	Jimenez-Preitner *et al.* (2011)	Plac8 is required for BAT differentiation and thermogenic capacity.
	Czyzyk *et al.* (2012)	δ-opioid receptor deficiency induces ↑ UCP1 and ↓ adiposity.
	Satyanarayana *et al.* (2012)	Id1 deficiency induces ↑ UCP1, ↑ EE, and ↑ fatty acid oxidation.
	Lin *et al*. (2011)	GHS-R ablation induces ↑ insulin sensitivity, ↑ EE, ↑ resting metabolic rate and ↑ UCP1 during ageing.
	Ma *et al*. (2011)	GHS-R regulates BAT NST, adiposity, metabolism and energy homeostasis during ageing.
	Mano-Otagiri *et al*. (2010)	GHS-R/ghrelin induces ↓ EE and ↑ EI by suppressing the SNS innervating BAT.
	Kiefer *et al.* (2012)	Rald induces ↑ transcription of brown fat markers in WAT.
	Bauwens *et al*. (2011)	α1-AMPK does not play a key role in NST and body mass.

↑= increase; ↓= decrease; α1-AMPK = α1-AMP-activated protein kinase; BAT = brown adipose tissue; BMP-7 = bone morphogenetic protein 7; EE = energy expenditure; EI = energy intake; FABP3 = fatty acid-binding protein 3; GHS-R = growth hormone secretagogue receptor; GRK2 = G-protein-coupled receptor kinase 2; Id1 = inhibitor of DNA binding 1; KO = knockout; LXR = liver-X receptor; NPs = natriuretic peptides; NPY = hypothalamic neuropeptide Y; NST = non-shivering thermogenesis; p38 MAPK = p38 mitogen-activated protein kinase; PGC-1α = peroxisome proliferator-activated receptor gamma co-activator 1-α; Plac8 = placenta-specific 8; POMC = proopiomelanocortin; PPAR-γ = peroxisome proliferator-activated receptor γ; PTP1B = protein tyrosine phosphatase 1B; Rald = retinaldehyde dehydrogenase 1; RIP140 = receptor interacting protein 140; Sirt3 = silent mating type information regulation 2, homolog 3; SLC25A25 = solute carrier family 25 (mitochondrial carrier; phosphate carrier), member 25; SNS = sympathetic nervous system; UCP1 = uncoupling protein-1; WAT = white adipose tissue.

Table 2. The "other studies" identified by our search criteria and their main results.

Group	Article	Main results
Molecule treatment	Lehr *et al.* (2009)	T3 in brown adipocyte medium induces differentiation of WAT stroma vascular cells in brown adipocytes-like cells.
	Bartolomucci *et al.* (2006)	TLQP-21 ↑EE and blocks the early phase of high-fat-diet-induced obesity.
	Kim *et al.* (2006)	PE extract ↑BAT thermogenesis and WAT fatty acid oxidation.
	Matsen *et al.* (2013)	Thyroid hormone β-selective agonist GC-1 induces ↑ UCP1, ↑EE, and ↓ adiposity.
	Ma *et al.* (2012)	L-menthol induces ↑ *T*c, ↑ UCP1, and ↓ body mass.
	Romero del Mar *et al.* (2009)	OE maintains thermogenic potential.
	Wargent *et al.* (2013)	ZAG induces no effect on UCP1 expression and NST activity.
	Moriya *et al.* (2006)	QRFP43 ↑feeding, ↓EE, and induces obesity.
Sex and polymorphisms	Rodriguez-Cuenca *et al.* (2007*a*)	Variation of sex steroid receptor expression in BAT of male, female, pregnant and lactating females.
	Rodriguez-Cuenca *et al.* (2007*b*)	Sex hormones affect mitochondrial transcription factors and mitochondriogenesis.
	Shore *et al.* (2012)	CpG methylation in the UCP1 promoter has no role in UCP1 expression.
	Rose *et al.* (2011)	UCP1 transcription is ↑ by progesterone and retinoic acid but ↓ by 17-β estradiol.
	Nikolic *et al.* (2011)	Sex-difference effect of PKG-I activation on BAT thermogenesis and WAT lipolysis.
Temperature	Wells *et al.* (2012)	Opa3 gene mutation indices ↓ NST and ↑ lipid storage in BAT.
	Oelkrug *et al.* (2013)	Original function of BAT in defending mammal high body temperature for migration to cold.
	Cypess *et al.* (2013)	Higher UCP1 expression in longus colli and carotid sheath than superficial BAT depots.
	van der Lans *et al.* (2013)	Cold acclimation induces ↑ BAT activity and ↑ NST but no effect on brite development.
	Yoneshiro *et al.* (2013)	Cold exposure induces ↑EE, ↑ BAT activity, and ↓ body fat mass.
	Li *et al.* (2013)	Cold exposure induces ↑ Bmal1 which is involved in lipid catabolism.
	Chappuis *et al.* (2013)	Cold exposure induces ↑ Per2 which is a co-activator of UCP1 transcription factors.
	Barger *et al.* (2006)	UCP1 is the only mediator of NST in BAT.
	Liu *et al.* (2009)	Low temperature ↑NST, ↑RMR and ↑total respiratory capacity of BAT.
	Zhang *et al.* (2009)	Cold exposure ↑EE, ↑thermogenic capacity, and ↑EI.
	Zhang *et al.* (2012)	Cold exposure induces ↑ UCP1, ↑body mass, and ↓ leptin.
	Kitao & Hashimoto (2012)	Hibernation induces ↑ BAT thermogenesis at low temperature.
	Chen *et al.* (2012)	Cold exposure and short photoperiod induce ↑ T3, ↑ UCP1, ↑NST,↓ leptin and↓ body mass.
Diet and reproductive state	Xiao *et al.* (2007)	Early postnatal over-nutrition induces adverse BAT impact reducing NST in adulthood.
	Zhao & Wang (2009)	Changes in nutritional fibre content impact BAT activity, basal metabolic rate, and NST.
	Primeaux *et al.* (2007)	Spinal cord injury induces ↓ body mass, ↓ WAT mass, ↓ UCP1 mRNA and ↑ caloric intake.
	Zhang *et al.* (2008)	Lactating voles ↑ caloric intake, ↑resting metabolic rate, ↓ UCP1 and ↓ body fat mass.
	Leitner & Bartness (2009)	MSG ↓BAT NST and induces obesity.
	Cheng *et al.* (2010)	Leucine deprivation induces ↑ EE, ↑ UCP1, ↓ EI, ↓ body mass.
	Du *et al.* (2012)	Isoleucine or valine deprivation induces ↑ EE, ↑ UCP1, ↓ EI, ↓ body mass.

Noatsch *et al.* (2011)		↑ proteins or leucine in diet have no effect on energy homeostasis and UCP1 expression.

↑= increase; ↓= decrease; BAT = brown adipose tissue; Bmal1 = brain and muscle arnt-l ke 1; CpG = cytosine–phosphate–guanine; EE = energy expenditure; EI = energy intake; GC-1 = 2-[4-[(4-hydroxy-3-propan-2-ylphenyl)methyl]-3,5-dimethylphenoxy]acetic acid; MSG = monosodium glutamate; NST = non-shivering thermogenesis; OE = oleoyl-oestrone; Opa3 = optic atrophy 3; PE = *Pinellia ternata*; Per2 = period2; PKG-I = cyclic guanosine monophosphate-dependent protein kinase I; QRFP43 = pyroglutamylated arginine-phenylalanine-amide peptide; RMR = resting metabolic rate;T3 = tri-iodothyronine; Tc = core temperature; TLQP-21 = VGF-derived peptide; UCP1 = uncoupling protein 1; WAT = white adipose tissue; ZAG = zinc-α2-glycoprotein.

RESULTS

(1) Knockout studies

The analysed studies adopting knockout (KO) gene analysis targeted: (*a*) UCP1, (*b*) molecules of the nervous system, or (*c*) receptors, enzymes, and transcription factors to analyse their impact on NST heat production and obesity. Thus, the "knockout studies" were separated into "UCP1-KO", "Brain", and "Receptors, enzymes, and transcription factors" groups, respectively (Table 1).

(a) UCP1-KO group

Fatty acid-binding protein 3 is essential for accelerating fatty acid flux into the tissue from the bloodstream and for stimulating UCP1 activity for NST in rat BAT (Yamashita et al. 2008). UCP1 activity prevents the development of obesity and is the only protein that can mediate diet-induced thermogenesis in mouse BAT (Feldmann et al. 2009). Specifically, β3-adrenergic stimulation induces BAT NST which is fully UCP1-dependent (Inokuma et al. 2006). UCP2 and UCP3 are not involved in this process but they play roles in the regulation of cellular energy levels and/or oxidation of fatty acids (Inokuma et al. 2006). Therefore, given that UCP1 is the only player in NST heat production, its ablation becomes obesogenic in mice fed with both high-fat and normal diets due to an inability to stimulate diet-induced thermogenesis (Feldmann et al. 2009). The UCP1-KO mice also demonstrate slow arousal from torpor because re-warming is less effective and requires additional energy (Oelkrug et al. 2011). Despite their dysfunctional NST, UCP1-KO mice are cold tolerant probably due to: (*i*) persistent muscle shivering (Shabalina et al. 2010); (*ii*) up-regulation of ATP-Mg^{2+}/Pi inner mitochondrial membrane solute transporter gene in skeletal muscle [which could be a candidate for shivering thermogenesis (Anunciado-Koza et al. 2011)]; and/or (*iii*) reduction of heat loss through adrenergic

vasoconstriction (Meyer et al. 2010). On the other hand, ectopic UCP1 expression in skeletal muscles results in reduced adiposity and augmented EE in mice (Adjeitey et al. 2013). Moreover, the activity of UCP1 in muscle mitigates the production of reactive oxygen species in the mitochondria but not in BAT (Adjeitey et al. 2013).

(b) Brain group

It is well known that the hypothalamus links the nervous system to endocrine secretion *via* the pituitary and that both the hypothalamus and the pituitary express factors involved in NST and the regulation of temperature homeostasis in mammals. Specifically, cytosolic brain-type creatine kinase deficiency in mice inhibits neuronal communication between different hypothalamic circuits involved in NST (Streijger et al. 2009). Moreover, dorsomedial hypothalamic neuropeptide Y knockdown in rats increases EE and the thermogenic response to cold, and stimulates brown adipocyte formation in inguinal white adipose tissue (WAT) (Chao et al. 2011). Other central circuits, including the pro-opiomelanocortin neurons that are expressed in the pituitary, also regulate energy balance (De Jonghe et al. 2011). Down-regulation of pro-opiomelanocortin-protein tyrosine phosphatase 1B, a negative regulator of leptin signalling, reduces food intake and body mass in mice and increases their core temperature. Furthermore, pro-opiomelanocortin-protein tyrosine phosphatase 1B knockout mice show an increase in BAT mass, UCP1 mRNA in BAT, and serum tri-iodothyronine (T3) and type II iodothyronine deiodinase in response to cold exposure despite stable core temperature, food intake, and body mass (De Jonghe et al. 2011). These results highlight the negative effect of the expression of dorsomedial hypothalamic neuropeptide Y and pro-opiomelanocortin-protein tyrosine phosphatase 1B on body mass regulation *via* food intake, adiposity, NST, and EE (Chao et al. 2011; De Jonghe et al. 2011).

(c) Receptors, enzymes, and transcription factors group

The brain plays an important role in metabolism and thermoregulation, yet the function of the heart in these pathways also appears to be important. This is due to the release of natriuretic peptides from myocardiocytes which can regulate UCP1 expression promoting the binding of its transcription factors (Bordicchia et al. 2012). Indeed, nuclear receptors (described in detail below) play an important role in the control of metabolism and thermoregulation, regulating the expression of specific genes involved in both mechanisms. The activity of these nuclear receptors is mediated by a variety of cofactors and enzymes (also described in detail below) whose activity, in turn, depends on specific G-protein-coupled receptors. To evaluate effectively the gene function of these receptors, enzymes and transcription factors on NST and metabolism, the relevant studies were separated into: positive-effect genes (the activation of which promotes NST and EE) and negative or null-effect genes (the activation of which decreases or does not affect BAT activity and metabolism, respectively).

(i) Positive-effect genes

Liver-X receptors α and β play key roles in both NST and metabolism in mice, controlling EE and body mass loss through UCP1 expression in BAT (Korach-Andréa et al. 2011). Other receptors directly involved in the control of EE and body mass balance include the G-protein-coupled receptor kinase 2 (Vila-Bedmar et al. 2012), the thyroid hormone receptor (Pelletier et al. 2008), and the receptor interacting protein 140 (Hudson-Davies et al. 2009). G-protein-coupled receptor kinase 2 hemizygous (+/-) adult mice exhibit increased EE, BAT activity, white and brown fat lipid catabolism as well as core temperature after a cold exposure compared with wild-type animals (Vila-Bedmar et al. 2012). On the other hand, studies using KO mice for thyroid hormone receptor or receptor interacting protein 140 report a

significant reduction in BAT mass associated with poor NST, as well as disturbed BAT metabolic gene expression (Hudson-Davies et al. 2009). These results indicate that the activation of these receptors results in a positive effect on NST and metabolism.

Transcription factors such as peroxisome proliferator-activated receptor γ (PPAR-γ) (Gray et al. 2006) as well as molecules including silent mating type information regulation 2, homolog 3 (Sirt3; (Giralt et al. 2011), cardiac natriuretic peptides (Bordicchia et al. 2012), bone morphogenetic protein 7 (Tseng et al. 2008) and placenta-specific gene 8 protein (Jimenez-Preitner et al. 2011) are involved in mouse NST playing key roles in both UCP1 activation and brown adipocyte differentiation. Specifically, the transcription factor peroxisome proliferator-activated receptor γ co-factor 1α (PGC-1α) is unable to activate the brown adipocyte differentiation and the full programme of thermogenic genes, such as UCP1 and type 2 iodothyronine deiodinase expression, in mice lacking Sirt3 (Giralt et al. 2011). Moreover, cardiac natriuretic peptides promote brite cell development (and, thus, brite mass) and UCP1 expression in both natriuretic peptide receptor C-null mice and *in vitro* in human white adipocytes through the activation of natriuretic peptide receptor A (Bordicchia et al. 2012).

(ii) Negative- or null-effect genes

Despite the aforementioned effect of specific receptors and transcription factors on increasing metabolism and NST, the expression of a group of G-protein-coupled receptors, δ-opioid receptors (Czyzyk et al. 2012), as well as inhibitor of DNA-binding protein 1 (Satyanarayana et al. 2012), attenuates the activity of UCP1 in mice. Indeed, δ-opioid receptor (Czyzyk et al. 2012) or inhibitor of DNA-binding protein 1 (Satyanarayana et al. 2012) deficient mice demonstrate increased NST and EE as well as reduced body mass. Similarly, the ablation of growth hormone secretagogue

receptor increases thermogenic capacity and EE in both mice and rats (Mano-Otagiri et al. 2010; Lin et al. 2011; Ma et al. 2011). The absence of this receptor under both standard and high-fat diets leads to a lean mouse phenotype as well as increased EE, BMR, BAT mass and UCP1 gene expression (Mano-Otagiri et al. 2010; Lin et al. 2011; Ma et al. 2011). Lack of this receptor also leads to increased insulin sensitivity and resistance to the effect of ghrelin on BAT especially in older mice (Mano-Otagiri et al. 2010; Lin et al. 2011; Ma et al. 2011).

Aldehyde dehydrogenase 1 family member A1 – expressed more in WAT than BAT – irreversibly converts retinaldehyde dehydrogenase 1 (Rald) to retinoic acid resulting in a lower WAT functional plasticity (Kiefer et al. 2012). Indeed, in aldehyde dehydrogenase 1 family member A1 deficient mice as well as human white adipocytes, Rald was not converted into retinoic acid and, thus, it could promote transcription of BAT markers in WAT (including UCP1, PPAR-γ, PGC-1α, PR (positive regulatory domain 1 binding factor 1 and retinoblastoma protein-interacting zinc-finger protein) domain containing 16 (PRDM16), and fatty acid-binding protein 3) (Kiefer et al. 2012). This finding demonstrates the key role of Rald in human brite cell development. In contrast to all aforementioned positive- and negative-effect genes, α_1-AMP-activated protein kinase is a metabolic regulator but does not play a role in mouse NST and body mass regulation (Bauwens et al. 2011).

(2) Other studies

To synthesise the available evidence systematically and highlight the critical advances of the evaluated studies, the papers included in the 'other studies' category were separated into four groups: "Molecule treatment", "Sex and polymorphisms", "Temperature", and "Diet and reproductive state" in which the effect molecules, sex, UCP1 gene polymorphisms, temperature, litter size and diet were analysed, respectively, in terms of metabolism and NST (Table 2).

(a) Molecule treatment group

Circulating hormones such as insulin and T3 as well as β_3-adrenoceptor agonist CL 316243 influence NST activity and stimulate brite cell development in WAT (Lehr et al. 2009). Such effects, however, are not exerted by circulating oleoyl-oestrone (Romero del Mar et al. 2009) and by the β_3-adrenoceptor agonist zinc-α_2-glycoprotein (Wargent et al. 2013). Mouse WAT stroma vascular cells that are cultured in brown adipocyte medium containing T3 and β_3-adrenoceptor agonist CL 316243 undergo brite cell transformation. However, natural substances such as L-menthol in mice (Ma et al. 2012) and *Pinellia ternata* extract in rats (Kim et al. 2006), as well as the administration of the thyroid hormone β-selective agonist 2-[4-[(4-hydroxy-3-propan-2-ylphenyl)methyl]-3,5-dimethylphenoxy]acetic acid (GC-1) in diabetic rats (Matsen et al. 2013) increase NST and EE and reduce adiposity, but are not involved in brite cell development. Moreover, treatments with specific neuropeptides lead to similar results on NST and EE. Indeed, the VGF-derived peptide TLQP-21 increases NST and EE, limiting mass gain in rats (Bartolomucci et al. 2006). By contrast, a different neuropeptide, pyroglutamylated arginine-phenylalanine-amide peptide (QRFP43), reduces mouse BAT-induced NST and results in obesity phenotype development (Moriya et al. 2006).

(b) Sex and polymorphisms group

The different gene expression of steroid receptors (i.e. oestrogen receptor α and androgen receptor) in BAT of male and female rats explains sex hormone effects on BAT physiology (Rodriguez-Cuenca et al. 2007a). Progesterone activates mitochondrial biogenesis by modifying the mRNA expression of several mitochondrial transcription factors. For instance, when combined with norepinephrine, progesterone increases the mRNA levels of PPAR-γ, but testosterone and 17β-

estradiol down-regulate its expression (Rodriguez-Cuenca et al. 2007b). Therefore, these sex hormones are responsible, at least in part, for the differences in mitochondrial biogenesis between the sexes (Rodriguez-Cuenca et al. 2007b). Additional human evidence shows that methylation of the cytosine–phosphate–guanine (CpG) islands in the promoter region of UCP1 does not play a role in UCP1 protein expression (Shore et al. 2012), but haplotypic variation in the 5'-enhancer region of this gene affects NST and metabolism by altering UCP1 protein levels (Rose et al. 2011). When this variation is present, 17-βestradiol and progesterone produce opposing effects on UCP1 transcription (Rose et al. 2011). Specifically, UCP1 transcription activity is increased by progesterone and retinoic acid and decreased by 17-βestradiol in the presence of polymorphisms A-3826-G and, primarily, C-3737-A in the UCP1 gene sequence (Rose et al. 2011). On the other hand, overexpression of cyclic guanosine monophosphate-dependent protein kinase I protects female but not male mice against diet-induced obesity by stimulating lipolysis in WAT as well as NST in BAT (Nikolic et al. 2011).

(c) Temperature group

The recent identification of active BAT in protoendothermic mammals (Oelkrug et al. 2013) supports the prevailing hypothesis that BAT evolved to defend body temperature for migration to cold environments. This hypothesis is also supported by the recent discovery of higher UCP1 expression in the human longus colli and carotid sheath compared to superficial BAT depots. Indeed, the anatomical localisation of these depots, which are adjacent to the sympathetic chain and the carotid arteries, permits a rapid response to cold stimuli as well as effective heating of the cerebral vasculature (Cypess et al. 2013). The recent finding that cold acclimation leads to increased EE and BAT activity in humans – without an effect on brite cell development in abdominal subcutaneous WAT (van der Lans et al. 2013; Yoneshiro

et al. 2013) – further supports the involvement of BAT in body temperature regulation. Indeed, cold exposure in mice stimulates NST and induces the expression of clock genes, such as brain and muscle arnt-like 1 (Li et al. 2013) and period2 (Chappuis et al. 2013), that are involved in lipid catabolism and co-activation of UCP1 transcription factors leading to increased EE. Despite these findings demonstrating a link between BAT and EE, it is important to mention that the presence of the mitochondrial regulator function optic atrophy 3 gene mutation leads to an increase of lipid storage in mouse BAT without NST activation (Wells et al. 2012).

Different lines of evidence suggest that low temperature increases EE, BMR and NST in BAT in non-acclimated Brandt's voles (*Lasiopodomys brandtii*) (Liu et al. 2009; Zhang et al. 2009) as well as in tree shrew (*Tupaia belangeri*) (Zhang et al. 2012). Interestingly, the effect of cold also has been confirmed in cold-acclimated mammals. For instance, prolonged cold exposure of Arctic ground squirrels (*Urocitellus parryii*) generates significant increases in UCP1 mRNA and protein levels in BAT (Barger et al. 2006). The same study demonstrated that this cold-induced NST is not produced by up-regulation of UCP3 in the muscle. A study on Syrian hamsters (*Mesocricetus auratus*) showed that the ability of cold exposure to induce BAT thermogenesis and reduce body mass is stronger in hibernating animals due to their greater BAT mass compared to cold- or warm-acclimated animals (Kitao and Hashimoto 2012). On the other hand, the effect of cold on body mass loss appears to be linked with photoperiod. Specifically, the combined effect of cold and short photoperiod (typically occurring in the winter and potentially serving as a seasonal cue for the acclimation of energy balance) leads to reduced body mass in Maximowiczi's voles (*Microtus maximowiczii*) (Chen et al. 2012).

(d) Diet and reproductive state group

It is well known that nutrition is considered an important aspect in both metabolism and NST playing a key role in obesity and energy balance. In this light, while BAT serves to maintain body temperature during exposure to cold, leading to excess EE (Kozak 2010), research has shown that BAT thermogenesis can be also influenced by dietary factors. Specifically, early postnatal over-feeding in rats leads to sympathetic nervous system-mediated permanent changes in BAT thermogenesis resulting in reduced NST rates during adulthood (Xiao et al. 2007). However, this effect on BAT activity is dependent on nutritional fibre content. Indeed, high-fibre diet acclimation in adult Mongolian gerbils (*Meriones unguiculatus*) decreases BMR and NST, but these changes are reversed after restoration to a low-fibre diet (Zhao and Wang 2009).

Adaptation to diet of different fibre content occurs mainly *via* phenotypic plasticity in digestive tract morphology which counteracts changes in body mass (Zhao and Wang 2009). Another example of organ adaptation involves high thoracic spinal cord injury which triggers a prolonged post-injury loss of body mass and a reduction in WAT mass in rats (Primeaux et al. 2007). Interestingly, these changes occur despite a decrease in BAT UCP1 gene expression and a higher cumulative caloric intake (Primeaux et al. 2007). Therefore, this phenotype is not due to hypophagia or an increase in sympathetic nervous system-induced thermogenesis, but is caused by permanent changes in gastrointestinal transit and absorption, as well as whole-body homeostatic mechanisms (Primeaux et al. 2007). This is also confirmed in lactating Brandt's voles that show a reduction in body fat mass and UCP1 content despite an increase in energy intake compared to non-reproductive animals. The fact that NST was not augmented during lactation despite a rise in BMR may be an energy-conservation strategy for milk production (Zhang et al. 2008).

Other dietary factors such as the inclusion of food additives and/or the removal of specific branched-chain amino acids can also influence NST and metabolism. Siberian hamsters (*Phodopus sungorus*) treated with monosodium

glutamate (a molecule used as a food additive) showed a reduction in BAT activity associated with obesity phenotype development (Leitner and Bartness 2009). This effect on NST and metabolism can also result from feeding animals diets rich in leucine (Cheng et al. 2010), valine and isoleucine (Du et al. 2012). Mice fed with leucine or valine or an isoleucine deprivation diet show an increase in EE, expression of β-oxidation genes, and lipolysis (Cheng et al. 2010; Du et al. 2012). In addition, lipogenic gene expression and fatty acid synthesis in WAT are diminished, together with a reduction in food intake primarily due to isoleucine and valine. These findings together with a higher UCP1 activity in BAT – despite a reduction in BAT mass – could explain the WAT loss observed in these isoleucine- or valine-deprived mice compared to controls (Cheng et al. 2010; Du et al. 2012). Finally, exposure to high-protein-content diets or leucine supplementation does not affect energy homeostasis and UCP1 expression (Noatsch et al. 2011).

DISCUSSION

The objective of this paper was to evaluate critically, using a systematic approach, recent evidence on the molecular pathways linking NST and obesity in mammals, focusing on the mechanisms involved in BAT development. Our results, summarised in Fig. 2, demonstrated that molecules such as fatty acid-binding protein 3 (Yamashita et al. 2008), cardiac natriuretic peptides (Bordicchia et al. 2012), *Pinellia ternate* extract (Kim et al. 2006), L-menthol (Ma et al. 2012), progesterone (Rose et al. 2011), bone morphogenetic protein 7 (Tseng et al. 2008), PPAR-γ (Gray et al. 2006), placenta-specific 8 (Jimenez-Preitner et al. 2011), T3 (Lehr et al. 2009), Sirt3 (Giralt et al. 2011), period2 (Chappuis et al. 2013) as well as cold stimuli (Barger et al. 2006; Liu et al. 2009; Zhang et al. 2009; Chappuis et al. 2013; van der Lans et al.

2013; Yoneshiro et al. 2013) can increase UCP1 expression in existing brown adipocytes (Fig. 2: mechanism A).

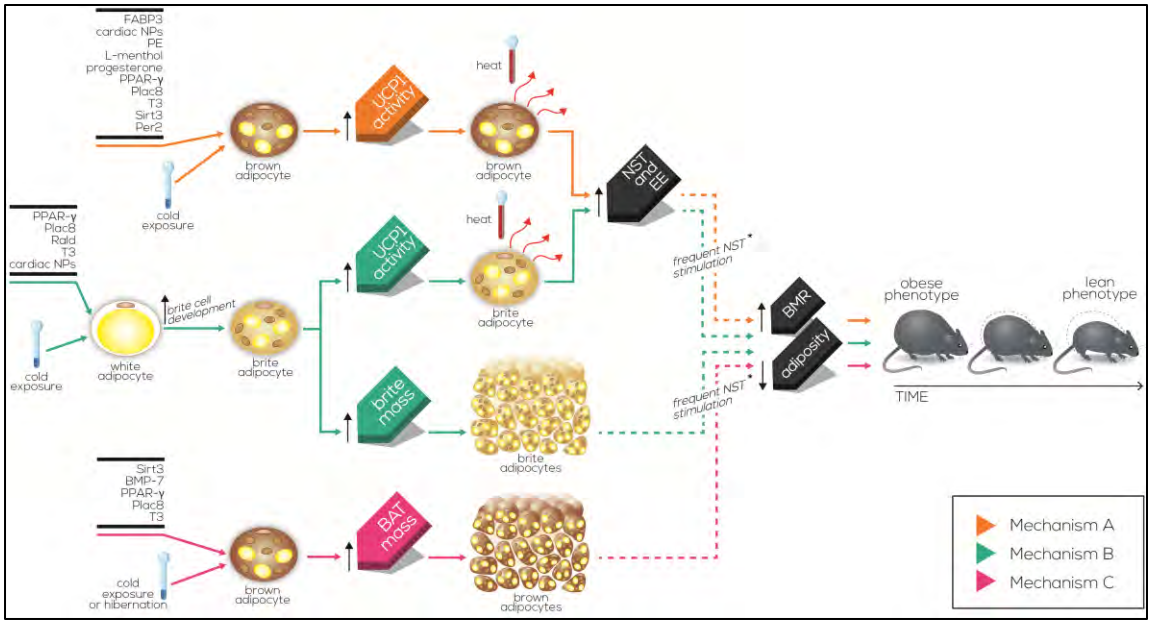

Figure 2. *Schematic representation of the effect of specific molecules, hibernation, and cold on brown adipose tissue (BAT)/brite development, non-shivering thermogenesis (NST) stimulation and adiposity based on the results of the present systematic analysis. In mechanism A, cold stimuli or specific molecules activate uncoupling protein-1 (UCP1) in the existing brown adipocytes. In mechanism B, certain molecules or cold exposure stimulate brite cell development, increasing the number of brite cells (i.e. brite mass) and the expression of UCP1 in brite adipocytes. In mechanism C, specific molecules, or hibernation, or cold exposure lead to increased BAT mass. The up-regulation of UCP1 expression in brown (mechanism A) and brite (mechanism B) adipocytes enhances NST and energy expenditure (EE). Finally, all three mechanisms can lead to augmented BMR and reduced adiposity levels in mammals when frequent NST stimulation without food intake compensation occurs. * = without food intake compensation; ↑ = increase; ↓ = decrease; BMP-7 = bone morphogenetic protein 7; BMR = basal metabolic rate; FABP3 = fatty acid-binding protein 3; NPs = natriuretic peptides; PE = Pinellia ternate extract; Per2 = Period2; Plac8 = placenta-specific 8; PPAR-γ = peroxisome proliferator-activated receptor γ; Rald = retinaldehyde dehydrogenase 1; Sirt3 = silent mating type information regulation 2, homolog 3; T3 = tri-iodothyronine.*

Specific molecules such as PPAR-γ (Gray et al. 2006), placenta-specific 8 (Jimenez-Preitner et al. 2011), Rald (Kiefer et al. 2012), T3 (Lehr et al. 2009), cardiac natriuretic peptides and cold exposure (Bordicchia et al. 2012) are implicated in brite cell development (Fig. 2: mechanism B). In turn, this leads to enhanced numbers of brite cells (i.e. brite mass) in WAT that contribute to increased UCP1 expression in WAT. It is important to note that the effect of cold exposure on white-to-brite transdifferentiation has been confirmed in rodents (Bordicchia et al. 2012), yet further

research is required to assess its efficacy in humans (van der Lans et al. 2013). On the other hand, cold exposure as well as molecules such as Sirt3 (Giralt et al. 2011), bone morphogenetic protein 7 (Tseng et al. 2008), PPAR-γ (Gray et al. 2006), placenta-specific 8 (Jimenez-Preitner et al. 2011), and T3 (Lehr et al. 2009) stimulate brown adipocyte differentiation (Fig. 2: mechanism C), leading to augmented BAT mass. Interestingly, the increase in BAT mass can also emerge from hibernation (Kitao and Hashimoto 2012) (Fig. 2: mechanism C), a concept discussed further below. The up-regulation of UCP1 gene and protein expression in brown and brite adipocytes through the aforementioned mechanisms A and/or B, respectively, leads to augmented NST and EE. Finally, frequent NST stimulation can result, eventually, in a rise of BMR and a reduction in adiposity levels (Koutedakis et al. 2005; Feldmann et al. 2009; Shabalina et al. 2010; Carrillo and Flouris 2011).

It is worth noting that the evaluated studies suggest that specific molecules such as fatty acid-binding protein 3 (Yamashita et al. 2008), *Pinellia ternate* extract (Kim et al. 2006), L-menthol (Ma et al. 2012), and progesterone (Rose et al. 2011) are involved in the activation of UCP1 in the existing brown adipocytes (Fig. 2: mechanism A) but do not contribute to BAT mass development. Thus, their effects on NST and metabolism depend on the available number of brown adipocytes. This is confirmed by the finding that cold exposure generates greater NST response and body mass reduction in hibernating animals that demonstrate larger BAT mass compared to warm- or cold-acclimated animals that demonstrate lower BAT mass (Kitao and Hashimoto 2012).

The transdifferentiation of white adipocytes to brite adipocytes (i.e. increasing brite mass) in mammals is a crucial step in the process towards increasing NST and metabolism, given the key role of brite mass in UCP1 expression. Stimulating a larger mass of cells to express UCP1 results in a more prominent increase of NST (Kitao and Hashimoto 2012) thus augmenting total EE by a magnitude proportional to the number of available brown and brite adipocytes. Moreover, frequent NST

stimulation, without food intake compensation, may lead to body mass loss. Several early studies showed that BAT is present in adult humans (Heaton 1972; Huttunen et al. 1981; Astrup et al. 1985) and that it is highly correlated with body mass index (Vijgen et al. 2011). Individuals with a larger BAT mass demonstrate greater cold-induced thermogenesis, EE, and BAT activity following cold exposure (Vijgen et al. 2011). Therefore, the increase of BAT/brite mass (through mechanisms B and C in Fig. 2) as well as frequent NST stimulation (through mechanisms A and B) may be promising in obesity treatment.

The current analysis produced an interesting concept regarding human brite cell development: one of the analysed studies showed that Rald (a molecule included in mechanism B of Fig. 2) induces white-to-brite transdifferentiation in human white adipocytes. This occurs by stimulating the WAT expression of the zinc-finger protein PR domain containing 16 (Kiefer et al. 2012). The latter is known to increase directly – or indirectly through the activation of PGC-1α – the type 2 deiodinase expression (Seale et al. 2007) that catalyses the conversion of thyroxine in T3 (Hall et al. 2010). Interestingly, several animal studies analysed herein suggested that T3 (Fig. 2: mechanism B) augments brite cell development, UCP1 transcription, NST, and EE resulting in lower adiposity levels (Lehr et al. 2009; Hall et al. 2010; De Jonghe et al. 2011; Chen et al. 2012). It is, therefore, logical to suggest that Rald may induce brite cell development in human WAT though the stimulation of thyroid hormone T3. However, the validity of this hypothesis remains to be confirmed by future research.

Systematic reviews determine the information to be obtained from a literature analysis using explicit inclusion and exclusion criteria (e.g. key words, years, and languages). Thus, the advantage of using a systematic analysis lies in reducing the likelihood of bias in identifying, selecting, and aggregating individual studies (Wieseler and McGauran 2010). While the systematic approach is likely to produce more accurate results regarding the effects of a specific phenomenon across a wide range of settings and empirical methods, it incorporates the risk of not including

relevant studies due to inadequate or incorrect methodology. In the present review we made considerable efforts to minimise these shortcomings by adopting published guidelines (Wieseler and McGauran 2010), using appropriate key words, and searching two of the largest databases available. Our systematic review is not a catalogue of everything that has been done, but rather a systematic synthesis of the work conducted since 2006 – the year when UCP1 was suggested to be the only mediator of NST in mammalian BAT (Barger et al. 2006). We attempted to ensure that our work provides concrete and unbiased added value and substance, draws together knowledge and highlights critical advances, thus creating new knowledge. In this light, our analysis suggests that future research in both animals and humans should address the interplay between body mass, BAT mass, as well as the main molecules involved in brite cell development.

CONCLUSIONS

(1) Specific molecules can enhance NST and metabolism by: (*i*) stimulating brite cell development in white adipose tissue, (*ii*) increasing UCP1 expression in brite adipocytes and in existing brown adipocytes, and (*iii*) augmenting BAT/brite mass.

(2) BAT mass also can be increased through low temperature, hibernation, and/or molecules involved in brown adipocyte differentiation.

(3) Cold stimuli and/or certain molecules activate UCP1 in existing brown adipocytes, thus increasing total energy expenditure by a magnitude proportional to the number of available brown adipocytes.

ACKNOWLEDGMENTS

The authors report no financial or personal relationships with other people or organisations that could inappropriately influence (bias) their actions. This work was supported by funding from the Education and Lifelong Learning Programme of the Greek Ministry of Education, Co-financed by Greece and the European Union (NSRF 2007-2013, IRAKLITOS II, grant no. 162), and the European Union 7th Framework Program (FP7-PEOPLE-IRG-2008 239521; FP7-PEOPLE-2009-IRSES 247631). The authors would like to express their gratitude to Miss Anna Carmen Patella for her assistance in designing the illustrations.

CHAPTER 3

Published as:

Valente A, Carrillo AE, Tzatzarakis MN, Vakonaki E, Tsatsakis AM, Kenny GP, Koutedakis Y, Jamurtas AZ, Flouris AD. The absorption and metabolism of a single L-menthol ORAL versus SKIN administration: Effects on thermogenesis and metabolic rate. Food Chem Toxicol. 2015 Sep 28.

The absorption and metabolism of a single l-menthol oral versus skin administration: effects on thermogenesis and metabolic rate

Angelica Valente,[1] Andres E. Carrillo,[2] Manolis N. Tzatzarakis,[3] Elena Vakonaki,[3] Aristidis M. Tsatsakis,[3] Glen P. Kenny,[4] Yiannis Koutedakis,[5,6] Athanasios Z. Jamurtas,[5] and Andreas D. Flouris[1,4]

ADDRESS FOR CORRESPONDENCE:

Andreas D. Flouris

FAME Laboratory

Department of Exercise Science

University of Thessaly

Karies, Trikala, 42100, Greece.

email: andreasflouris@gmail.com

Tel: +302431500601, Fax: +302431063191

[1]FAME Laboratory, Department of Exercise Science, University of Thessaly, Trikala, Greece.

[2]Department of Exercise Science, Chatham University, Pittsburgh, PA 15232, USA.

[3]Centre of Toxicology Science and Research, Medical School, University of Crete, Heraklion, Greece.

[4]Human and Environmental Physiological Research Unit, University of Ottawa, Ontario, Canada.

[5]School of Physical Education and Exercise Science, University of Thessaly, Greece.

[6]Institute of Sport, Faculty of Education, Health, and Wellbeing, University of Wolverhampton, WV1 1LY, UK.

ABSTRACT

We investigated the absorption and metabolism pharmacokinetics of a single L-menthol oral versus skin administration and the effects on human thermogenesis and metabolic rate. Twenty healthy adults were randomly distributed into oral (capsule) and skin (gel) groups and treated with 10 $mg \cdot kg^{-1}$ L-menthol ($ORAL_{MENT}$; $SKIN_{MENT}$) or control (lactose capsule: $ORAL_{CON}$; water application: $SKIN_{CON}$) in a random order on two different days. Levels of serum L-menthol increased similarly in $ORAL_{MENT}$ and $SKIN_{MENT}$ ($p>0.05$). L-menthol glucuronidation was greater in $ORAL_{MENT}$ than $SKIN_{MENT}$ ($p<0.05$). Cutaneous vasoconstriction, rectal temperature and body heat storage showed greater increase following $SKIN_{MENT}$ compared to $ORAL_{MENT}$ and control conditions ($p<0.05$). Metabolic rate increased from baseline by 18% in $SKIN_{MENT}$ and 10% in $ORAL_{MENT}$ and respiratory exchange ratio decreased more in $ORAL_{MENT}$ (5.4%) than $SKIN_{MENT}$ (4.8%) compared to control conditions ($p<0.05$). Levels of plasma adiponectin and leptin as well as heart rate variability were similar to control following either treatment ($p>0.05$). Participants reported no cold, shivering, discomfort, stress or skin irritation. We conclude that a single L-menthol skin administration increased thermogenesis and metabolic rate in humans. These effects are minor following L-menthol oral administration probably due to faster glucuronidation and greater blood menthol glucuronide levels.

KEYWORDS: brown adipose tissue; non-shivering thermogenesis; UCP1; partitional calorimetry; energy consumption; cardiovascular diseases.

INTRODUCTION

Uncoupling protein 1 (UCP1) is the main player in non-shivering thermogenesis (NST) process which takes place in mammal brown and brown-like (beige) adipocytes (Feldmann et al. 2009). Frequent stimulation of UCP1 results in an increase of basal metabolic rate and a reduction of adiposity levels in rodents as the fat energy storage is used for body heat production (Inokuma et al. 2006; Yamashita et al. 2008; Feldmann et al. 2009; Yoneshiro et al. 2013; Valente et al. 2014). Specifically, the oxidation of free fatty acids generates an electrochemical gradient across the mitochondrial inner membrane and when protons bypass the ATP synthase entrance and return to the mitochondrial matrix through UCP1, the energy of the electrochemical gradient is dissipated as heat (Feldmann et al. 2009; Mattson 2010). Animal studies reported that L-menthol is one of the molecules involved in the activation of UCP1 through the stimulation of the transient receptor potential melastatin 8 ion channel (Tajino et al. 2007; Ma et al. 2012; Valente et al. 2014). This receptor is the principal sensor of thermal stimuli in the peripheral nervous system (Romanovsky 2007; Flouris 2011). It is predominantly located on the cell membrane of sensory neurons while its expression has also been recently discovered on the membrane of brown and white adipocytes (Wang and Woolf 2005; Bautista et al. 2007; Colburn et al. 2007; Dhaka et al. 2007; Tajino et al. 2011; Ma et al. 2012; Rossato et al. 2014). Once in the body, L-menthol stimulates its receptor and induces a reversible rise in the intracellular Ca^{2+} with a subsequent protein kinase A phosphorylation in brown adipocytes that leads to UCP1 activation (Ma et al. 2012). This effect on Ca^{2+} current and UCP1 activation is stereochemically selective as D-menthol is half as active as its stereoisomer L-menthol (Wright et al. 1998).

A single application of L-menthol to the skin of the whole trunk in mice induces heat production and a rise in core temperature through skin vasoconstriction, muscle shivering, and NST activity (Tajino et al. 2007). Moreover, a 7-month dietary

L-menthol administration in mice increases core temperature, UCP1 expression in brown adipose tissue (BAT), NST activity and insulin sensitivity leading to attenuated body weight gain (Ma et al. 2012).

Similarly to rodents, a single skin L-menthol application in humans evokes cold sensation and cutaneous vasoconstriction (Yosipovitch et al. 1996; Olive et al. 2010; Topp et al. 2011; Gillis et al. 2015). A single oral administration of L-menthol, however, does not influence blood pressure or skin temperature (Gelal et al. 1999). Pharmacokinetics results show that, when taken orally, L-menthol is rapidly absorbed from the small intestine and extracted in the urine predominantly (~65%) as menthol glucuronide (Hiki et al. 2011). These findings suggest that the glucuronidation process which leads to low levels of L-menthol in the blood, may attenuate the aforementioned physiological effect upon oral L-menthol administration. Interestingly, the recent discovery of BAT and the white to brown-like transdifferentiation process in adult humans has provoked a plethora of theories and scientific experiments on its metabolic capabilities and potential for increasing energy expenditure (van Marken Lichtenbelt et al. 2009; Virtanen et al. 2009; Muzik et al. 2012; Rossato et al. 2014; Dinas et al. 2015; Flouris and Dinas 2015). Indeed, a recent in vitro study on human white adipocytes reported that L-menthol induces white to brown-like adipocyte transdifferentiation, stimulates UCP1 expression in brown-like adipocytes, and increases glucose uptake and heat production (Rossato et al. 2014). These findings emphasize the requirement of in vivo studies to confirm L-menthol as a potential molecule involved in controlling energy metabolism in humans. However, no physiological or clinical data are available on the effect of L-menthol on NST and energy expenditure in humans as well as on the comparison between oral and skin L-menthol administration in eliciting these effects.

The purpose of the present study was to compare, for the first time, the absorption and metabolism pharmacokinetics of a single L-menthol oral versus skin administration and investigate their effects on thermogenesis and metabolic rate in

healthy men and women. Based on previous animal studies assessing the effects of a single skin and daily oral L-menthol administration on NST and metabolism (Yosipovitch et al. 1996; Gelal et al. 1999; Tajino et al. 2007; Olive et al. 2010; Topp et al. 2011; Ma et al. 2012; Rossato et al. 2014; Valente et al. 2014) as well as considering the increase in human cutaneous vasoconstriction and rectal temperature upon a single skin L-menthol administration, we hypothesized that both oral and skin L-menthol administration would increase thermogenesis and metabolic rate in humans. Moreover, considering a limited contribution of the skin to the body's total phase II drug metabolism in humans (Manevski et al. 2015), L-menthol transdermal absorption may attenuate and/or delay the glucuronidation process leading to the entrance of a greater amount of L-menthol into the bloodstream compared to gastrointestinal absorption (Gelal et al. 1999; Hiki et al. 2011). Therefore, we also hypothesized that the skin administration would be more potent at eliciting these effects.

METHODS

Participants

The study conformed to the standards set by the Declaration of Helsinki and was approved by the University of Thessaly Department of Exercise Science Ethics Committee. A minimum required sample size of <5 participants per group was determined (statistical power: 0.95; α error probability: 0.05) based on plasma menthol glucuronide concentration observed before (17.8 ± 13.9 ng/ml) and 1 hour after (5617.5 ± 1918.1 ng/ml) a single oral L-menthol administration in a previously-published study (Hiki et al. 2011). Thus, 10 male and 10 female healthy volunteers [25.3 ± 6.2 years, 23.8 ± 3.0 $kg \cdot m^2$ body mass index (BMI), 20.2 ± 9.9 body fat percentage (mean ± standard deviation)] were recruited for this study. All volunteers

were recreationally active individuals and none of them were competitive athletes. Exclusion criteria included smoking, history or presence of metabolic, cardiac or pulmonary disease, thyroid or thermoregulatory disorders, use of any medication or oral contraception and pregnancy for females. Participants were informed about all experimental procedures, associated risks and discomforts and were asked to provide written informed consent. Female participants were tested during the early follicular phase (days 1-6) of their menstrual cycle.

Volunteers were randomly placed into the oral (ORAL) or skin (SKIN) administration group, each consisting of 10 participants. The study was conducted between June 2013 and June 2014 and participants of the two groups (ORAL and SKIN) were randomly allocated among the four seasons and tested for both control and L-menthol administration within 4-6 days. The randomization of the participants into the two groups as well as among seasons was performed using a random allocation algorithm incorporated in the SPSS Statistics Software (version 19; SPSS Inc., Chicago, IL, USA) in order to eliminate the eventual effects of adaptation/stress to the experimental procedures as well as to season temperature on the obtained results. No differences in age (ORAL: 26.2 ± 8.0 years; SKIN: 24.4 ± 3.9 years), body weight (ORAL: 65.9 ± 11.9 Kg; SKIN: 77.0 ± 11.3 Kg), height (ORAL: 1.7 ± 0.1 m; SKIN: 1.8 ± 0.1 m), BMI (ORAL: 22.6 ± 2.1 $Kg \cdot m^2$; SKIN: 25 ± 3.4 $Kg \cdot m^2$), or body fat percentage (ORAL: 17.8 ± 6.8 %; SKIN: 22.6 ± 12.1 %), were detected between the two groups (mean ± SD, $p>0.05$). Participants in the ORAL group were administered L-menthol ($ORAL_{MENT}$) via a capsule containing 10 $mg \cdot kg^{-1}$ body weight of L-menthol crystals (natural L-menthol FU-BP-USP; A.C.E.F. spa, Fiorenzuola d'Arda, Italy). This represents the highest daily orally dose that has been safely administrated to humans (Eisenberg et al. 1955). Participants in the SKIN group were administered L-menthol ($SKIN_{MENT}$) by applying a gel on skin surface of the neck and right arm and leg containing the same relative amount of L-menthol crystals (i.e., 10 $mg \cdot kg^{-1}$ body weight). The L-menthol gel was formulated according to previously published

procedures (Kounalakis et al. 2010) by mixing 10 mL of warm water (~40°C) and crystals of L-menthol for five minutes immediately prior to application. Both groups also completed a control treatment that consisted of a capsule containing lactose for the ORAL group ($ORAL_{CON}$) and warm water (~40°C) application for the SKIN ($SKIN_{CON}$). The administration of L-menthol or control was conducted in a random order on two different days separated by at least 72 hours. All measurements (described in the following paragraphs) were conducted by the same trained researchers using identical pre-calibrated equipment. Double-blind procedures were adopted only in the ORAL group. Due to the strong smell of menthol, a double-blind design was not possible in the SKIN group.

Experimental procedures

For each participant, the dietary intakes of the day before each administration (i.e., control or L-menthol oral administration as well as control or L-menthol skin administration) were similar. Indeed, on the day before to the first administration (i.e., control or L-menthol), participants chose their food consumption recording all the nutrients and the relative amount of their dietary intake using a log as well as their physical activity using a pedometer (Digi-Walker SW–200, Yamax, United Kingdom). These data were used as a guide for the participants to follow during the day prior to the second administration, and they were asked to adhere to it as much as possible. All participants were asked to not consume any products containing menthol, abstain from alcohol, caffeine, and environmental tobacco smoke, avoid any physical or mental stress and extreme temperature environments, and fast for 12 hours prior to each administration. Moreover, the National Weather Service Website was used to record the environmental temperature in the surrounding area of the day before each administration (i.e., control or L-menthol) for both groups (ORAL or SKIN).

During the treatment days, participants were asked to report to the laboratory (which was maintained at 25.1 ± 0.9 °C and 35.8 ± 3.4 % relative humidity during the

entire assessment period) at 08:30 following a 12-hr fast. They were asked to refrain from excessive stressors between wake-up time and arrival at the laboratory. All participants were transported to the laboratory via car and they were asked to wear the same clothing for both treatment days. Food consumption was not permitted during data collection. Although room-temperature water was provided *ad libitum*, Mann-Whitney U test showed that participants in ORAL (151 ± 78.0 g) and SKIN (220 ± 83.6 g) groups consumed the same quantity during treatment days ($p>0.05$).

After the participant's arrival in the lab, body mass and body fat percentage were assessed using a body composition analyser (Tanita BF522W, Tokyo, Japan). Rectal temperature (T_{re}), skin blood flow (SkBF), mean skin temperature (T_{sk}), and body heat storage (S) were assessed to determine the effect of L-menthol administration on thermogenesis, while metabolic rate (M) and respiratory exchange ratio (RER) were measured to determine the effect of L-menthol on metabolism and substrate utilization. Therefore, various sensors for these physiological variables measurements were applied on the participants' body. Specifically, a thin and flexible core temperature thermistor (Mon-A-Therm Core, Mallinkrodt Medical, St Louis, USA) was self-inserted 15 cm beyond the anal sphincter to measure T_{re} every 8 sec using the BioTemp^{TM} (model 3.1, Biomnic Ltd., Greece), as previously described (Hartley et al. 2012). A laser-Doppler velocimetry (PeriFlux System 5000, main control unit; PF5010 LDPM, function unit; Perimed, Stockholm, Sweden) was applied on the epidermis at the distal end of the left first toe (i.e. hallux) to measure SkBF, using previous procedures (Flouris and Cheung 2009). The probe (PR 407 small straight probe; Perimed) was held in place with a plastic apparatus (diameter: 5 mm; PH 07-5; Perimed) and double-sided adhesive strips (PF 105-3; Perimed). The T_{sk}, S, M and RER were measured non-invasively using partitional calorimetric techniques. Seven pre-calibrated heat flow sensors incorporating temperature thermistors were placed on the skin surface of the forehead, abdomen, forearm, hand, quadriceps, shin, and foot and held in place with surgical tape (Leukoplast,

BSN medical, Hamburg, Germany) and were used to record data every 8 sec using the BioTemp^{TM} (model 3.1, Biomnic Ltd., Greece). Moreover, to assess autonomic modulation, participants were outfitted with a heart rate chest strap and heart rate variability (HRV) was measured through short-range telemetry at 1,000 Hz with a Polar RS800CX (Polar Electro, Kempele, Finland).

At 09:45, participants were asked to sit on a comfortable chair and remain seated for the next 7 hours and 30 min. For all participants, data collection started at 09:45 and the first 15 minutes (i.e., 09:45-10:00) were used as baseline data. The treatment (i.e., L-menthol or control) was always administered at 10:00 which consisted of ingestion of the L-menthol/lactose capsules for participants in ORAL and application of L-menthol gel/water to the back of the neck and the front of the right arm and leg for SKIN participants. Data collection (the first 15 min of every hour) continued for 7 hours and 15 minutes (i.e., from 10:00 until 17:15) following the administration of the treatment. During data collection participants were instructed to remain silent and as calm and still as possible while between measurements, participants remained seated and either were watching a movie or reading a book. Following the final data collection (i.e., 17:00-17:15), all sensors were removed and the participants were discharged.

Blood biomarkers

Four venous blood samples (~10 mL each) were collected from an antecubital vein at baseline and at 1, 2, and 6 hours following each administration and then separated in serum-separator and EDTA tubes. The serum-separator-samples were first kept at room temperature for ~20 min before centrifugation at 3000 rpm for 10 min at 4°C while the EDTA-samples were immediately centrifuged at 3000 rpm for 10 min at 4°C. The serum and plasma supernatants were collected and stored at -80°C until analysis.

Serum samples were analysed for L-menthol and its primary metabolite, menthol glucuronide that was calculated as the difference in L-menthol concentrations before and after the samples were treated with β-glucuronidase. Specifically, for the determination of free L-menthol, 1 mL of serum was placed in an 8 mL solid phase microextraction vial. One ml of ultrapure water, 0.25 gr of NaCl and 40 ng of internal standard 1,2,3,4-tetrachloronaphthalene (TCN) were added. For the determination of total L-menthol 1 mL of serum, 0.25 gr NaCl, 875 μL of buffer solution pH=6 (Carl Roth GmbH), 25 μL of the β-glucuronidase enzyme (Type HP-2, Helix pomatia, Sigma), 100 μL of ultrapure water and 40 ng of TCN were placed in solid phase microextraction vials (Hiki et al. 2011). Solid phase microextraction vials were sealed with polytetrafluoroethylene/silicon septum caps and placed in a gas chromatography-mass spectrometry tray. Online extraction followed with a polydimethylsiloxane/divinylbenzene type extraction fibre at 50°C for 30 min with an agitation speed of 250 rpm. After the completion of the absorption process, the fibre tip was inserted in the injection port of the gas chromatography-mass spectrometry, where it remained for 3 min until the complete release of the analytes. Serum samples with no detected levels of L-menthol were used as blank samples, fortified at different concentration levels (0, 1, 2, 5, 10, 20, 40 and 80 ng/mL for free L-menthol and 0, 5, 10, 20, 40, 80, 160, 320, 640 and 1280 ng/mL for total L-menthol) and used as spiked samples for the preparation of the calibration curves. Samples were analysed with a Shimadzu (Kyoto, Japan) QP-2010 gas chromatography-mass spectrometry equipment. The system was equipped with a split/splitless injection inlet and an AOC-5000 robotic autosampler with the appropriate functions to operate in solid phase microextraction mode. Gas chromatography-mass spectrometry solution software was used for instrument control and data analysis. Gas chromatography analysis was conducted on a Supelco SLBtm-5ms (Bellefonte PA, USA) capillary column of 30 m length, 0.25 mm i.d, and 0.25 μm film thicknesses. The AOC-5000 solid phase microextraction autosampler was equipped with a syringe with a 65 um

polydimethylsiloxane/divinylbenzene Metal Alloy fibre from Supelco (Bellefonte PA, USA). The following conditions were used: Helium with a constant flow rate of 1 mL/min as a carrier gas, inlet temperature 250°C, splitless injection for 1 min, mass spectrometer interface and ion source temperatures were 300°C and 220°C, respectively. The column temperature was initially held at 65°C for 5 min, raised at 10°C·min^{-1} to 140°C and increase at a rate of 30°C·min^{-1} until 310°C were it remained for 2 min. Under the above conditions the retention times of L-menthol and internal standard were 11.80 and 17.57 min, respectively. The mass spectrometer detector was operated at the selected ion-monitoring mode (SIM). The qualification m/z ions of L-menthol were m/z=71, 81, 95, 123 and 138 (with target ion m/z=95) while the m/z ions for internal standard were 266 and 194 (with target ion 266).

The plasma samples were analysed for adiponectin (Human adiponectin/Acrp30 ELISA, order number RAB0005, analytical sensitivity <25 pg/mL, intra assay <10%, inter assay <12%; Sigma-Aldrich, St Louis, MO 63013, USA) and leptin concentration (Human Leptin ELISA, order number RAB0333, analytical sensitivity <2 pg/mL, intra assay <10%, inter assay <12%; Sigma-Aldrich, St Louis, MO 63013, USA) – being both hormones involved in UCP1 activity (Asano et al. 2013; Qiao et al. 2014), regulation of energy expenditure and glucose and fatty acid breakdown (Giby and Ajith 2014) – using commercially available ELISA kits that were performed according to the instructions of the manufacturer. Briefly, all plasma samples were diluted 30000 times for adiponectin and 20 times for leptin with sample diluent before performing each hormone analysis. Standard series and samples were added in duplicate to the plate and adiponectin or leptin presented in each sample was bound to the wells by the corresponding immobilized antibody. The wells were washed with a washing solution and biotinylated anti-human adiponectin or leptin antibodies were added. After washing away unbound biotinylated antibody, horseradish peroxidase-conjugated streptavidin was pipetted to the wells. The wells were again washed, a 3,3′,5,5′-tetramethylbenzidine substrate solution was added to

the wells and colour developed in proportion to the amount of adiponectin or leptin bound. The stop solution changed the colour from blue to yellow, and the intensity of the colour was measured at a wavelength of 450 nm.

Thermal comfort and sensation

At the beginning of baseline and each data collection time, participants were asked to indicate a number for thermal comfort and thermal sensation using previously published scales (Gagge et al. 1969). The range of the thermal comfort scale was from 1 through 5, where 1 = “comfortable”, 2 = “slightly uncomfortable”, 3 = “uncomfortable”, 4 = “very uncomfortable”, 5 = “extremely uncomfortable”; participants could also indicate intermediate numbers (i.e., 1.5, 2.5, 3.5, and 4.5). The range of the thermal sensation scale was from 0 through 10, where 0 = “unbearably cold”, 1 = “very cold”, 2 = “cold”, 3 = “cool”, 4 = “slightly cool”, 5 = “neutral”, 6 = “slightly warm”, 7 = “warm”, 8 = “hot”, 9 = “very hot”, 10 = “unbearably hot”. Moreover, during the entire assessment period, participants were frequently asked to report any kind of stress, discomfort, and/or shivering. Moreover, participants in the SKIN group were also constantly inspected for skin irritation.

Data computations

Physiological data (i.e., SkBF, T_{sk}, T_{re}, S, M, RER, and HRV indices) were used to calculate 1-min averages for each 15-min data collection time point. Thereafter, these values were used for subsequent computations as described below. Data for total L-menthol and free L-menthol concentrations were used to calculate menthol glucuronide concentration. The serum concentration of total L-menthol represents the total L-menthol absorption, the free L-menthol serum concentration represents the amount of L-menthol in the body, while the serum menthol glucuronide concentration is an indicator of the metabolism of L-menthol.

Partitional calorimetric estimates of the rates of heat storage were calculated according to the conceptual heat balance equation:

$$S = M - W\ (C + R + E_{sk} + C_{res} + E_{res})\ (W \cdot m^{-2})$$

As previously (Nishi 1981), M was calculated as:

$$M = \frac{VO_2 \cdot \frac{\left(\frac{RER - 0.7}{0.3}\right) \cdot e_c + \left(\frac{1 - RER}{0.3}\right) \cdot e_f}{1000} \cdot 1000\ (W \cdot m^{-2})}{60}$$

where VO_2 is the rate of oxygen consumption ($mL \cdot min^{-1}$); RER is the respiratory exchange ratio (non-dimensional); while e_c and e_f are the energetic equivalents of carbohydrate (21.116 $kJ \cdot L^{-1}$ O_2) and fat (19.606 $kJ \cdot L^{-1}$ O_2), respectively. The VO_2 and RER were based on indirect calorimetry data obtained as participants breathed (during data collection time) through a low resistance one-way valve attached to a face mask. Exhaled gases were assessed using a gas analyser (Oxycon Mobile, CareFusion, San Diego, USA) and RER was calculated as the ratio between CO_2 removed from the body and O_2 consumed. External workload (W) was 0 as the participants remained relaxed in a seated position throughout the experiment.

The combined respiratory heat exchange via convection (C_{res}) and evaporation (E_{res}) was calculated as:

$$C_{res} + E_{res} = [0.0014 \cdot H_p \cdot (34 - T_a)] + [0.0173 \cdot H_p \cdot (5.87 - P_a)]\ (W \cdot m^{-2})$$

where H_p is the rate of metabolic heat production calculated as the difference between M and W (in $W \cdot m^{-2}$); T_a is the ambient temperature (°C); and P_a is the ambient vapour pressure in kilopascals (kPa).

Heat exchange via convection (C) and radiation (R) was calculated as:

$$C + R = \frac{T_{sk} - T_o}{R_{cl} + \frac{1}{f_{cl} \cdot h}}\ (W \cdot m^{-2})$$

where: R_{cl} is the thermal resistance of clothing ($m^2 \cdot °C \cdot W^{-1}$) which was assumed to be negligible due to minimal clothing insulation (i.e., ~0.2-0.3 clo) and, in any case, systematic as participants wore the same clothing on both assessment days; f_{cl} is the

non-dimensional area-weighted clothing factor (assumed to be 1.0 with minimal clothing); h is the combined heat transfer coefficient ($W \cdot m^{-2} \cdot °C^{-1}$) calculated as the sum of convective (h_c) and radiant (h_r) heat transfer coefficients (see calculation procedures below). The operative temperature (T_o) was estimated as:

$$T_o = \frac{h_c \cdot T_a + h_r \cdot T_r}{h_r + h_c} \ (°C)$$

where T_r is the radiant temperature (°C) assumed to be equal to T_a.

The h_c and h_r were calculated as follows:

$$h_c = 8.3v^{0.6} \ (W \cdot m^{-2} \cdot C^{-1})$$

$$h_r = 4\varepsilon\sigma \frac{A_r}{A_D} \left(273.15 + \frac{T_{cl} + T_r}{2}\right)^3 \ (W \cdot m^{-2} \cdot °C^{-1})$$

where: v is air velocity ($m \cdot s^{-1}$); ε is the area-weighted emissivity of the skin, estimated as 0.95; σ is the Stefan-Boltzmann constant ($5.67 \cdot 10^{-8}$ $W \cdot m^{-2} \cdot °C^{-4}$); $\frac{A_r}{A_D}$ is the effective radiant surface area (non-dimensional), estimated to be 0.7 for a seated individual (Fanger 1970); and T_{cl} is the temperature of the clothing (°C) which was assumed to be equal to T_{sk}. Evaporative heat loss was assumed to be negligible as no sweating was apparent.

For the HRV analysis, the heart rate monitor signal was transferred to the Polar Precision Performance Software (release 3.00; Polar Electro Oy), and RR intervals (time intervals between consecutive R waves in the electrocardiogram) were analysed in order to assess the modulation of sympathetic and parasympathetic activities as previously described (Flouris and Cheung 2009). Frequency domain, time domain and nonlinear method analysis was performed using HRV software version 1.1 (Finland; Biomedical Signal Analysis Group, Department of Applied Physics, University of Kuopio, Finland 2002) evaluating the RR interval time series automatically obtained from the raw signals (Rajendra Acharya et al. 2006). The frequency domain with the low frequency, high frequency, and low frequency to high frequency ratio variables were analysed to discriminate between sympathetic and

parasympathetic contribution to HRV. For the time domain method, both statistical and geometric parameters were considered for the analysis of Mean RR, Mean HR, standard deviation of RR and heart rate, the square root of the mean of squared differences between successive intervals, the percentage of the differences of successive normal-to-normal intervals 50 ms normalized to all differences within the interval, the number of pairs of successive normal-to-normal that differ by more than 50 ms, the HRV triangular index, and the triangular interpolation of normal-to-normal interval histogram. Nonlinear method was used to analyse the standard deviation of fast and long term RR variability, mean line length, maximum line length, recurrence rate, determinism, Shannon Entropy, approximate entropy, sample entropy, Detrended Fluctuation Analysis α 1 and 2, and correlation dimension.

Statistical analyses

Environmental temperature in the surrounding area of the day before each administration and all dependent variables (serum L-menthol and menthol glucuronide, plasma adiponectin, leptin and leptin/adiponectin ratio as well as SkBF, T_{sk} T_{re}, S, M, RER, HRV, thermal comfort and thermal sensation) showed a non-normal distribution therefore non-parametric tests were used throughout. Mann-Whitney U and Wilcoxon Signed-Rank tests were used to compare environmental temperatures in the surrounding area between groups for the same treatment (i.e., $ORAL_{MENT}$ vs. $SKIN_{MENT}$ and $ORAL_{CON}$ vs. $SKIN_{CON}$) and between treatments within the same group (i.e., $ORAL_{CON}$ vs. $ORAL_{MENT}$ and $SKIN_{CON}$ vs. $SKIN_{MENT}$), respectively. Moreover, for each dependent variable, Mann–Whitney U tests were used for the comparisons between groups for the same treatment (i.e., $ORAL_{MENT}$ vs. $SKIN_{MENT}$ and $ORAL_{CON}$ vs. $SKIN_{CON}$) at baseline and each assessment hour separately. Wilcoxon Signed-Rank test was used for the comparisons between treatments within the same group (i.e., $ORAL_{CON}$ vs. $ORAL_{MENT}$ and $SKIN_{CON}$ vs. $SKIN_{MENT}$) at baseline and each assessment hour separately as well as to assess

dependent variables differences across time (i.e., differences between baseline and each following assessment hour as well as between consecutive assessment hours within each treatment). All analyses were conducted with SPSS Statistics (version 19; SPSS Inc., Chicago, IL, USA). The data are reported as mean ± SEM and p-values < 0.05 were regarded as statistically significant. We did not adjust for multiple comparisons in our study due to the errors and misplaced emphasis associated with such procedures when applied in actual natural observations (Rothman 1990; Perneger 1998; Feise 2002; Rothman 2014).

RESULTS

Environmental temperatures in the surrounding area

In order to test our primary and secondary hypothesis, we first examined the impact of the environmental temperature in the surrounding area. Mann-Whitney U and Wilcoxon Signed-Rank tests showed that the environmental temperature in the surrounding area on the day before each administration were not significant different ($p>0.05$) between groups for the same treatment (i.e., $ORAL_{MENT}$: 20.5 ± 1.7 °C vs. $SKIN_{MENT}$: 16.4 ± 1.8 °C; $ORAL_{CON}$: 19.8 ± 2.0 °C vs. $SKIN_{CON}$ 15.6 ± 1.6 °C) and between treatments within the same group (i.e., $ORAL_{CON}$: 19.8 ± 2.0 °C vs. $ORAL_{MENT}$: 20.5 ± 1.7 °C; $SKIN_{CON}$: 15.6 ± 1.6 °C vs. $SKIN_{MENT}$: 16.4 ± 1.8 °C).

Serum L-menthol and menthol glucuronide concentration

Regarding our primary hypothesis, results from Wilcoxon Signed-Rank tests demonstrated that L-menthol and menthol glucuronide concentrations were significantly different between treatments within the same group (i.e., $ORAL_{CON}$ vs. $ORAL_{MENT}$ and $SKIN_{CON}$ vs. $SKIN_{MENT}$) (Figure 1, $p<0.05$). Regarding our secondary hypothesis, results from Mann-Whitney U tests demonstrated that menthol

glucuronide concentrations ($p<0.05$) but not L-menthol ($p>0.05$), were significantly different between groups for the same treatment (i.e., $ORAL_{MENT}$ vs. $SKIN_{MENT}$). Specifically, the body absorption of L-menthol (i.e., total L-menthol) was higher in $ORAL_{MENT}$ (3385.9 ± 1681.1 ng/mL) compared to $SKIN_{MENT}$ (214.8 ± 112.7 ng/mL) (Figure 1, $p<0.05$). The changes observed in the amount of L-menthol in the body (i.e., free L-menthol) were similar in $ORAL_{MENT}$ and $SKIN_{MENT}$ ($p>0.05$), showing an increase within 1 hour after treatments (Figure 1, $p<0.05$). Within 1 hour after $ORAL_{MENT}$, menthol glucuronide was ~38.0 times higher than L-menthol (3299.6 ± 1636.3 ng/mL menthol glucuronide and 86.4 ± 44.7 ng/mL L-menthol) (Figure 1).

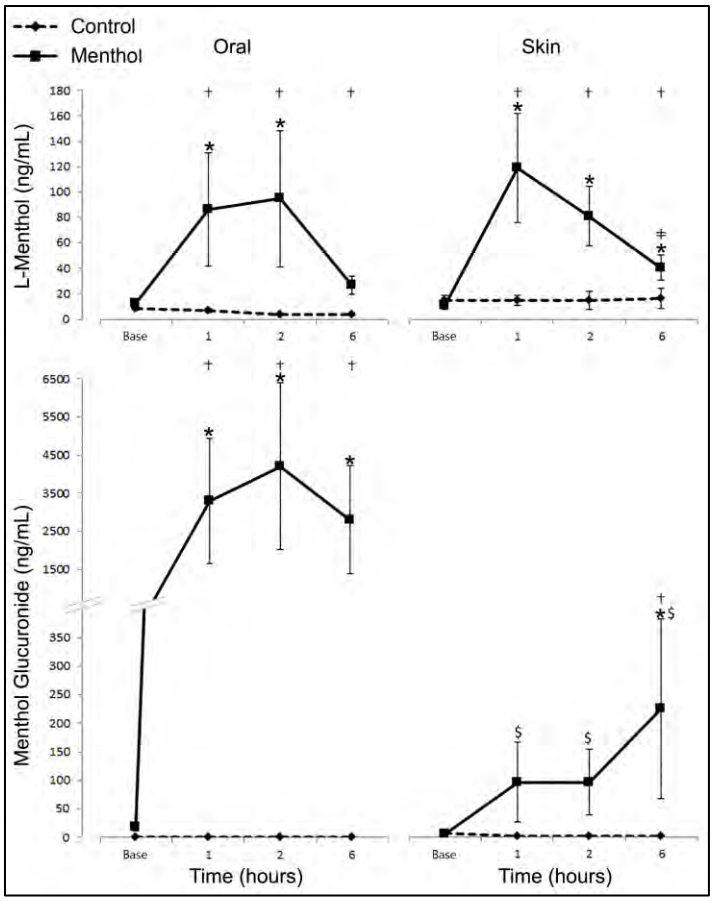

Figure 1. *Results (mean ± SEM) and comparisons for serum L-menthol and menthol glucuronide levels at baseline (Base) and 1, 2 and 6 hours after oral and skin treatments. Note: * = significant differences from baseline within the same treatment (Wilcoxon Signed-Rank tests; p<0.05); ǂ = significant differences from the previous time-point within the same treatment (Wilcoxon Signed-Rank tests; p<0.05); † = significant differences between control and L-menthol treatments within the same group for the same time-point (Wilcoxon Signed-Rank tests; p<0.05); $ = significant differences between SKIN vs. ORAL group for the same treatment and time-point (Mann-Whitney U tests; p<0.05).*

The peak of menthol glucuronide (4201.2 ± 2189.9 ng/mL) was reached 2 hours after $ORAL_{MENT}$ (Figure 1, $p<0.05$). On the other hand, within 1 hour after $SKIN_{MENT}$, menthol glucuronide was ~1.2 times smaller than L-menthol (95.5 ± 69.7 ng/mL menthol glucuronide and 119.4 ± 42.9 ng/mL L-menthol, Figure 1). The peak of menthol glucuronide was reached 6 hours after $SKIN_{MENT}$ (Figure 1, $p<0.05$), showing a concentration ~5.5 times higher than that of L-menthol (223.8 ± 157.0 ng/mL menthol glucuronide and 40.5 ± 10.0 ng/mL L-menthol). However, even at its peak, menthol glucuronide concentration in $SKIN_{MENT}$ was significantly lower than in $ORAL_{MENT}$ (Figure 1, $p<0.05$).

Thermogenesis and metabolic response

Regarding our first hypothesis, figure 2 shows that SkBF was reduced ($p<0.05$) within 1 hour following both $ORAL_{MENT}$ (66.5% reduction) and $ORAL_{CON}$ (79.5% reduction); the latter reduction being significantly greater ($p<0.05$).

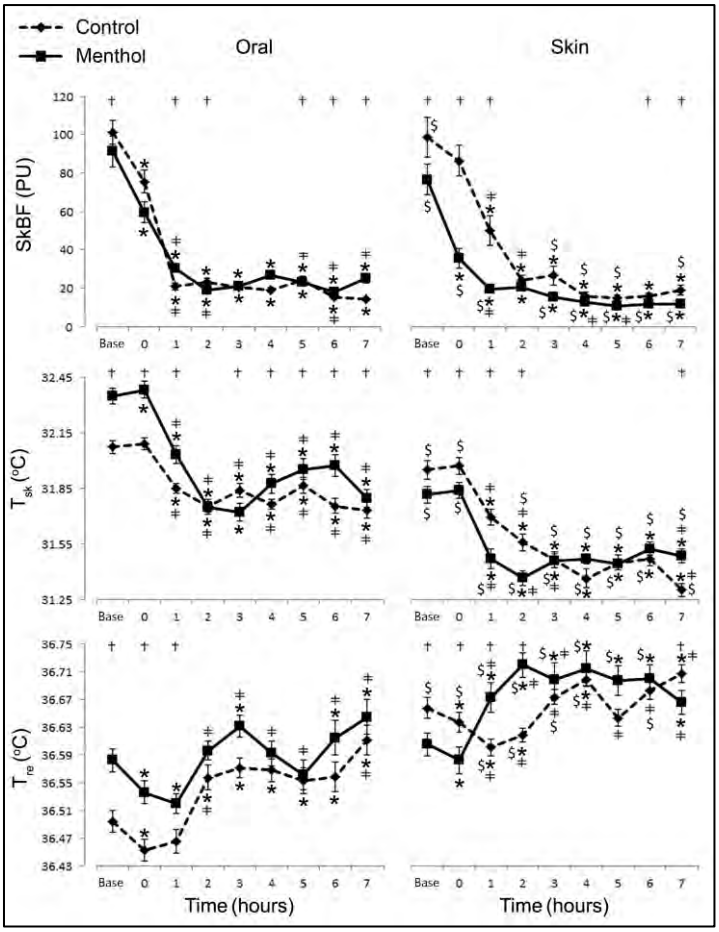

Figure 2: *Results (mean ± SEM) and comparisons for skin blood flow [SkBF in perfusion units (PU)], mean skin temperature (Tsk), and rectal temperature (Tre) at baseline (Base) and for 7 hours after oral and skin treatments. Note: * = significant differences from baseline within the same treatment (Wilcoxon Signed-Rank tests, p<0.05); ǂ = significant differences from the previous time-point within the same treatment (Wilcoxon Signed-Rank tests, p<0.05); † = significant differences between control and L-menthol treatments within the same group for the same time-point (Wilcoxon Signed-Rank tests, p<0.05); $ = significant differences between SKIN vs. ORAL group for the same treatment and time-point (Mann-Whitney U tests, p<0.05).*

The changes observed in T_{sk} and T_{re} were similar in $ORAL_{MENT}$ and $ORAL_{CON}$ (Figure 2, p>0.05). Indeed, after treatments T_{sk} was attenuated by 1% within 1 hour (p<0.05) while T_{re} was increased by 0.1% within 3 hours (p<0.05).

SkBF was reduced within 15 min (at time 0) following only $SKIN_{MENT}$ (55% reduction; Figure 2, p<0.05). Within 1 hour from the treatment, SkBF was reduced in both $SKIN_{MENT}$ (75% reduction) and $SKIN_{CON}$ (49% reduction); the former reduction being significantly greater (Figure 2, p<0.05). The changes observed in T_{sk} and T_{re} were more evident in $SKIN_{MENT}$ compared to $SKIN_{CON}$ (Figure 2, p<0.05). Specifically,

in $SKIN_{MENT}$, T_{sk} was attenuated by 1.1% within 1 hour and by 1.4% within 2 hours ($p<0.05$) after treatment, while T_{re} was increased by 0.2% within 1 hour and by 0.3% within 2 hours ($p<0.05$) after treatment. In contrast, in $SKIN_{CON}$, T_{sk} was attenuated by only 0.8% within 1 hour and by 1.2% within 2 hours ($p<0.05$) after treatment, while T_{re} was decreased by 0.1% within 1 hour ($p<0.05$) after treatment (Figure 2).

Mann-Whitney U tests indicated that S, M, and RER were significantly different between groups for the same treatment (i.e., $ORAL_{MENT}$ vs. $SKIN_{MENT}$ and $ORAL_{CON}$ vs. $SKIN_{CON}$; Figure 3, $p<0.05$), while Wilcoxon Signed-Rank tests showed that significant differences between treatments within the same group (i.e., $ORAL_{CON}$ vs. $ORAL_{MENT}$ and $SKIN_{CON}$ vs. $SKIN_{MENT}$) were observed only in RER (Figure 3, $p<0.05$). Specifically, during the first 5 hours from the treatment, the increase observed in S during $ORAL_{MENT}$ was similar to that observed in $ORAL_{CON}$ (Figure 3, $p<0.05$); the former increase being slightly lower ($p>0.05$).

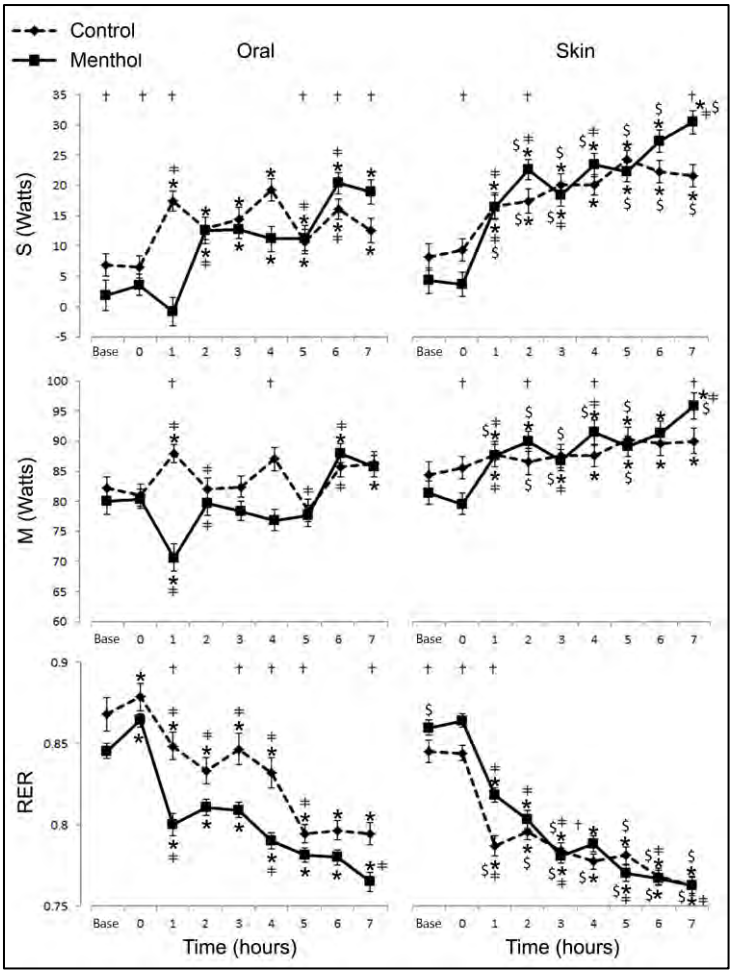

Figure 3: *Results (mean ± SEM) and comparisons for heat storage (S), metabolic rate (M) and respiratory exchange ratio (RER) at baseline (Base) and for 7 hours after oral and skin treatments. Note: * = significant differences from baseline within the same treatment (Wilcoxon Signed-Rank tests; p<0.05); ǂ = significant differences from the previous time-point within the same treatment (Wilcoxon Signed-Rank tests; p<0.05); † = significant differences between control and L-menthol treatments within the same group for the same time-point (Wilcoxon Signed-Rank tests; p<0.05); Ṩ = significant differences between SKIN vs. ORAL group for the same treatment and time-point (Mann-Whitney U tests; p<0.05).*

Nevertheless, within 6 hours from the treatment, the increase observed in S was more pronounced during $ORAL_{MENT}$ (1000%) compared to $ORAL_{CON}$ (136%) (Figure 3, p<0.05). By 7 hours from the treatment, S increased by 943% (p<0.05) during the $ORAL_{MENT}$ and by only 83% (p<0.05) during the $ORAL_{CON}$. The changes observed in M during the $ORAL_{MENT}$ and the $ORAL_{CON}$ were opposite in trend (Figure 3, p<0.05). Specifically, in $ORAL_{MENT}$, M was attenuated by 12% (p<0.05) within 1 hour from the treatment and it subsequently demonstrated an upward trend reaching an increase of 10% within 6 hours from the treatment (Figure 3, p<0.05). In contrast, in $ORAL_{CON}$, M

was significantly increased by 7% ($p<0.05$) within 1 hour from the treatment and it was subsequently attenuated reaching baseline levels within 2 hours from the treatment (Figure 3, $p>0.05$). The RER was reduced within 1 hour after the treatment in both $ORAL_{MENT}$ (5.4% reduction; $p<0.05$) and $ORAL_{CON}$ (2.3% reduction, $p<0.05$); the former reduction being significantly greater (Figure 3, $p<0.05$).

Statistically significant increases in S and M were observed in $SKIN_{MENT}$ and $SKIN_{CON}$; the former increase being significantly greater (Figure 3, $p<0.05$). Specifically, within 2 hours from the treatment, S was increased by 522% ($p<0.05$) in $SKIN_{MENT}$ and by only 110% ($p<0.05$) in $SKIN_{CON,}$ while M was increased by 11% ($p<0.05$) in $SKIN_{MENT}$ and by only 3% ($p<0.05$) in $SKIN_{CON}$. Within 7 hours from the treatment, S was increased by 700% ($p<0.05$) in $SKIN_{MENT}$ and by only 160% ($p<0.05$) in $SKIN_{CON,}$ while M was increased by 18% ($p<0.05$) in $SKIN_{MENT}$ and by only 6.7% ($p<0.05$) in $SKIN_{CON}$. Within 1 hour after the treatment, the RER was reduced in both $SKIN_{MENT}$ (4.8% reduction, $p<0.05$) and $SKIN_{CON}$ (7% reduction, $p<0.05$); the latter reduction being significantly greater (Figure 3, $p<0.05$).

Plasma hormones concentration

Mann-Whitney U tests showed that leptin ($p<0.05$) but not adiponectin or leptin/adiponectin ratio ($p>0.05$), was significantly different between groups for the same treatment. $ORAL_{MENT}$ (5.5 ± 1.2 ng/mL at baseline vs. 3.6 ± 0.5 ng/mL at 1-hour) and $ORAL_{CON}$ (4.5 ± 0.7 ng/mL at baseline vs. 2.7 ± 0.3 ng/mL at 1-hour) resulted in a significant decrease of leptin within 1 hour ($p<0.05$), while $SKIN_{MENT}$ (2.9 ± 1.27 ng/mL at baseline vs. 1 ± 0.3 ng/mL at 6-hours) and $SKIN_{CON}$ (1.4 ± 0.4 ng/mL at baseline vs. 1 ± 0.3 ng/mL at 6-hours) demonstrated significant reductions in leptin within 6 hours ($p<0.05$).

Autonomic modulation

Results from Mann-Whitney U and Wilcoxon Signed-Rank tests indicated that the analysed HRV indices from the frequency, time and nonlinear domains were not significant different between groups for the same treatment and between treatments within the same group, showing a similar trend in $ORAL_{MENT}$, $ORAL_{CON}$, $SKIN_{MENT}$ and $SKIN_{CON}$ without any significant variation throughout the entire assessment period ($p>0.05$).

Thermal comfort and sensation response

Mann-Whitney U test indicated that responses in thermal comfort and sensation were significant different between groups for the same treatment (i.e., $ORAL_{MENT}$ vs. $SKIN_{MENT}$ and $ORAL_{CON}$ vs. $SKIN_{CON}$) (Figure 4, $p<0.05$).

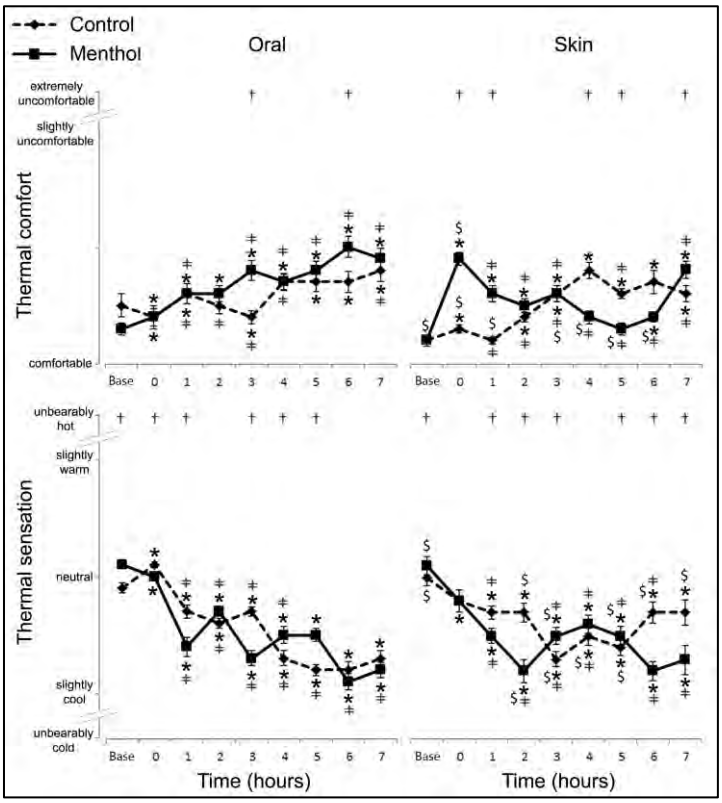

Figure 4: *Results (mean ± SEM) and comparisons for thermal comfort and sensation at baseline (Base) and for 7 hours after oral and skin treatments. Note: * = significant differences from baseline within the same treatment (Wilcoxon Signed-Rank tests; p<0.05); ǂ = significant differences from the previous time-point within the same treatment (Wilcoxon Signed-Rank tests; p<0.05); † = significant differences between control and L-menthol treatments within the same group for the same time-point (Wilcoxon Signed-Rank tests; p<0.05); Ṣ = significant differences between SKIN vs. ORAL group for the same treatment and time-point (Mann-Whitney U tests; p<0.05).*

Thermal comfort response showed significant differences between $ORAL_{MENT}$ and $ORAL_{CON}$ (Figure 4, $p<0.05$). Indeed, within 3 hours from the treatment, the participants in $ORAL_{MENT}$ reported being more uncomfortable than in $ORAL_{CON}$ (Figure 4, $p<0.05$). On the other hand, thermal sensation response showed no significant difference between $ORAL_{MENT}$ and $ORAL_{CON}$ (Figure 4, $p>0.05$).

Thermal comfort response showed no significant difference between $SKIN_{MENT}$ and $SKIN_{CON}$ (Figure 4, $p>0.05$). However, immediately after the treatment (at time 0, $p<0.05$) participants in $SKIN_{MENT}$ reported being more uncomfortable than during $SKIN_{CON}$ (Figure 4, $p<0.05$). Within 4 hours following treatment in $SKIN_{MENT}$ the thermal comfort response returned to baseline (i.e., “comfortable”; Figure 4, $p>0.05$). Thermal sensation response showed significant difference between $SKIN_{MENT}$ and $SKIN_{CON}$ (Figure 4, $p<0.05$). Specifically, within 1 hour after the treatment ($p<0.05$), participants in $SKIN_{MENT}$ reported being cooler than in $SKIN_{CON}$ (Figure 4, $p<0.05$).

All participants reported no stress, discomfort or shivering during the entire assessment period. Moreover, participants in $SKIN_{MENT}$ perceived no skin irritation after the treatment administration and for at least 7 days past the test day.

DISCUSSION

This is the first study aiming to assess and compare the absorption and metabolism pharmacokinetics of a single L-menthol oral versus skin administration and investigate their effects on thermogenesis and metabolic rate in men and women. We found that a single skin L-menthol administration can increase thermogenesis and metabolic rate in humans while these effects are minor following a single oral L-menthol administration.

Our novel findings show that the administration of L-menthol through the skin (i.e., gel) leads to very low absorption in the body. Indeed, the total L-menthol following $SKIN_{MENT}$ represented 6% of that observed following $ORAL_{MENT}$. Nevertheless, when administered through the skin, the metabolism of L-menthol was very slow, as indicated by the low menthol glucuronide concentration within 1 and 6 hours following administration. This slow metabolism of L-menthol when administered through the skin may explain the reduced heat loss (as seen through attenuated skin blood flow and mean skin temperature) and augmented thermogenesis (as seen through metabolic rate) which, in turn, lead to increased body heat storage and rectal temperature. Moreover, L-menthol administration through the skin (i.e., gel), but not through the gastrointestinal tract (i.e., capsule), results in a greater RER – corresponding to an increased carbohydrate oxidation compared to the control condition – within 1 hour.

Administration of L-menthol through the gastrointestinal tract leads to a very high absorption in the body. Indeed, the total L-menthol observed following $ORAL_{MENT}$ was ~16 times higher than that observed following $SKIN_{MENT}$. Nevertheless, when administered through the gastrointestinal tract, the metabolism of L-menthol was very fast, as indicated by higher menthol glucuronide concentration within 1 and 2 hours following oral administration compared to the skin. L-menthol levels following oral administration were similar to that following skin administration, therefore the very high menthol glucuronide concentration observed when L-menthol was administered through the gastrointestinal tract may explain the minor effects observed in heat loss attenuation and thermogenesis following administration. Our findings on the high metabolism of L-menthol when administered through the gastrointestinal tract are in line with previous studies (Gelal et al. 1999; Hiki et al. 2011) reporting that L-menthol gastrointestinal absorption results in low (or undetectable) levels of L-menthol and high levels of menthol glucuronide in the blood. Interestingly, we found that the peak of menthol glucuronide concentration in

the blood (1-2 hours after the L-menthol capsule ingestion) corresponded to a strong reduction in metabolic rate compared to the control condition and L-menthol gel application, suggesting an inhibitory effect on metabolism by the menthol glucuronide and/or glucuronidation process. Altogether these results suggest that L-menthol concentration in the blood should be high enough, without the interference of its glucuronide form, to activate an unknown mechanism which augments carbohydrate oxidation and thermogenesis.

The overall increase in energy expenditure – as measured by the gain in metabolic rate – after the L-menthol gel application is in accordance with the results of a previous in vitro study which reported that L-menthol induces an increase in glucose uptake and heat production in human white adipocytes (Rossato et al. 2014). Moreover, in accordance with previous studies, our analysis shows that a single application of L-menthol gel resulted in a significant decrease in skin blood flow (Yosipovitch et al. 1996; Olive et al. 2010; Topp et al. 2011; Gillis et al. 2015) and mean skin temperature (Yosipovitch et al. 1996; Olive et al. 2010; Topp et al. 2011) as well as in a significant increase in rectal temperature (Gillis et al. 2015). In contrast to our results, the latter study reported no effects of a single L-menthol skin spray solution on mean skin temperature and mean body temperature (Gillis et al. 2015). This may be explained by the lower L-menthol concentration (about 1/3 of that used in our experiment) as well as the thermometrically-derived calculation of mean body temperature used in the study by Gillis et al. (2015).

Our data indicate that L-menthol capsule ingestion caused a decrease in skin blood flow and mean skin temperature, unlike a previous study which reported no such effects after the ingestion of 10 mg L-menthol (Gelal et al. 1999). These contradictory results may be explained by the difference in L-menthol dosage. For instance, in the previous oral administration study, the lower L-menthol dose administrated (which resulted in undetectable blood L-menthol levels due to its rapid

conversion in the glucuronide form) could have suppressed the effect on skin blood flow and mean skin temperature (Gelal et al. 1999).

Since BAT activation was not assessed in the present analysis, the observed L-menthol gel application effect in increasing human thermogenesis and metabolic rate could not be certainly attributed to the activation of UCP1 mediated by blood L-menthol as reported in previous animal studies (Tajino et al. 2007; Ma et al. 2012). In our study, participants rested and fasted for the entire assessment period in a thermoneutral environment. Thus, considering the absence of physical activity, diet-induced thermogenesis or shivering, it seems reasonable to suggest that the gain in thermogenesis after L-menthol gel application, may be mediated by non-shivering thermogenesis. Specifically, our results suggest that the increase in body heat storage observed within the first 2 hours after skin L-menthol administration resulted from both the increase in metabolic rate and attenuation in cutaneous vasoconstriction which is due to mainly for the resting and fasting condition in a thermoneutral environment, as similar results were also observed after the control conditions. Thereafter, the further increase in body heat storage was primarily due to an increase in metabolic rate since no further reduction in cutaneous vasoconstriction was observed. Nevertheless, further analysis should clarify the involvement of BAT activity in increasing body temperature and metabolism in humans after a single L-menthol gel application as well as evaluate if a daily application may lead to a reduction of body weight and adiposity levels in humans. Moreover, as the capsule ingestion resulted in a very high L-menthol absorption but the increased menthol glucuronide interfered with the effects of L-menthol on metabolism activation, it would be interesting to use an inhibitory mechanism for the conversion of L-menthol in its glucuronide form and then evaluate the efficacy of ingestible L-menthol on thermogenesis and metabolism.

An animal study reported that daily oral L-menthol administration in mice increases insulin sensitivity (Ma et al. 2012). Moreover, human studies reported that

there is high correlation between insulin sensitivity and leptin/adiponectin ratio in both adults and children with a lower leptin/adiponectin ratio corresponding to higher insulin sensitivity (Hung et al. 2006; Finucane et al. 2009; Oberhauser et al. 2012). The present study showed that a single L-menthol oral or skin administration does not have effect on the levels of leptin, adiponectin or leptin/adiponectin ratio in the blood. Indeed, the decrease of leptin after either L-menthol gel or capsule administration was probably caused by the fasting condition during the entire assessment period which, in turns, resulted in the increase of participants' hunger, as similar results were also observed after the control conditions. In this light, it is worth mentioning that the prolonged fasting could have interfered in part with the L-menthol administration and therefore, besides explaining some of the observed results (i.e., decrease of leptin), may have masked part of L-menthol effects. Thus, further studies should analyse a long term effect after daily L-menthol gel and capsule administration on insulin and carbohydrate metabolism in humans.

Menthol products have shown different healthy physiological effects. They have been successfully used for many decades as a natural analgesic gel for pain (Fang et al. 2008) and as an oral treatment for disinfection (Iscan et al. 2002). Both oral and skin L-menthol administration were very well tolerated by the participants as thermal comfort and sensation ranged from "comfortable" to "slightly uncomfortable" and from "neutral" to "slightly cool", respectively. Moreover, participants reported no discomfort, shivering, skin irritation, or stress (which was evident also from the unchanged HRV indices) throughout the assessment period. A previous study reported that half of the participants sprayed with an L-menthol solution perceived skin irritation, indicating that a cream solution may be more appropriate as well as that there may be large inter-individual variation in the perception of irritation after a single skin L-menthol application (Gillis et al. 2015). The current results showed no apparent detrimental cardiovascular effects (as evidenced by stable heart rate variability recordings) after a single dose of 10 $mg \cdot kg^{-1}$ body weight of L-menthol

which, in contrast, are evident following specific drugs that also boost metabolic rate (Cypess et al. 2012; Vosselman et al. 2012; Carey et al. 2013; Cypess et al. 2015). Finally, it is important to note that very small differences at baseline between treatments which were deemed as statistically significant by our statistical analysis (e.g., a 0.1°C difference in T_{re} between $ORAL_{MENT}$ and $ORAL_{CON}$) are of no physiological significance as they are within the normal day-to-day variation. Therefore, these differences are not considered in the context of this study's findings. On the other hand, consistent differences in rectal temperature as high as 0.23 °C within 2 hours that cannot be explained by factors other than L-menthol treatment are of major physiological significance.

In conclusion, we show that a single administration of L-menthol via a gel cream increased thermogenesis and metabolic rate in humans. These effects are minor following oral L-menthol administration probably due to a faster metabolism of L-menthol (i.e., glucuronidation process) that occurs when the molecule is absorbed through the gastrointestinal tract leading to higher menthol glucuronide concentration following the oral administration compared to the skin. Considering the tolerability of a single L-menthol administration, future chronic studies are necessary to confirm L-menthol as promising candidate treatment for human cardio-metabolic diseases.

ACKNOWLEDGMENTS

The authors report no financial or personal relationships with other people or organisations that could inappropriately influence (bias) their actions. This work was supported by funding from the Education and Lifelong Learning Programme of the Greek Ministry of Education, Co-financed by Greece and the European Union (NSRF 2007-2013, IRAKLITOS II, grant no. 162), and the European Union 7th Framework Program (FP7-PEOPLE-2013-IRSES grant no. 612547).

CHAPTER 4

Daily L-menthol skin administration effects on metabolism, body composition and white adipose tissue plasticity

Angelica Valente,[1,2] Petros C. Dinas,[3] Marnie Granzotto,[4] Natalie A. Davies,[5] Andres E. Carrillo,[5] Marco Rossato,[4] Roberto Vettor,[4] Athanasios Z. Jamurtas,[6] and Andreas D. Flouris[1,7]

ADDRESS FOR CORRESPONDENCE:

Andreas D. Flouris

FAME Laboratory

Department of Exercise Science

University of Thessaly

Karies, Trikala, 42100, Greece.

email: andreasflouris@gmail.com

Tel: +302431500601, Fax: +302431063191

[1]FAME Laboratory, Department of Exercise Science, University of Thessaly, Trikala, Greece.

[2]Department of Human Physiology, Vrije Universiteit Brussel, Brussels, Belgium.

[3]Institute of Sport, Faculty of Education Health and Wellbeing, University of Wolverhampton, Walsall, West Midlands, WS1 3BD, UK

[4]Department of Medicine – DIMED, Internal Medicine 3, University of Padova, Italy.

[5]Department of Exercise Science, Chatham University, Pittsburgh, PA 15232, USA.

[6]School of Physical Education and Exercise Science, University of Thessaly, Greece.

[7]Human and Environmental Physiological Research Unit, University of Ottawa, Ontario, Canada.

ABSTRACT

We analysed, for the first time, the effect and dose-dependent effect, of 1-month daily L-menthol cream administration on metabolism, body composition, and white adipose tissue plasticity in humans. Twenty-one healthy volunteers (33.8 ± 6.3 years, 26.1 ± 3.5 kg·m2 body mass index, 23.4 ± 8.9 body fat percentage) were randomly placed in the control (0 mg·kg-1 body weight of L-menthol crystals), low L-menthol concentration (10 mg·kg-1 body weight of L-menthol crystals) or high L-menthol concentration (20 mg·kg-1 body weight of L-menthol crystals) group and they were asked to apply on the skin surface of their legs, arms, neck, chest and belly, the L-menthol or control creams once a day for 30 days. Physical activity, dietary nutrient intake, thermal comfort and sensation were recorded three days/week while analysis of resting metabolic rate, heart rate variability, and body composition, as well as abdominal skin and subcutaneous adipocytes biopsies were performed at baseline and one day after the last application. Daily application of either lower or higher L-menthol creams showed no effect on body composition, metabolism and white adipose tissue plasticity. The increase of adiponectin in white adipocytes could indicate that a process for increasing metabolism may have started with no changes in body composition and metabolism maybe due to the short period. Further analysis on protein expression and activity of factors involved in metabolism and white adipose tissue plasticity as well as on human cold-sensitive gating receptors are essential to clarify the effect of L-menthol on human metabolism and thermogenesis.

KEYWORDS: brown adipose tissue; brite adipocytes; non-shivering thermogenesis; obesity; TRPM8; TRPA1; sodium intake.

INTRODUCTION

White, brown and brown-like (“brite”) cells represent the three different kinds of adipocytes in mammals. White adipocytes play a role in storing energy while brown and brite adipocytes are involved in heat production, showing metabolic capabilities and potential for increasing energy expenditure through the activation of a mitochondrial inner membrane protein, uncoupling protein 1 (UCP1) (Inokuma et al. 2006; Feldmann et al. 2009; Mattson 2010; Valente et al. 2014). A systematic analysis from our group suggests that frequent stimulation of UCP1 in mammal brown and brite adipocytes results in an increase of basal metabolic rate and a reduction of adiposity levels in rodents (Inokuma et al. 2006; Yamashita et al. 2008; Feldmann et al. 2009; Yoneshiro et al. 2013; Valente et al. 2014). Animal studies identified L-menthol as an activator of UCP1 in rodent brown adipocytes through the stimulation of the transient receptor potential melastatin 8 ion channel (TRPM8) which is the principal sensor of thermal stimuli in the peripheral nervous system (Romanovsky 2007; Tajino et al. 2007; Flouris 2011; Tajino et al. 2011; Ma et al. 2012; Valente et al. 2014). TRPM8 is predominantly located on the cell membrane of sensory neurons while its expression has also been recently discovered on the membrane of brown and white adipocytes (Wang and Woolf 2005; Bautista et al. 2007; Colburn et al. 2007; Dhaka et al. 2007; Tajino et al. 2011; Ma et al. 2012; Rossato et al. 2014). It seems that alternative mRNA splicing of this receptor is an important regulatory process for its activity as shorter isoforms (TRPM8α and TRPM8β, reported here as TRPM8-S) of the full-length TRPM8 (reported here as TRPM8-L) are translated in a non-functional ion channel receptor (Bidaux et al. 2012; Fernandez et al. 2012).

Animal studies report that a single L-menthol skin application on the whole trunk in mice induces heat production and a rise in core temperature through skin

vasoconstriction, muscle shivering, and UCP1 activity in brown adipocytes (Tajino et al. 2007). Moreover, a 7-month dietary L-menthol administration in mice increases core temperature, UCP1 expression and activity in BAT, and insulin sensitivity leading to attenuated body weight gain (Ma et al. 2012).

Our recent work indicates that a single administration of L-menthol via a gel cream increased thermogenesis and metabolic rate in humans maybe through UCP1 activation (Valente et al. 2015). However, these effects are minor following oral L-menthol administration probably due to a faster metabolism of L-menthol (i.e., glucuronidation process) that occurs when the molecule is absorbed through the gastrointestinal tract leading to higher menthol glucuronide concentration following the oral administration compared to the skin (Hiki et al. 2011; Valente et al. 2015). Moreover, an in vitro study on human white adipocytes reported that L-menthol induces UCP1 expression and activation in white adipose tissue, and increases glucose uptake and heat production (Rossato et al. 2014). Altogether, these findings suggest a possible role for L-menthol in controlling energy metabolism and energy balance in humans, although, chronic studies are necessary to confirm L-menthol as promising candidate treatment for human metabolic diseases.

The purpose of the present work is to analyse, for the first time, the effect of 1-month daily L-menthol cream administration on metabolism, body composition, and white adipose tissue plasticity in humans. We also tested the eventual L-menthol dose-dependent effect using lower and higher L-menthol concentration creams. Based on the aforementioned results of L-menthol effects in boosting human and rodent metabolism (Tajino et al. 2007; Ma et al. 2012; Valente et al. 2014; Valente et al. 2015), we hypothesized that 1-month daily L-menthol cream administration would increase human metabolism, decrease body weight and adiposity. Moreover, considering that L-menthol stimulates UCP1 in human white adipocytes (Rossato et al. 2014), we also hypothesized that daily L-menthol cream administration would

stimulate subcutaneous adipose tissue plasticity with UCP1 expression increased in subcutaneous white adipocytes.

METHODS

Participants

The study conformed to the standards set by the Declaration of Helsinki and was approved by the University of Thessaly Department of Exercise Science Ethics Committee. A minimum required sample size of 6 participants per group was determined (statistical power: 0.95; α error probability: 0.05) based on body fat mass calculated before (11.7 ± 0.7 Kg) and after (10.9 ± 0.35 Kg) 6 weeks of cold exposure in a previous published study (Yoneshiro et al. 2013). Thus, 21 sedentary male healthy volunteers [33.8 ± 6.3 years, 26.1 ± 3.5 $kg \cdot m^2$ body mass index (BMI), 23.4 ± 8.9 body fat percentage] were recruited for this study. Exclusion criteria included smoking, use of any medication, history or presence of metabolic, cardiac or pulmonary disease, thyroid or thermoregulatory disorders. Participants were informed about all experimental procedures, associated risks and discomforts and were asked to provide written informed consent.

Volunteers were randomly placed into the control (0 $mg \cdot kg^{-1}$ body weight of L-menthol crystals, CON), low L-menthol concentration (10 $mg \cdot kg^{-1}$ body weight of L-menthol crystals, LM) or high L-menthol concentration (20 $mg \cdot kg^{-1}$ body weight of L-menthol crystals, HM) group, each consisting of 7 participants. No differences in age (CON: 34.9 ± 8.4 years; LM: 33.9 ± 3.3 years; HM: 32.7 ± 6.9 years), body mass (CON: 79 ± 13.5 Kg; LM: 86.7 ± 13.7 Kg; HM: 85.1 ± 13.4 Kg), BMI (CON: 25.4 ± 4.7 $Kg \cdot m^2$; LM: 26.8 ± 2.9 $Kg \cdot m^2$; HM: 26.1 ± 3.1 $Kg \cdot m^2$), or body fat percentage (CON: 22.6 ± 9.1 %; LM: 23.6 ± 8.1 %; HM: 23.9 ± 10.6 %), were detected among the tree groups (mean ± SD, $p>0.05$).

Cream preparation and research design

Participants were asked to apply on the skin surface of their legs, arms, neck, chest and belly, the L-menthol or control creams once a day between 7:00 and 9:00 am for a total of 30 days. For an equal daily L-menthol distribution on the three areas of the body cream application (legs, arms, and neck-chest-belly), the total relative amount of L-menthol crystals (natural L-menthol FU-BP-USP; A.C.E.F. spa, Fiorenzuola d'Arda, Italy) was equally split and mixed in three cans cream containing each 10% of urea and 5 gr of base cream which composed by vaseline, olive oil, soy oil, avocado oil, macadamia oil, evening primrose oil and jojoba oil (A.C.E.F. spa, Fiorenzuola d'Arda, Italy). Control creams were composed by the base cream to which was added only 10% of urea. Thus, all participants received one little container of cream per day for legs, arms, and neck-chest-belly respectively, for a total of ninety containers cream which were kept in the refrigerator at 6-7 °C until use.

Due to the strong smell of menthol, a double-blind design was adopted only in terms of L-menthol crystals concentration used to prepare the cream. All participants (including those in CON) as well as the researchers who performed dietary nutrient intake analysis, abdominal skin and subcutaneous adipose tissue biopsies, and gene expression analysis (described in the following paragraphs) were not informed about the L-menthol crystals concentration contained in the cream of each group (i.e., 0, low or high concentration).

Experimental procedures

The experimental protocol consisted of 1 week of baseline (from day -7 to day -1) following by 4 weeks of daily cream application (from day 0 to day 29) during which, all participants were asked to maintain their physical activity and dietary nutrient intake (food and beverage) as before the experimental period. During both baseline and each week of the cream application period, physical activity and dietary nutrient

intake were assessed using a pedometer (Digi-Walker SW–200, Yamax, United Kingdom) and a 24h diet recall interview, respectively, to eliminate the eventual impact on changes in metabolism and body composition. Participants were instructed to wear the pedometer on the right hip-pants, use it every day during the entire experimental period (baseline week and following 4 weeks of cream application) and remove it only for sleep and shower. To minimize the potential for changes in physical activity or eating, participants were blinded to the telephone recall schedule which was set for randomly three days/week (two week days and one weekend day) for the all experimental period.

Measurements were performed on both day -4 (baseline week) and day 30 (one day after the last cream application) and participants were asked to abstain from alcohol, caffeine, and environmental tobacco smoke, to avoid any physical or mental stress and extreme temperature environments for 24-hour prior to each measurement day. Both measurement days all participants were transported to the laboratory via car to avoid excessive stressors between wake-up time and arrival at the laboratory. They reported to the laboratory (which was maintained at 23.1 ± 0.9 °C and 35.8 ± 3.4 % relative humidity) 30 min after waking (between 06:00 h and 07:30 h) and after 12-hour overnight fast. Then, measurements of resting metabolic rate, HRV, body mass, height, body mass index, body fat percentage as well as subcutaneous adipose tissue biopsies (described in the following paragraphs) were performed at the same hour of the day and by the same trained researchers using identical pre-calibrated equipment.

Dietary nutrient intake analysis

All recorded food and beverages consumption were analyzed by one trained investigator using Nutritionist Pro, Version 5.4.0, Axxya Systems (Redmond, WA, USA). This software (i.e. Nutritionist Pro) has been previously used for research purposes (Michaliszyn et al. 2009; Stuempfle et al. 2013). For the analysis, a search

was conducted in Nutritionist Pro for each food and beverage consumed. Details regarding the amount and preparation of each food and/or beverage were also included. Once all the relevant information regarding the food or beverage was entered into the software, a corresponding list of macro and micronutrient content was provided and subsequently saved. This process was repeated for all food and beverages listed on the diet record. If a particular food or beverage was not found within the Nutritionist Pro database, the investigator manually entered the macro and micronutrient content of that particular food and saved it to the database for future use. The feedback provided by the software for each food or beverage included the following dietary variables: weight (g), kilocalories (kcal), protein (g), carbohydrate (g), total fat (g), alcohol (g), cholesterol (mg), saturated fat (g), monounsaturated fat (g), polyunsaturated fat (g), oleic acid (g), linoleic acid (g), linolenic acid (g), eicosapentaenoic acid (g), docosahexaenoic acid (g), trans fatty acid (g), sodium (mg), potassium (mg), vitamin A (IU), beta-carotene (μg), alpha-carotene (μg), lutein (+ zeaxanthin) (μg), beta-cryptoxanthin (μg), lycopene (μg), vitamin C (mg), calcium (mg), iron (mg), vitamin D (IU), vitamin E (IU), alpha-tocopherol (mg), thiamin (mg), riboflavin (mg), niacin (mg), pyridoxine (mg), total folate (μg), folate (DFE) (μg), cobalamin (μg), biotin (μg), pantothenic acid (mg), vitamin K (μg), phosphorus (mg), iodine (μg), magnesium (mg), zinc (mg), copper (mg), manganese (mg), selenium (μg), fluoride (μg), chromium (mg), molybdenum (μg), total dietary fiber (g), soluble fiber (g), insoluble fiber (g), crude fiber (g), total sugar (g), glucose (g), galactose (g), fructose (g), sucrose (g), lactose (g), maltose (g), sugar alcohol (g), other carbohydrate (g), tryptophan (mg), threonine (mg), isoleucine (mg), leucine (mg), lysine (mg), methionine (mg), cysteine (mg), phenylalanine (mg), tyrosine (mg), valine (mg), arginine (mg), histidine (mg), alanine (mg), aspartic acid (mg), glutamic acid (mg), glycine (mg), proline (mg), serine (mg), moisture (g), ash (g), caffeine (mg). The data of three-day diet records were divided by 3 in order to obtain for each week average results for kilocalories and each nutrient expressed as daily intake.

Resting metabolic rate and body composition analyses

Resting metabolic rate was assessed to determine the effect of daily L-menthol cream application on metabolism. All measurements were conducted with participants in the supine position on a comfortable medical bed inside a semi-darkened, temperature-controlled room (23.1 ± 0.9 °C) with other distractions minimized. Participants were asked to refrain from sleeping and hyperventilating during the procedure. Breath-by-breath data were collected using an automated gas analyser (Vmax, CareFusion, USA) which was calibrated before each test using standard gases of known concentrations. Respiratory variables were recorded every 20 seconds for a total of 30 minutes data collection. The first and the last 5 minutes were excluded from the 30 minutes data collection to ensure participants' habituation and avoid over restless interference (Adriaens et al. 2003). Resting metabolic rate was expressed per 24-hour and calculated as the average value of the 20 minutes data collection.

Body weight and body fat percentage were assessed to determine the effect of daily L-menthol cream administration on body composition. All measurements were performed using bioelectrical impendence method with a body composition device (Fresenius Medical Care AG & Co. KGaA D-61346 Bad Homburg, Germany).

HRV analysis

To assess autonomic modulation, participants were outfitted with a heart rate chest strap and HRV was measured through short-range telemetry at 1,000 Hz with a Polar RS800CX (Polar Electro, Kempele, Finland). The heart rate monitor signal was transferred to the Polar Precision Performance Software (release 3.00; Polar Electro Oy), and RR intervals (time intervals between consecutive R waves in the electrocardiogram) were analysed in order to assess the modulation of sympathetic and parasympathetic activities as previously described (Flouris and Cheung 2009).

Frequency domain, time domain and nonlinear method analysis was performed using HRV software version 1.1 (Finland; Biomedical Signal Analysis Group, Department of Applied Physics, University of Kuopio, Finland 2002) evaluating the RR interval time series automatically obtained from the raw signals (Rajendra Acharya et al. 2006). The frequency domain with the low frequency, high frequency, and low frequency to high frequency ratio variables were analysed to discriminate between sympathetic and parasympathetic contribution to HRV. For the time domain method, both statistical and geometric parameters were considered for the analysis of Mean RR, Mean HR, standard deviation of RR and heart rate, the square root of the mean of squared differences between successive intervals, the percentage of the differences of successive normal-to-normal intervals 50 ms normalized to all differences within the interval, the number of pairs of successive normal-to-normal that differ by more than 50 ms, the HRV triangular index, and the triangular interpolation of normal-to-normal interval histogram. Nonlinear method was used to analyse the standard deviation of fast and long term RR variability, mean line length, maximum line length, recurrence rate, determinism, Shannon Entropy, approximate entropy, sample entropy, Detrended Fluctuation Analysis α 1 and 2, and correlation dimension.

Abdominal dermis and subcutaneous adipose tissue biopsies

A non-diathermy method was used to obtained abdominal dermis and subcutaneous adipose tissue biopsies. Each participant was positioned on a surgical bed in a supine position. The spot of the incision was disinfected and a 10 ml of xylocaine 2%-no adrenaline was injected in the region of the incision for local anaesthesia. An incision on the dermis and subcutaneous tissue until adipose tissue was revealed, was executed approximately 3-5 cm on the right (on day -4) and symmetrically on the left (on day 30) from the navel. The incision length was approximately 2-2.5 cm. Subsequently, 50 mg of dermis and 500 mg of subcutaneous adipose tissue were

removed with an operating scissors. All samples were immediately frozen in liquid nitrogen and then stored at -80° C.

Gene expression analysis

Gene expression of Ucp1, Ppar-γ, Rald, Plac8, and Npra in white adipocytes was assessed to determine the effect of daily L-menthol cream application on white adipose tissue plasticity (Gray et al. 2006; Feldmann et al. 2009; Jimenez-Preitner et al. 2011; Kiefer et al. 2012; Valente et al. 2014). Gene expression of Pgc1-α, Cox IV, Leptin, Adiponectin, Ppar-α, Pgk1, Fabp3, and Glut4 in white adipocytes was assessed to determine the effect on metabolism activation in white adipose tissue (Virtanen et al. 2009; Bostrom et al. 2012; Vaughan et al. 2014). Gene expression of Trpm8-L and Trpm8-S in dermis was assessed to determine the levels of the functional receptor that could be activated by L-menthol and also eventual body adaptation to the daily application (Bidaux et al. 2012). Thus, total RNA was extracted from abdominal dermis and adipose tissue biopsies using RNeasy Lipid Tissue mini kit (QIAGEN) and ReliaPrep RNA Tissue Miniprep Systems (PROMEGA) respectively and following the manufacturer's protocol. First-strand cDNAs were synthetized from equal amounts of total RNA using random primers and M-MLV reverse trascriptase (Promega). Quantitative real time PCR was performed using Sybr Green fluorofore. The change in fluorescence at every cycle was monitored and a threshold cycle above background for each reaction was calculated. A melt curve analysis was performed following every run to ensure a single amplified product for every reaction. All reactions were carried duplicates for every sample. 18S rRNA or RPL0 genes were constantly expressed under all experimental conditions and was then used as a reference gene for normalization.

Thermal comfort and sensation

During the 4-week cream application, participants were frequently asked to report any kind of stress, discomfort or skin irritation as well as they were randomly asked 3 days/week to indicate a number for thermal comfort and thermal sensation for each body area of the cream application (arms, legs, and neck-chest-belly) using previously published scales (Gagge et al. 1969). The range of the thermal comfort scale was from 1 through 5, where 1 = “comfortable”, 2 = “slightly uncomfortable”, 3 = “uncomfortable”, 4 = “very uncomfortable”, 5 = “extremely uncomfortable”. The range of the thermal sensation scale was from 0 through 10, where 0 = “unbearably cold”, 1 = “very cold”, 2 = “cold”, 3 = “cool”, 4 = “slightly cool”, 5 = “neutral”, 6 = “slightly warm”, 7 = “warm”, 8 = “hot”, 9 = “very hot”, 10 = “unbearably hot”.

Statistical analysis

All dependent variables showed a non-normal distribution therefore non-parametric tests were used throughout. Mann–Whitney U tests were used for the comparisons between groups (i.e., CON vs LM; CON vs HM; LM vs HM) at the same time measurements. Wilcoxon Signed-Rank tests were used to compare values between baseline and day 30 within the same group. Moreover, for week-recording variables (diet nutrient intake, number of steps, thermal comfort and sensation), Wilcoxon Signed-Rank tests were used for the comparisons within the same group between baseline and each following week, between consecutive weeks as well as between baseline and the average of 4-week treatment period. All analyses were conducted with SPSS Statistics (version 19; SPSS Inc., Chicago, IL, USA). The data are reported as mean ± SD and p-values < 0.05 were regarded as statistically significant.

RESULTS

Physical activity and diet nutrient intake

At baseline, steps/day were similar between groups (Figure 1-A; $p>0.05$). During the 4-week cream application, steps/day did not change from baseline in CON, LM, and HM ($p>0.05$), showing similar levels of physical activity between groups (Figure 1-A; $p>0.05$). However, during the last week of cream application (week 4), steps/day significantly increased from the baseline in LM (Figure 1-A; $p<0.05$).

At baseline, the daily intake of kilocalories, total fat, protein, carbohydrate, maltose, sodium, vitamin D and E was similar between CON and LM ($p>0.05$) as well as between CON and HM (Figure 1 – B, C, D, E, F, H, I, L; $p>0.05$). During the baseline week, the daily intake of galactose was lower in LM compared to CON (Figure 1 – G; $p<0.05$); the daily intake of kilocalories, total fat and protein was lower in LM compared to HM (Figure 1 – B, C, D; $p<0.05$). During the cream application period (from week 1 to week 4), kilocalories and protein daily intake increased from baseline only in CON (Figure 1 – B and D; $p<0.05$), while maltose, galactose and sodium daily intake increased from baseline only in LM (Figure 1 – F, G, H; $p<0.05$). On the other hand, the daily intakes of vitamin D and E decreased from baseline only in LM during week 4 and week 2 and 4, respectively (Figure 1 – I, L; $p<0.05$).

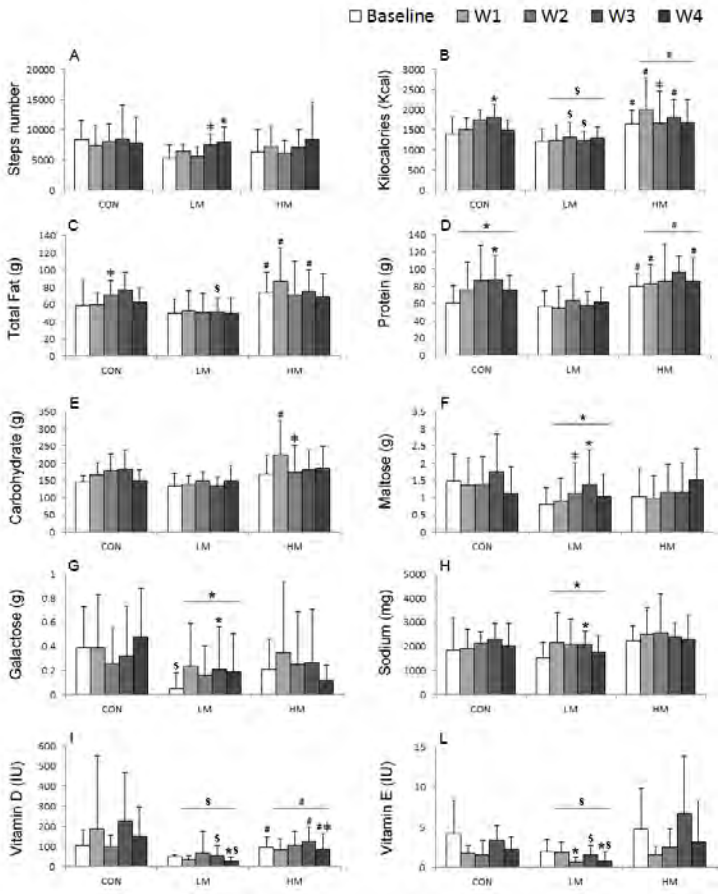

Figure 1. *Results (mean ± SD) of Steps number (A), Kilocalories (B), Total fat (C), Protein (D), Carbohydrate (E), Maltose (F), Galactose (G), Sodium (H), Vitamin D (I), and Vitamin E (L), at baseline and the following week 1, 2, 3, and 4 of the cream application period in CON (0 mg·kg^{-1} body weight of L-menthol crystals), LM (10 mg·kg^{-1} body weight of L-menthol crystals), and HM (20 mg·kg^{-1} body weight of L-menthol crystals) groups. Note: * = significant differences from baseline within the same group; ǂ = significant differences from the previous week within the same group; $ = significant differences versus CON for the same week; # = significant differences HM vs LM for the same week; ——— = average of cream application period (from week 1 to week 4).*

Moreover, kilocalories and vitamin D daily intake during the cream application period (average from week 1 to week 4) in LM was lower compared to those in HM and CON (Figure 1 – B, I; $p<0.05$) as well as protein and vitamin E daily intake in LM was lower compared to those in HM and CON, respectively (Figure 1 – D, L; $p<0.05$).

The daily intake of all the other analysed nutrients was not significant different among groups at both baseline and day 30, showing any significant variation from baseline throughout the entire cream application period in CON, LM, or HM (from week 1 to week 4) ($p>0.05$).

Body composition, body weight and RMR

Table 1 shows that at baseline, BW, BMI, body fat %, RER, but not REE ($p<0.05$), were similar between groups ($p>0.05$). REE was significantly higher in LM and HM compared to CON ($p<0.05$) showing, however, similar levels between LM and HL ($p>0.05$). BW, BMI, body fat %, REE, and RER were similar between baseline and day 30 in CON, LM, and HM ($p>0.05$), although RER in LM showed a light attenuation after 30 days of L-menthol cream application ($p>0.05$). Moreover, at day 30, BW, BMI, body fat %, REE, and RER were similar among groups ($p>0.05$).

Table 1. Daily L-menthol cream administration effects on body weight, body mass index, body fat percentage, resting metabolic rate, and respiratory exchange ratio.

Variable	CON		LM		HM	
	Baseline	day 30	Baseline	day 30	Baseline	day 30
BW (kg)	79.0±13.5	79.1±13.7	86.7±13.7	86.5±14.5	85.1±13.4	85.3±13.9
BMI (Kg·m^2)	25.5±4.7	25.5±4.7	26.8±2.8	26.7±2.9	26.2±3.1	26.2±3.3
Body fat (%)	22.6±9.1	22.5±9.0	23.6±8.1	23.7±7.3	24.0±10.6	23.1±10.9
RMR (Kcal)	1411.6±188.8	1588.7±285.8	1801.1±265.0$^{\$}$	1897.3±311.7	1717.5±93.5$^{\$}$	1761.8±97.7
RER	0.81±0.07	0.83±0.07	0.81±0.04	0.78±0.09	0.78±0.05	0.80±0.09

Note:); $ = significant differences vs. CON group for the same time-point (Mann-Whitney U tests; $p<0.05$).
Key: CON = control group (0 mg·kg^{-1} body weight of L-menthol crystals); LM = low L-menthol concentration group (10 mg·kg-1 body weight of L-menthol crystals); HM = high L-menthol concentration group (20 mg·kg-1 body weight of L-menthol crystals); BW = body weight; BMI = body mass index; RMR = resting metabolic rate; RER = respiratory exchange ratio.

Autonomic modulation

HRV indices from the frequency, time and nonlinear domains were not significant different among groups at both baseline and day 30, showing a similar trend in CON, LM, and HM without any significant variation from baseline throughout the entire experimental period (from week 1 to week 4) ($p>0.05$).

Abdominal dermis and subcutaneous adipose tissue gene expression

Figure 2 show that the expression of Trpm8-L at both baseline and day 30 is significantly lower than that of Trpm8-S in both LM and HM groups, with the long and short isoforms representing ~1% and ~ 99% of the Trpm8 expressed in dermis, respectively. However, in both LM and HM groups the expression of Trpm8-L and

Trpm8-S isoforms did not change from baseline following 30 days of L-menthol cream application.

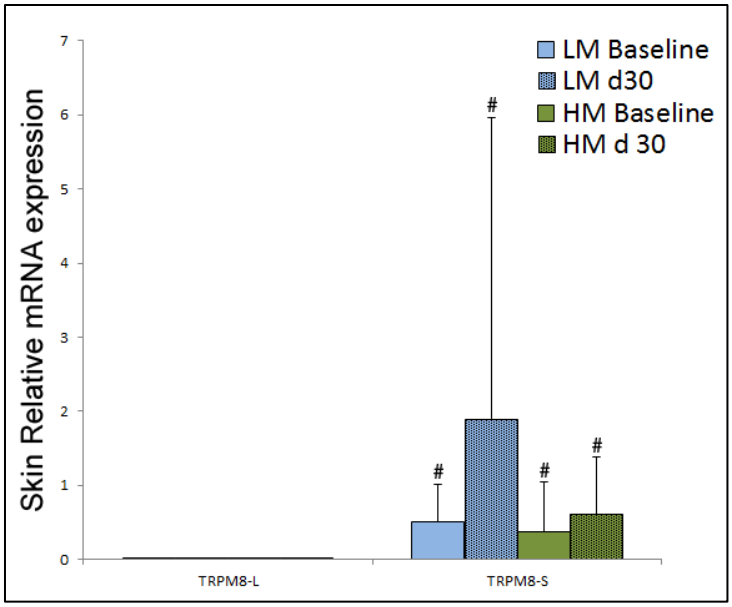

Figure 2: *Results (mean ± SD) of dermis relative mRNA expression of TRPM8-L (full-length functional isoform) and TRPM8-S (short non-functional TRPM8α and TRPM8β isoforms) at baseline and the day after the last cream application (day 30) in LM (10 mg·kg^{-1} body weight of L-menthol crystals) and HM (20 mg·kg^{-1} body weight of L-menthol crystals) groups. Note: # = significant differences for TRPM8-S versus TRPM8-L within the same group for the same time-point.*

Figure 3 show that the subcutaneous adipose tissue expression of Ucp1, Rald, Plac8, Npra, Pgc1-α, Cox IV, Ppar-γ, Leptin, Adiponectin, Ppar-α, Pgk1, Fabp3, Glut4, Trpm8-L at both baseline and day 30 was not different among CON, LM, and HM. Moreover, the expression level of all analysed genes was unchanged from baseline after 4 weeks of daily cream application in CON, LM, and HM, expect for Adiponectin in HM group. Indeed, Adiponectin increased following 4 weeks of daily L-menthol cream application only in HM group. Interestingly, the expression of Trpm8-S was not detectable in subcutaneous adipocytes, with TRPM8-L being the single isoform expressed in subcutaneous adipose tissue.

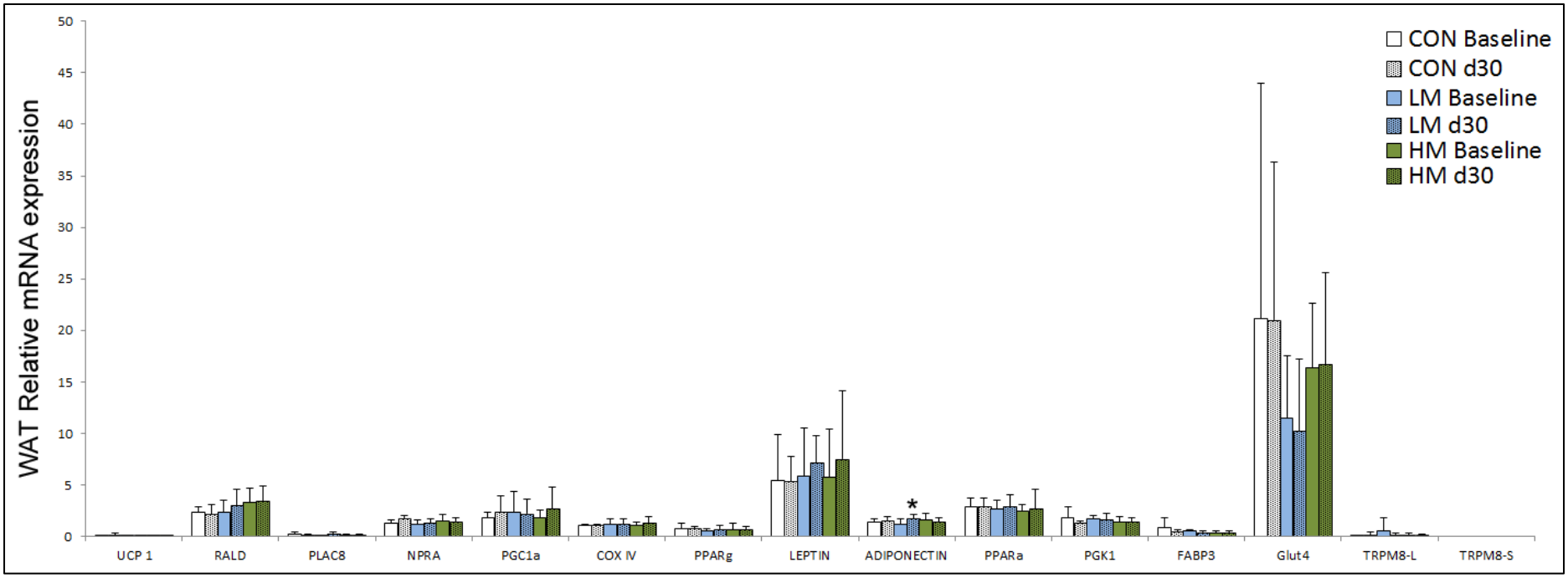

Figure 3: *Results (mean ± SD) of white adipose tissue relative mRNA expression of UCP1, RALD, PLAC8, NPRA, PGC1α, COX IV, PPARγ, Leptin, Adiponectin, PPARα, PGK1, FABP3, Glut4, TRPM8-L, and TRPM8-S, at baseline and the day after the last cream application (day 30) in CON (0 mg·kg^{-1} body weight of L-menthol crystals), LM (10 mg·kg^{-1} body weight of L-menthol crystals) and HM (20 mg·kg^{-1} body weight of L-menthol crystals) groups. Note: * = significant differences from baseline within the same group.*

Thermal comfort and sensation response

Thermal comfort response did not show significant differences among CON, HM, and LM ($p>0.05$) as well as among arms, legs or chest-belly body areas in each group (Figure 4, $p>0.05$). Indeed, participants in all groups reported being between slightly uncomfortable and uncomfortable throughout the entire cream application period (from week 1 to week 4) without any significant differences among arms, legs and chest-belly body areas ($p>0.05$).

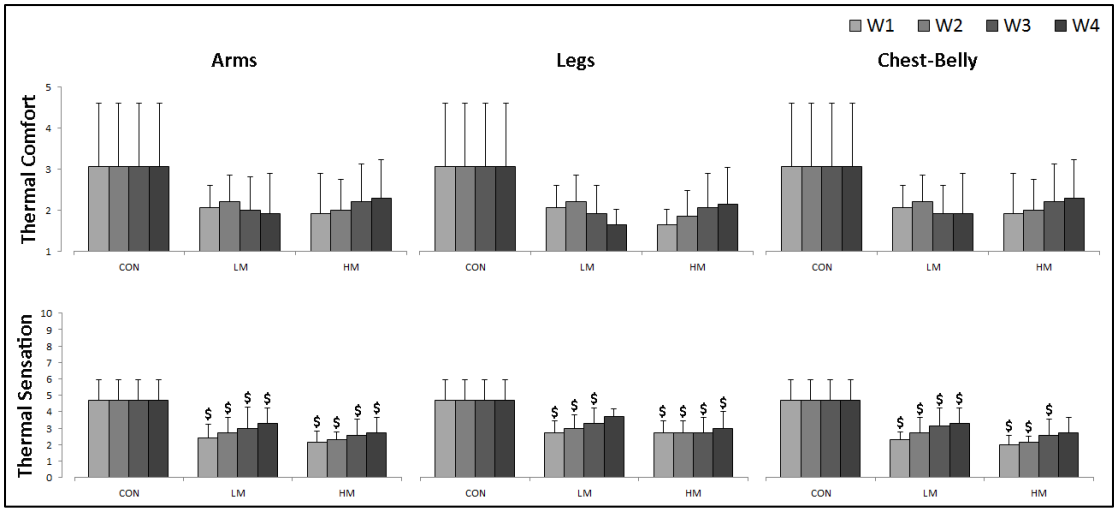

Figure 4: *Results (mean ± SD) of thermal comfort and sensation of arms, legs, and chest-belly at week 1, 2, 3, and 4 of the cream application period in CON (0 mg·kg^{-1} body weight of L-menthol crystals), LM (10 mg·kg^{-1} body weight of L-menthol crystals), and HM (20 mg·kg^{-1} body weight of L-menthol crystals) groups. Note: $ = significant differences versus CON for the same week.*

Thermal sensation response showed significant differences between CON and LM or HM for arms, legs and chest-belly body areas (Figure 4; $p<0.05$). Indeed, participants in CON reported being neutral while participants in both LM and HM reported similar sensation ($p>0.05$) between slightly cool and cold without any significant differences among arms, legs and chest-belly body areas ($p>0.05$).

All participants reported no stress, discomfort or skin irritation during the entire cream application period and for at least 7 days past the last cream application day.

DISCUSSION

This is the first study aiming to assess the effect of 1-month daily L-menthol skin administration on metabolism, body composition and subcutaneous white adipose tissue plasticity in humans. Also, we assessed the eventual L-menthol dose-dependent effect using lower (10 $mg \cdot kg^{-1}$ body weight of L-menthol crystals, LM) and higher (20 $mg \cdot kg^{-1}$ body weight of L-menthol crystals, HM) L-menthol concentration creams. We found that 1-month of daily application of either lower or higher L-menthol creams did not have an effect on metabolism, body composition and white adipose tissue plasticity in humans.

Our novel findings show that body weight, BMI, body fat percentage, resting metabolic rate and respiratory exchanged ratio did not change following 1-month of daily L-menthol cream application. Moreover, factors involved in the subcutaneous white adipose tissue plasticity (i.e, Ucp1, Ppar-γ, Rald, Plac8, Npra, and T3) as well as factors involved in metabolism activation (i.e, Pgc1-α, Cox IV, Leptin, Ppar-α, Pgk1, Fabp3, and Glut4) did not change their gene expression in subcutaneous white adipose tissue following 1-month of daily L-menthol cream application.

At baseline, the dermis of participants in both LM and HM groups expressed higher levels of the short isoform of Trpm8 compared to the long isoform. On the other hand, subcutaneous white adipocytes of LM, HM, and control groups expressed only the full-length isoform of Trpm8, with undetectable levels of the short isoforms. The full-length isoform of Trpm8 which is the only one that can be translated in a functional ion channel, represented ~1% and 100% of the Trpm8 expressed in dermis and subcutaneous adipose tissue, respectively. Thus, L-menthol cream applied on the skin may have stimulated only 1% of the TRPM8. A better stimulation of this receptor could have been achieved on the surface of white adipocytes after the absorption of L-menthol in the blood, although the following glucuronidation process seems to interfere with L-menthol-mediated TRPM8

activation (Valente et al. 2015). L-menthol cream application did not influence the alternative splicing of Trpm8 because the day after the last L-menthol cream application in LM and HM groups, both full-length and short isoform of Trpm8 did not change their expression levels in either dermis or white adipocytes. Therefore, the failure of daily L-menthol cream application in increasing metabolism and white adipose plasticity as well as decreasing adiposity may be attributed to the very low expression of the full-length isoform of Trpm8 in dermis at baseline rather than to a higher expression of the short TRPM8 isoforms. However, analysis on TRPM8 protein levels is necessary for confirmation. An alternative reason could be the increase of skin glucuronidation due to the daily exposure of dermis to L-menthol leading to high menthol glucuronide levels in the body. However this alternative is unlikely because a previous study reported a limited contribution of the skin to the body's total phase II drug metabolism in humans (Manevski et al. 2015). Moreover, considering that a single L-menthol administration has beneficial effect in increasing metabolism and thermogenesis in both human in vivo and in vitro white adipocytes (Rossato et al. 2014; Valente et al. 2015), we can hypothesize that an eventual body adaptation to the daily L-menthol cream application through a pathway TRPM8-indipendent may also explain the observed results.

Adiponectin gene expression was the only factor that increased in subcutaneous white adipocytes following 1-month of daily application of the lower L-menthol concentration cream. Adiponectin plays a role in modulating a number of metabolic processes, including glucose regulation and fatty acid oxidation (Fang and Sweeney 2006; Chiarugi and Fiaschi 2010; Lim et al. 2014), thus these results may indicate that a process for increasing human metabolism may have started. However, since the cream application lasted 1 month, it is possible that the action of adiponectin in increasing metabolism may have not been strong enough and durable to increase resting metabolic rate and decrease body weight and adiposity. Interestingly, the increase in adiponectin was significant only in white adipocytes of

LM group but not of HM group. In-vitro studies showed that L-menthol increased TRPM8 expression and activity in a dose-dependent manner in human white adipocytes (Rossato et al. 2014) and lymph node carcinoma of the prostate cells as well as Chinese hamster ovary and monkey fibroblast-like cells (Mahieu et al. 2007). Our novel findings showed that dermis expressed both functional and non-functional TRPM8 isoforms while subcutaneous white adipose tissue expressed only the functional isoform, indicating a major role for dermis in responding and adapting to different thermal stimuli. As literature does not report a dose-dependent effect of L-menthol on dermis TRPM8, it is reasonable to presume that the daily application of higher L-menthol concentration cream on the skin would have resulted in a possible desensitization or would have inhibited protein transcription or activity of the dermis TRPM8 in HM group through a negative feedback regulation, as dermis of participants showed no changes in mRNA expression of both TRPM8 isoforms following the application period. Future studies on TRPM8 protein levels are required to clarify the eventual dose-dependent effect on dermis TRPM8 expression and/or activity.

During the 4 weeks of cream application, all participants reported no changes in their nutrients and kilocalories intake as well as in their physical activity explaining the unchanged results observed in body composition and metabolism. Interestingly, participants in LM group increased their physical activity only in the last week (week 4) of cream application compared to the baseline. This may explain in part the increase in adiponectin gene expression in white adipocytes of LM group as exercise increases blood adiponectin levels in humans (Kriketos et al. 2004; Saunders et al. 2012). Moreover, participants in LM group reported an increment in sodium intake during the whole cream application period compared to the baseline. Although the sodium intake increased only by 1-fold, this may also explain in part the increase observed in adiponectin gene expression in subcutaneous white adipocytes since previous animal and human studies reported that an increment of 4- or 20-fold in

sodium intake leads to increased blood adiponectin through renin-angiotensin-aldosterone system suppression (Lely et al. 2007; Kamari et al. 2010; Krikken et al. 2012; Mallamaci et al. 2013). However, the effect of sodium intake on adiponectin is still controversial as a study on mice reported that sodium restriction diet increased mRNA expression of adiponectin in visceral adipose tissue (Baudrand et al. 2014). Also, other human studies reported that the shift from high to low sodium intake does not have an effect on blood adiponectin levels (Campbell et al. 2014; Zhu et al. 2014). It is worth noting that a human study reported that high sodium diet increases adiponectin in normotensive salt-resistant but not in salt-sensitive subjects (Liu et al. 2012). In the present study we did not test the sensitivity to sodium of our participants, therefore whether the effect of L-menthol cream application in increasing adiponectin would have been larger in LM group if the rise in sodium intake had been prevented is one of the questions raised by this study. Further analyses on renin-angiotensin-aldosterone system suppression following L-menthol cream application are required to clarify the process that increases adiponectin in subcutaneous white adipocytes.

Our study showed that Ucp1 did not increase in white adipocytes following daily L-menthol administration, although further analysis on protein levels are necessary to confirm the effect of L-menthol on white adipose tissue plasticity. In accordance with our results, previous studies showed that UCP1 expression levels in rodent and human white adipocytes did not change following daily oral L-menthol administration and 10 days of cold exposure, respectively (Ma et al. 2012; van der Lans et al. 2013). Our human studies showed a significant but slight increase in metabolism and thermogenesis following a single L-menthol cream administration (Valente et al. 2015) and no effect on resting metabolic rate, body weight, and adiposity following 1-month of daily L-menthol cream application. In accordance with these results, human body weight did not change after chronic cold exposure of 6h/day at 15-16 °C for a total of 10 days or 2h/day at 17 °C for a total of 6 weeks,

while fat mass decreased following the 6 weeks but not the 10 days, of cold exposure (van der Lans et al. 2013; Yoneshiro et al. 2013). In contrast to our results, animal studies reported that skin or oral L-menthol administration increased metabolism and non-shivering thermogenesis activation in rodents with higher levels of UCP1 in brown adipocytes as well as a great reduction in body weight gain and adiposity following daily oral L-menthol administration (Tajino et al. 2007; Ma et al. 2012). These controversial results between humans and rodents could be explained by divergence in thermal sensitivity that may be a result of adaptive evolution. Our results showed that, despite changes in season temperatures, dermis of all participants showed a higher expression of the non-active isoform of TRPM8 compared to the active isoform, thus similar analysis in rodents may reveal an eventual divergence in thermal sensitivity. Moreover, a recent work reported that L-menthol activates rodents but not primate transient receptor potential cation channel, subfamily A, member 1 (TRPA1) due to a variation of a single residue – G878 in rodents but V875 in primate – within S5 transmembrane domain of the receptor, with the residue G878 being determinant for species-specific L-menthol responses (Chen et al. 2013). This suggests that as in rodents L-menthol may stimulate both TRPA1 and TRPM8, in humans may stimulate only TRPM8, explaining the controversial effect of L-menthol on human metabolism and thermogenesis activation (Karashima et al. 2007; Tajino et al. 2007; Tajino et al. 2011; Ma et al. 2012; Rossato et al. 2014; Valente et al. 2015). Interestingly, the protein sequences alignment in BLAST between mouse and human showed that 222 residues are different for TRPA1 and 69 residues are different for TRPM8. Considering the identification of a single residue critical for L-menthol TRPA1 activation, it is reasonable to presume that L-menthol-mediated TRPM8 activation in humans may be to a much less degree compared to that in rodents due to residues variation, which could represent an alternative or even further explanation of the observed results. Thus, molecular determinants analysis of cold-sensitive gating between TRPM8 of different species may be relevant for a

deeper understanding of L-menthol-mediated TRPM8 stimulation of human metabolism and thermogenesis.

There are a number of limitations to the present study, some of which like the missing analysis at protein levels of the factors involved in metabolism activation, white adipose tissue plasticity and TRPM8 activity, have previously been discussed. Our estimation of dietary nutrients intake was based on self-reported 24-hour diet records three days a week that may underestimate the usual nutrient intake. Body fat percentage was assessed using bioelectrical impendence method which is not as accurate as other methods like dual-energy X-ray absorptiometry (DEXA). The eventual and uncontrolled evaporation of the menthol cream could have affected blood menthol levels and thus the overall results. Limitations due to the self-applied cream by the participants were minimized by calling each participant <4 times a week asking for confirmation of cream application, feelings about the cream, eventual skin irritation, thermal comfort and sensation.

In conclusion, we showed that 1-month of daily L-menthol cream application did not increase metabolism or white adipose tissue plasticity and did not affect body composition. However, the increase of adiponectin in white adipocytes could indicate that a process for increasing human metabolism may have started. The short cream application period and/or divergence in thermal sensitivity between rodents and humans may have resulted in a weaker stimulation of human metabolism leading to unchanged results in body weight, body composition and resting metabolic rate following L-menthol cream application. Thus, further analysis on protein expression and activity of factors involved in metabolism, white adipose tissue plasticity as well as on molecular determinants of human TRPM8 cold-sensitive gating are essential to clarify the effect of L-menthol-mediated TRPM8 stimulation on human metabolism and thermogenesis.

ACKNOWLEDGMENTS

The authors report no financial or personal relationships with other people or organisations that could inappropriately influence (bias) their actions. This work was supported by funding from the Education and Lifelong Learning Programme of the Greek Ministry of Education, Co-financed by Greece and the European Union (NSRF 2007-2013, IRAKLITOS II, grant no. 162), and the European Union 7th Framework Program (FP7-PEOPLE-2013-IRSES grant no. 612547).

CHAPTER 5

GENERAL CONCLUSION

The present PhD project aims to identify factors that increase human metabolism and treat adipose excess through UCP1 activation. By integrating the results of the evaluated animal and human studies, our systematic analysis identified L-menthol as one of the molecules that can activate rodent UCP1 in brown and brite adipocytes (Valente et al. 2014). Indeed, the activation of UCP1 by L-menthol-mediated TRPM8 stimulation increases rodent metabolism with a decrease in adiposity following frequent UCP1 activation (Tajino et al. 2007; Tajino et al. 2011; Ma et al. 2012).

Our results showed that a single administration of L-menthol via a gel cream increased thermogenesis and metabolic rate in humans (Valente et al. 2015). These effects were minor following oral L-menthol administration probably due to a faster metabolism of L-menthol (i.e., glucuronidation process) that occurs when the molecule is absorbed through the gastrointestinal tract leading to higher menthol glucuronide concentration following the oral administration compared to the skin (Hiki et al. 2011; Valente et al. 2015). Thus, the research hypothesis 1 is rejected while the research hypothesis 2 is accepted as skin L-menthol administration increased human metabolism and thermogenesis with minor effect following the oral administration. On the other hand, we found that 1-month of daily application of either lower or higher L-menthol creams did not increase metabolism or white adipose tissue plasticity and did not affect body composition in humans rejecting, therefore, the research hypotheses 3, 4 and 5.

These results may be attributed to different reasons. First, the very low expression of the full-length isoform of Trpm8 in dermis may have resulted in low levels of the functional receptor activated by L-menthol. Second, an increase in skin glucuronidation process due to daily L-menthol cream application may have resulted in higher menthol glucuronide levels in the body interfering with TRPM8 stimulation. Third, a body adaptation to the daily L-menthol cream application through a pathway

TRPM8-indipendent may also be considered to justify the observed results. Another important aspect to be considered is the activity of TRPA1 and TRPM8 in rodents and humans. Indeed, in rodents L-menthol can stimulate both TRPA1 and TRPM8, while in humans L-menthol can stimulate only TRPM8 but not TRPA1 due to a single residue variation in human TRPA1 sequence that makes this receptor non-functional (Chen et al. 2013). As human TRPM8 sequence presents 69 residues that are different from rodent TRPM8 and a single residue is critical for L-menthol TRPA1 activation, it is reasonable to assume that L-menthol-mediated TRPM8 activation in humans may be to a much less degree compared to that in rodents, explaining the greater effect of L-menthol on rodent metabolism, thermogenesis and adiposity loss compared to our results in humans.

Given the above, future analysis on protein expression and activity of factors involved in metabolism and white adipose tissue plasticity following daily L-menthol administration, on human TRPM8 cold-sensitive gating and the consideration of the body fat percentage rather than the body mass of participants for L-menthol concentration cream are essential to clarify the effect of L-menthol-mediated TRPM8 stimulation on human metabolism and thermogenesis and to confirm together with a healthy nutrition and physical activity, L-menthol as promising candidate treatment for human cardio-metabolic diseases.

CHAPTER 6

REFERENCES

Adjeitey, C. N., Mailloux, R. J., Dekemp, R. A. and Harper, M. E. 2013. Mitochondrial uncoupling in skeletal muscle by UCP1 augments energy expenditure and glutathione content while mitigating ROS production. American Journal of Physiology - Endocrinology and Metabolism **305**(3): E405-415.

Adriaens, M. P., Schoffelen, P. F. and Westerterp, K. R. 2003. Intra-individual variation of basal metabolic rate and the influence of daily habitual physical activity before testing. Br J Nutr **90**(2): 419-423.

Anunciado-Koza, R. P., Zhang, J., Ukropec, J., Bajpeyi, S., Koza, R. A., Rogers, R. C., Cefalu, W. T., Mynatt, R. L. and Kozak, L. P. 2011. Inactivation of the mitochondrial carrier SLC25A25 (ATP-Mg2+/Pi transporter) reduces physical endurance and metabolic efficiency in mice. The Journal of Biological Chemistry **286**(13): 11659-11671.

Asano, H., Yamada, T., Hashimoto, O., Umemoto, T., Sato, R., Ohwatari, S., Kanamori, Y., Terachi, T., Funaba, M. and Matsui, T. 2013. Diet-induced changes in Ucp1 expression in bovine adipose tissues. Gen Comp Endocrinol **184**: 87-92.

Astrup, A., Bulow, J., Madsen, J. and Christensen, N. J. 1985. Contribution of BAT and skeletal muscle to thermogenesis induced by ephedrine in man. American Journal of Physiology **248**(5 Pt 1): E507-515.

Barger, J. L., Barnes, B. M. and Boyer, B. B. 2006. Regulation of UCP1 and UCP3 in arctic ground squirrels and relation with mitochondrial proton leak. Journal of Applied Physiology **101**(1): 339-347.

Bartolomucci, A., La Corteb, G., Possentid, R., Locatellif, V., Rigamontig, A. E., Torsellof, A., Brescianif, E., Bulgarellif, I., Rizzie, R., Pavonea, F., D'Amatoa, F. R., Severinid, C., Mignognah, G., Giorgih, A., Schinina`, M. E., Eliai, G., Branciaj, C., Ferrij, G.-L., Contik, R., Cianik, B., Pascuccil, T., Dell'Omom, G., Mullerg, E. E., Levic, A. and Molesa, A. 2006. TLQP-21, a VGF-derived peptide, increases energy expenditure and prevents the early phase of diet-induced obesity. PNAS **103**: 14584–14589.

Baudrand, R., Lian, C. G., Lian, B. Q., Ricchiuti, V., Yao, T. M., Li, J., Williams, G. H. and Adler, G. K. 2014. Long-term dietary sodium restriction increases adiponectin expression and ameliorates the proinflammatory adipokine profile in obesity. Nutr Metab Cardiovasc Dis **24**(1): 34-41.

Bautista, D. M., Siemens, J., Glazer, J. M., Tsuruda, P. R., Basbaum, A. I., Stucky, C. L., Jordt, S. E. and Julius, D. 2007. The menthol receptor TRPM8 is the principal detector of environmental cold. Nature **448**(7150): 204-208.

Bauwens, J. D., Schmuck, E. G., Lindholm, C. R., Ertel, R. L., Mulligan, J. D., Hovis, I., Viollet, B. and Saupe, K. W. 2011. Cold tolerance, cold-induced hyperphagia, and nonshivering thermogenesis are normal in alpha(1)-AMPK-/- mice. American Journal of Physiology - Regulatory, Integrative and Comparative Physiology **301**(2): R473-483.

Bidaux, G., Beck, B., Zholos, A., Gordienko, D., Lemonnier, L., Flourakis, M., Roudbaraki, M., Borowiec, A. S., Fernandez, J., Delcourt, P., Lepage, G., Shuba, Y., Skryma, R. and Prevarskaya, N. 2012. Regulation of activity of transient receptor potential melastatin 8 (TRPM8) channel by its short isoforms. J Biol Chem **287**(5): 2948-2962.

Bischoff, S. C., Damms-Machado, A., Betz, C., Herpertz, S., Legenbauer, T., Low, T., Wechsler, J. G., Bischoff, G., Austel, A. and Ellrott, T. 2012. Multicenter evaluation of an interdisciplinary 52-week weight loss program for obesity with regard to body weight, comorbidities and quality of life--a prospective study. International Journal of Obesity **36**(4): 614-624.

Bordicchia, M., Liu, D., Amri, E. Z., Ailhaud, G., Dessi-Fulgheri, P., Zhang, C., Takahashi, N., Sarzani, R. and Collins, S. 2012. Cardiac natriuretic peptides act via p38 MAPK to induce the brown fat thermogenic program in mouse and human adipocytes. The Journal of Clinical Investigation **122**(3): 1022-1036.

Bostrom, P., Wu, J., Jedrychowski, M. P., Korde, A., Ye, L., Lo, J. C., Rasbach, K. A., Bostrom, E. A., Choi, J. H., Long, J. Z., Kajimura, S., Zingaretti, M. C., Vind, B. F., Tu, H., Cinti, S., Hojlund, K., Gygi, S. P. and Spiegelman, B. M. 2012. A PGC1-alpha-dependent myokine that drives brown-fat-like development of white fat and thermogenesis. Nature **481**(7382): 463-468.

Campbell, K. L., Johnson, D. W., Bauer, J. D., Hawley, C. M., Isbel, N. M., Stowasser, M., Whitehead, J. P., Dimeski, G. and McMahon, E. 2014. A randomized trial of sodium-restriction on kidney function, fluid volume and adipokines in CKD patients. BMC Nephrol **15**: 57.

Carey, A. L., Formosa, M. F., Van Every, B., Bertovic, D., Eikelis, N., Lambert, G. W., Kalff, V., Duffy, S. J., Cherk, M. H. and Kingwell, B. A. 2013. Ephedrine activates brown adipose tissue in lean but not obese humans. Diabetologia **56**(1): 147-155.

Carrillo, A. E. and Flouris, A. D. 2011. Caloric restriction and longevity: effects of reduced body temperature. Ageing Research Reviews **10**(1): 153-162.

Carrillo, A. E., Flynn, M. G., Pinkston, C., Markofski, M. M., Jiang, Y., Donkin, S. S. and Teegarden, D. 2013. Impact of vitamin D supplementation during a resistance training intervention on body composition, muscle function, and glucose tolerance in overweight and obese adults. Clinical Nutrition **32**(3): 375-381.

Chao, P. T., Yang, L., Aja, S., Moran, T. H. and Bi, S. 2011. Knockdown of NPY Expression in the Dorsomedial Hypothalamus Promotes Development of Brown Adipocytes and Prevents Diet-Induced Obesity. Cell Metabolism **13** 573–583.

Chappuis, S., Ripperger, J. A., Schnell, A., Rando, G., Jud, C., Wahli, W. and Albrecht, U. 2013. Role of the circadian clock gene Per2 in adaptation to cold temperature. Molecular metabolism **2**(3): 184-193.

Chen, J., Kang, D., Xu, J., Lake, M., Hogan, J. O., Sun, C., Walter, K., Yao, B. and Kim, D. 2013. Species differences and molecular determinant of TRPA1 cold sensitivity. Nat Commun **4**: 2501.

Chen, J. F., Zhong, W. Q. and Wang, D. H. 2012. Seasonal changes in body mass, energy intake and thermogenesis in Maximowiczi's voles (Microtus maximowiczii) from the Inner Mongolian grassland. Journal of Comparative Physiology B **182**(2): 275-285.

Cheng, Y., Meng, Q., Wang, C., Li, H., Huang, Z., Chen, S., Xiao, F. and Guo, F. 2010. Leucine deprivation decreases fat mass by stimulation of lipolysis in white adipose tissue and upregulation of uncoupling protein 1 (UCP1) in brown adipose tissue. Diabetes **59**(1): 17-25.

Chiarugi, P. and Fiaschi, T. 2010. Adiponectin in health and diseases: from metabolic syndrome to tissue regeneration. Expert Opin Ther Targets **14**(2): 193-206.

Colburn, R. W., Lubin, M. L., Stone, D. J., Jr., Wang, Y., Lawrence, D., D'Andrea, M. R., Brandt, M. R., Liu, Y., Flores, C. M. and Qin, N. 2007. Attenuated cold sensitivity in TRPM8 null mice. Neuron **54**(3): 379-386.

Cypess, A. M., Chen, Y. C., Sze, C., Wang, K., English, J., Chan, O., Holman, A. R., Tal, I., Palmer, M. R., Kolodny, G. M. and Kahn, C. R. 2012. Cold but not sympathomimetics activates human brown adipose tissue in vivo. Proc Natl Acad Sci U S A **109**(25): 10001-10005.

Cypess, A. M., Weiner, L. S., Roberts-Toler, C., Elia, E. F., Kessler, S. H., Kahn, P. A., English, J., Chatman, K., Trauger, S. A., Doria, A. and Kolodny, G. M. 2015. Activation of Human Brown Adipose Tissue by a beta3-Adrenergic Receptor Agonist. Cell Metab **21**(1): 33-38.

Cypess, A. M., White, A. P., Vernochet, C., Schulz, T. J., Xue, R., Sass, C. A., Huang, T. L., Roberts-Toler, C., Weiner, L. S., Sze, C., Chacko, A. T., Deschamps, L. N., Herder, L. M., Truchan, N., Glasgow, A. L., Holman, A. R., Gavrila, A., Hasselgren, P. O., Mori, M. A., Molla, M. and Tseng, Y. H. 2013. Anatomical localization, gene expression profiling and functional characterization of adult human neck brown fat. Nature Medicine **19**(5): 635-639.

Czyzyk, T. A., Romero-Pico, A., Pintar, J., McKinzie, J. H., Tschop, M. H., Statnick, M. A. and Nogueiras, R. 2012. Mice lacking delta-opioid receptors resist the development of diet-induced obesity. FASEB journal **26**(8): 3483-3492.

De Jonghe, B. C., Hayes, M. R., Banno, R., Skibicka, K. P., Zimmer, D. J., Bowen, K. A., Leichner, T. M., Alhadeff, A. L., Kanoski, S. E., Cyr, N. E., Nillni, E. A., Grill, H. J. and Bence, K. K. 2011. Deficiency of PTP1B in POMC neurons leads to alterations in energy balance and homeostatic response to cold exposure. American Journal of Physiology - Endocrinology and Metabolism **300**(6): E1002-1011.

Dhaka, A., Murray, A. N., Mathur, J., Earley, T. J., Petrus, M. J. and Patapoutian, A. 2007. TRPM8 Is Required for Cold Sensation in Mice. Neuron **54**: 371–378.

Dinas, P. C., Nikaki, A., Jamurtas, A. Z., Prassopoulos, V., Efthymiadou, R., Koutedakis, Y., Georgoulias, P. and Flouris, A. D. 2015. Association between habitual physical activity and brown adipose tissue activity in individuals undergoing PET-CT scan. Clin Endocrinol (Oxf) **82**(1): 147-154.

Du, Y., Meng, Q., Zhang, Q. and Guo, F. 2012. Isoleucine or valine deprivation stimulates fat loss via increasing energy expenditure and regulating lipid metabolism in WAT. Amino Acids **43**(2): 725-734.

Ducharme, N. A. and Bickel, P. E. 2008. Lipid droplets in lipogenesis and lipolysis. Endocrinology **149**(3): 942-949.

Eisenberg, F., Jr., Field, J. B. and Stetten, D., Jr. 1955. Studies on glucuronide conjugation in man. Arch Biochem Biophys **59**(1): 297-299.

Fang, C., Liu, Y., Ye, X., Rong, Z. X., Feng, X. M., Jiang, C. B. and Chen, H. Z. 2008. Synergistically enhanced transdermal permeation and topical analgesia of tetracaine gel containing menthol and ethanol in experimental and clinical studies. Eur J Pharm Biopharm **68**(3): 735-740.

Fang, X. and Sweeney, G. 2006. Mechanisms regulating energy metabolism by adiponectin in obesity and diabetes. Biochem Soc Trans **34**(Pt 5): 798-801.

Fanger, P. O. 1970. Thermal comfort. Analysis and applications in environmental engineering., Danish Technical Press, Copenhagen: 1-244.

Feise, R. J. 2002. Do multiple outcome measures require p-value adjustment? BMC Med Res Methodol **2**: 8.

Feldmann, H. M., Golozoubova, V., Cannon, B. and Nedergaard, J. 2009. UCP1 Ablation Induces Obesity and Abolishes Diet-Induced Thermogenesis in Mice Exempt from Thermal Stress by Living at Thermoneutrality. Cell Metabolism **9**: 203–209.

Fernandez, J. A., Skryma, R., Bidaux, G., Magleby, K. L., Scholfield, C. N., McGeown, J. G., Prevarskaya, N. and Zholos, A. V. 2012. Short isoforms of the cold receptor TRPM8 inhibit channel gating by mimicking heat action rather than chemical inhibitors. J Biol Chem **287**(5): 2963-2970.

Finucane, F. M., Luan, J., Wareham, N. J., Sharp, S. J., O'Rahilly, S., Balkau, B., Flyvbjerg, A., Walker, M., Hojlund, K., Nolan, J. J. and Savage, D. B. 2009. Correlation of the leptin:adiponectin ratio with measures of insulin resistance in non-diabetic individuals. Diabetologia **52**(11): 2345-2349.

Finucane, M. M., Stevens, G. A., Cowan, M. J., Danaei, G., Lin, J. K., Paciorek, C. J., Singh, G. M., Gutierrez, H. R., Lu, Y., Bahalim, A. N., Farzadfar, F., Riley, L. M. and Ezzati, M. 2011. National, regional, and global trends in body-mass index since 1980: systematic analysis of health examination surveys and

epidemiological studies with 960 country-years and 9.1 million participants. Lancet **377**(9765): 557-567.
Flouris, A. D. 2011. Functional architecture of behavioural thermoregulation. Eur J Appl Physiol **111**(1): 1-8.
Flouris, A. D., Bouziotas, C., Christodoulos, A. D. and Koutedakis, Y. 2008. Longitudinal preventive-screening cutoffs for metabolic syndrome in adolescents. International Journal of Obesity **32**(10): 1506-1512.
Flouris, A. D. and Cheung, S. S. 2009. Influence of thermal balance on cold-induced vasodilation. J Appl Physiol **106**(4): 1264-1271.
Flouris, A. D. and Dinas, P. C. 2015. Impact of regular exercise on classical brown adipose tissue. Clin Endocrinol (Oxf): in press.
Gagge, A. P., Stolwijk, J. A. and Saltin, B. 1969. Comfort and thermal sensations and associated physiological responses during exercise at various ambient temperatures. Environ Res **2**(3): 209-229.
Gelal, A., Jacob, P., 3rd, Yu, L. and Benowitz, N. L. 1999. Disposition kinetics and effects of menthol. Clin Pharmacol Ther **66**(2): 128-135.
Giby, V. G. and Ajith, T. A. 2014. Role of adipokines and peroxisome proliferator-activated receptors in nonalcoholic fatty liver disease. World J Hepatol **6**(8): 570-579.
Gillis, D. J., Weston, N., House, J. R. and Tipton, M. J. 2015. Influence of repeated daily menthol exposure on human temperature regulation and perception. Physiology & Behavior **139**: 511-518.
Giralt, A., Hondares, E., Villena, J. A., Ribas, F., Diaz-Delfin, J., Giralt, M., Iglesias, R. and Villarroya, F. 2011. Peroxisome proliferator-activated receptor-gamma coactivator-1alpha controls transcription of the Sirt3 gene, an essential component of the thermogenic brown adipocyte phenotype. The Journal of Biological Chemistry **286**(19): 16958-16966.
Golubovic, M. V., Dimic, D., Antic, S., Radenkovic, S., Djindjic, B. and Jovanovic, M. 2013. Relationship of adipokine to insulin sensitivity and glycemic regulation in obese women--the effect of body weight reduction by caloric restriction. Vojnosanitetski Pregled **70**(3): 284-291.
Gray, S. L., Dalla Nora, E., Backlund, E. C., Manieri, M., Virtue, S., Noland, R. C., O'Rahilly, S., Cortright, R. N., Cinti, S., Cannon, B. and Vidal-Puig, A. 2006. Decreased brown adipocyte recruitment and thermogenic capacity in mice with impaired peroxisome proliferator-activated receptor (P465L PPARgamma) function. Endocrinology **147**(12): 5708-5714.
Hall, J. A., Ribich, S., Christoffolete, M. A., Simovic, G., Correa-Medina, M., Patti, M. E. and Bianco, A. C. 2010. Absence of thyroid hormone activation during development underlies a permanent defect in adaptive thermogenesis. Endocrinology **151**(9): 4573-4582.
Hartley, G. L., Flouris, A. D., Plyley, M. J. and Cheung, S. S. 2012. The effect of a covert manipulation of ambient temperature on heat storage and voluntary exercise intensity. Physiol Behav **105**(5): 1194-1201.
Heaton, J. M. 1972. The distribution of brown adipose tissue in the human. Journal of anatomy **112**(Pt 1): 35-39.
Hiki, N., Kaminishi, M., Hasunuma, T., Nakamura, M., Nomura, S., Yahagi, N., Tajiri, H. and Suzuki, H. 2011. A phase I study evaluating tolerability, pharmacokinetics, and preliminary efficacy of L-menthol in upper gastrointestinal endoscopy. Clin Pharmacol Ther **90**(2): 221-228.
Hudson-Davies, R., Pocock, V., White, R., Parker, M. and Milligan, S. R. 2009. Disturbances in core body temperature in RIP140-null mice. Journal of Thermal Biology **34**: 100–108.
Hung, Y. J., Chu, N. F., Wang, S. C., Hsieh, C. H., He, C. T., Lee, C. H. and Fan, S. C. 2006. Correlation of plasma leptin and adiponectin with insulin sensitivity

and beta-cell function in children - the Taipei Children Heart Study. Int J Clin Pract **60**(12): 1582-1587.

Huttunen, P., Hirvonen, J. and Kinnula, V. 1981. The occurrence of brown adipose tissue in outdoor workers. European journal of applied physiology and occupational physiology **46**(4): 339-345.

Inokuma, K., Okamatsu-Ogura, Y., Omachi, A., Matsushita, Y., Kimura, K., Yamashita, H. and Saito, M. 2006. Indispensable role of mitochondrial UCP1 for antiobesity effect of beta3-adrenergic stimulation. American Journal of Physiology - Endocrinology and Metabolism **290**(5): E1014-1021.

Iscan, G., Kirimer, N., Kurkcuoglu, M., Baser, K. H. and Demirci, F. 2002. Antimicrobial screening of Mentha piperita essential oils. J Agric Food Chem **50**(14): 3943-3946.

Jimenez-Preitner, M., Berney, X., Uldry, M., Vitali, A., Cinti, S., Ledford, J. G. and Thorens, B. 2011. Plac8 is an inducer of C/EBPbeta required for brown fat differentiation, thermoregulation, and control of body weight. Cell Metabolism **14**(5): 658-670.

Kamari, Y., Shimoni, N., Koren, F., Peleg, E., Sharabi, Y. and Grossman, E. 2010. High-salt diet increases plasma adiponectin levels independent of blood pressure in hypertensive rats: the role of the renin-angiotensin-aldosterone system. J Hypertens **28**(1): 95-101.

Karashima, Y., Damann, N., Prenen, J., Talavera, K., Segal, A., Voets, T. and Nilius, B. 2007. Bimodal action of menthol on the transient receptor potential channel TRPA1. J Neurosci **27**(37): 9874-9884.

Kiefer, F. W., Vernochet, C., O'Brien, P., Spoerl, S., Brown, J. D., Nallamshetty, S., Zeyda, M., Stulnig, T. M., Cohen, D. E., Kahn, C. R. and Plutzky, J. 2012. Retinaldehyde dehydrogenase 1 regulates a thermogenic program in white adipose tissue. Nature Medicine **18**(6): 918-925.

Kim, Y. J., Shin, Y. O., Ha, Y. W., Lee, S., Oh, J. K. and Kim, Y. S. 2006. Anti-obesity effect of Pinellia ternata extract in Zucker rats. Biological & Pharmaceutical Bulletin **29**(6): 1278-1281.

Kitao, N. and Hashimoto, M. 2012. Increased thermogenic capacity of brown adipose tissue under low temperature and its contribution to arousal from hibernation in Syrian hamsters. American Journal of Physiology - Endocrinology and Metabolism **302**(1): R118-125.

Korach-Andréa, M., Archera, A., Barros, R. P., Parinia, P. and Gustafsson, J. A. 2011. Both liver-X receptor (LXR) isoforms control energy expenditure by regulating Brown Adipose Tissue activity. PNAS **108**: 403–408.

Kounalakis, S. N., Botonis, P. G., Koskolou, M. D. and Geladas, N. D. 2010. The effect of menthol application to the skin on sweating rate response during exercise in swimmers and controls. Eur J Appl Physiol **109**(2): 183-189.

Koutedakis, Y., Bouziotas, C., Flouris, A. D. and Nelson, P. N. 2005. Longitudinal modeling of adiposity in periadolescent Greek schoolchildren. Medicine & Science in Sports & Exercise **37**(12): 2070-2074.

Kozak, L. P. 2010. Brown fat and the myth of diet-induced thermogenesis. Cell Metabolism **11**(4): 263-267.

Kriketos, A. D., Gan, S. K., Poynten, A. M., Furler, S. M., Chisholm, D. J. and Campbell, L. V. 2004. Exercise increases adiponectin levels and insulin sensitivity in humans. Diabetes Care **27**(2): 629-630.

Krikken, J. A., Dallinga-Thie, G. M., Navis, G. and Dullaart, R. P. 2012. Short term dietary sodium restriction decreases HDL cholesterol, apolipoprotein A-I and high molecular weight adiponectin in healthy young men: relationships with renal hemodynamics and RAAS activation. Nutr Metab Cardiovasc Dis **22**(1): 35-41.

Lehr, L., Canola, K., Leger, B. and Giacobino, J. P. 2009. Differentiation and characterization in primary culture of white adipose tissue brown adipocyte-like cells. International Journal of Obesity **33**(6): 680-686.

Leitner, C. and Bartness, T. J. 2009. Acute brown adipose tissue temperature response to cold in monosodium glutamate-treated Siberian hamsters. Brain Research **1292**: 38-51.

Lely, A. T., Krikken, J. A., Bakker, S. J., Boomsma, F., Dullaart, R. P., Wolffenbuttel, B. H. and Navis, G. 2007. Low dietary sodium and exogenous angiotensin II infusion decrease plasma adiponectin concentrations in healthy men. J Clin Endocrinol Metab **92**(5): 1821-1826.

Li, S., Yu, Q., Wang, G. X. and Lin, J. D. 2013. The biological clock is regulated by adrenergic signaling in brown fat but is dispensable for cold-induced thermogenesis. PLoS One **8**(8): e70109.

Lim, S., Quon, M. J. and Koh, K. K. 2014. Modulation of adiponectin as a potential therapeutic strategy. Atherosclerosis **233**(2): 721-728.

Lin, L., Saha, P. K., Ma, X., Henshaw, I. O., Shao, L., Chang, B. H., Buras, E. D., Tong, Q., Chan, L., McGuinness, O. P. and Sun, Y. 2011. Ablation of ghrelin receptor reduces adiposity and improves insulin sensitivity during aging by regulating fat metabolism in white and brown adipose tissues. Aging Cell **10**(6): 996-1010.

Liu, F., Mu, J., Yuan, Z., Wu, G., Liu, E., Zheng, S., Lian, Q., Ren, K. and Xu, H. 2012. High salt intake fails to enhance plasma adiponectin in normotensive salt-sensitive subjects. Nutrition **28**(4): 422-425.

Liu, J. S., Yang, M., Sun, R. Y. and Wang, D. H. 2009. Adaptive thermogenesis in Brandt's vole (Lasiopodomys brandti) during cold and warm acclimation Journal of Thermal Biology **34**: 60–69.

Ma, S., Yu, H., Zhao, Z., Luo, Z., Chen, J., Ni, Y., Jin, R., Ma, L., Wang, P., Zhu, Z., Li, L., Zhong, J., Liu, D. and Nilius, B. 2012. Activation of the cold-sensing TRPM8 channel triggers UCP1-dependent thermogenesis and prevents obesity. J mol cell biology **4**(2): 88-96.

Ma, X., Lin, L., Qin, G., Lu, X., Fiorotto, M., Dixit, V. D. and Sun, Y. 2011. Ablations of ghrelin and ghrelin receptor exhibit differential metabolic phenotypes and thermogenic capacity during aging. PLoS One **6**(1): e16391.

Mahieu, F., Owsianik, G., Verbert, L., Janssens, A., De Smedt, H., Nilius, B. and Voets, T. 2007. TRPM8-independent menthol-induced Ca2+ release from endoplasmic reticulum and Golgi. J Biol Chem **282**(5): 3325-3336.

Mallamaci, F., Leonardis, D., Pizzini, P., Cutrupi, S., Tripepi, G. and Zoccali, C. 2013. Procalcitonin and the inflammatory response to salt in essential hypertension: a randomized cross-over clinical trial. J Hypertens **31**(7): 1424-1430; discussion 1430.

Manevski, N., Swart, P., Balavenkatraman, K. K., Bertschi, B., Camenisch, G., Kretz, O., Schiller, H., Walles, M., Ling, B., Wettstein, R., Schaefer, D. J., Itin, P., Ashton-Chess, J., Pognan, F., Wolf, A. and Litherland, K. 2015. Phase II metabolism in human skin: skin explants show full coverage for glucuronidation, sulfation, N-acetylation, catechol methylation, and glutathione conjugation. Drug Metab Dispos **43**(1): 126-139.

Mano-Otagiri, A., Iwasaki-Sekino, A., Nemoto, T., Ohata, H., Shuto, Y., Nakabayashi, H., Sugihara, H., Oikawa, S. and Shibasaki, T. 2010. Genetic suppression of ghrelin receptors activates brown adipocyte function and decreases fat storage in rats. Regulatory peptides **160**(1-3): 81-90.

Matsen, M. E., Thaler, J. P., Wisse, B. E., Guyenet, S. J., Meek, T. H., Ogimoto, K., Cubelo, A., Fischer, J. D., Kaiyala, K. J., Schwartz, M. W. and Morton, G. J. 2013. In uncontrolled diabetes, thyroid hormone and sympathetic activators induce thermogenesis without increasing glucose uptake in brown adipose

tissue. American journal of physiology. Endocrinology and metabolism **304**(7): E734-746.
Mattson, M. P. 2010. Perspective: Does brown fat protect against diseases of aging? Ageing Research Reviews **9**(1): 69-76.
Meyer, C. W., Willershauser, M., Jastroch, M., Rourke, B. C., Fromme, T., Oelkrug, R., Heldmaier, G. and Klingenspor, M. 2010. Adaptive thermogenesis and thermal conductance in wild-type and UCP1-KO mice. American Journal of Physiology - Regulatory, Integrative and Comparative Physiology **299**(5): R1396-1406.
Michaliszyn, S. F., Shaibi, G. Q., Quinn, L., Fritschi, C. and Faulkner, M. S. 2009. Physical fitness, dietary intake, and metabolic control in adolescents with type 1 diabetes. Pediatr Diabetes **10**(6): 389-394.
Mitchell, C. S., Savage, D. B., Dufour, S., Schoenmakers, N., Murgatroyd, P., Befroy, D., Halsall, D., Northcott, S., Raymond-Barker, P., Curran, S., Henning, E., Keogh, J., Owen, P., Lazarus, J., Rothman, D. L., Farooqi, I. S., Shulman, G. I., Chatterjee, K. and Petersen, K. F. 2010. Resistance to thyroid hormone is associated with raised energy expenditure, muscle mitochondrial uncoupling, and hyperphagia. The Journal of Clinical Investigation **120**(4): 1345-1354.
Moriya, R., Sano, H., Umeda, T., Ito, M., Takahashi, Y., Matsuda, M., Ishihara, A., Kanatani, A. and Iwaasa, H. 2006. RFamide peptide QRFP43 causes obesity with hyperphagia and reduced thermogenesis in mice. Endocrinology **147**(6): 2916-2922.
Muzik, O., Mangner, T. J. and Granneman, J. G. 2012. Assessment of oxidative metabolism in brown fat using PET imaging. Front Endocrinol (Lausanne) **3**: 15.
Nikolic, D. M., Li, Y., Liu, S. and Wang, S. 2011. Overexpression of constitutively active PKG-I protects female, but not male mice from diet-induced obesity. Obesity (Silver Spring) **19**(4): 784-791.
Nishi, Y. 1981. Measurement of thermal balance in man. In: Cena, K., Clark, J.A. (eds) Bioengineering, thermal physiology and comfort. , New York: Elsevier, 29-39.
Noatsch, A., Petzke, K. J., Millrose, M. K. and Klaus, S. 2011. Body weight and energy homeostasis was not affected in C57BL/6 mice fed high whey protein or leucine-supplemented low-fat diets. European journal of nutrition **50**(6): 479-488.
Oberhauser, F., Schulte, D. M., Faust, M., Gudelhofer, H., Hahn, M., Muller, N., Neumann, K., Krone, W. and Laudes, M. 2012. Weight loss due to a very low calorie diet differentially affects insulin sensitivity and interleukin-6 serum levels in nondiabetic obese human subjects. Horm Metab Res **44**(6): 465-470.
Oelkrug, R., Goetze, N., Exner, C., Lee, Y., Ganjam, G. K., Kutschke, M., Muller, S., Stohr, S., Tschop, M. H., Crichton, P. G., Heldmaier, G., Jastroch, M. and Meyer, C. W. 2013. Brown fat in a protoendothermic mammal fuels eutherian evolution. Nature communications **4**: 2140.
Oelkrug, R., Heldmaier, G. and Meyer, C. W. 2011. Torpor patterns, arousal rates, and temporal organization of torpor entry in wildtype and UCP1-ablated mice. Journal of Comparative Physiology B **181**(1): 137-145.
Olive, J. L., Hollis, B., Mattson, E. and Topp, R. 2010. Vascular conductance is reduced after menthol or cold application. Clin J Sport Med **20**(5): 372-376.
Pelletier, P., Gauthier, K., Sideleva, O., Samarut, J. and Silva, J. E. 2008. Mice lacking the thyroid hormone receptor-alpha gene spend more energy in thermogenesis, burn more fat, and are less sensitive to high-fat diet-induced obesity. Endocrinology **149**(12): 6471-6486.
Perneger, T. V. 1998. What's wrong with Bonferroni adjustments. BMJ **316**(7139): 1236-1238.

Petrovic, N., Walden, T. B., Shabalina, I. G., Timmons, J. A., Cannon, B. and Nedergaard, J. 2010. Chronic peroxisome proliferator-activated receptor gamma (PPARgamma) activation of epididymally derived white adipocyte cultures reveals a population of thermogenically competent, UCP1-containing adipocytes molecularly distinct from classic brown adipocytes. The Journal of Biological Chemistry **285**(10): 7153-7164.

Primeaux, S. D., Tong, M. and Holmes, G. M. 2007. Effects of chronic spinal cord injury on body weight and body composition in rats fed a standard chow diet. American Journal of Physiology - Regulatory, Integrative and Comparative Physiology **293**(3): R1102-1109.

Qiao, L., Yoo, H., Bosco, C., Lee, B., Feng, G. S., Schaack, J., Chi, N. W. and Shao, J. 2014. Adiponectin reduces thermogenesis by inhibiting brown adipose tissue activation in mice. Diabetologia **57**(5): 1027-1036.

Rajendra Acharya, U., Paul Joseph, K., Kannathal, N., Lim, C. M. and Suri, J. S. 2006. Heart rate variability: a review. Med Biol Eng Comput **44**(12): 1031-1051.

Rodriguez-Cuenca, S., Monjo, M., Frontera, M., Gianotti, M., Proenza, A. M. and Roca, P. 2007a. Sex steroid receptor expression profile in brown adipose tissue. Effects of hormonal status. Cellular Physiology and Biochemistry **20**(6): 877-886.

Rodriguez-Cuenca, S., Monjo, M., Gianotti, M., Proenza, A. M. and Roca, P. 2007b. Expression of mitochondrial biogenesis-signaling factors in brown adipocytes is influenced specifically by 17beta-estradiol, testosterone, and progesterone. American Journal of Physiology - Endocrinology and Metabolism **292**(1): E340-346.

Romanovsky, A. A. 2007. Thermoregulation: some concepts have changed. Functional architecture of the thermoregulatory system. Am J Physiol Regul Integr Comp Physiol **292**(1): R37-46.

Romero del Mar, M., Fernandez-Lopez, J. A., Esteve, M. and Alemany, M. 2009. Oleoyl-oestrone inhibits lipogenic, but maintains thermogenic, gene expression of brown adipose tissue in overweight rats. Bioscience Reports **29** (4): 237–243.

Rose, G., Crocco, P., D'Aquila, P., Montesanto, A., Bellizzi, D. and Passarino, G. 2011. Two variants located in the upstream enhancer region of human UCP1 gene affect gene expression and are correlated with human longevity. Experimental gerontology **46**(11): 897-904.

Rossato, M., Granzotto, M., Macchi, V., Porzionato, A., Petrelli, L., Calcagno, A., Vencato, J., De Stefani, D., Silvestrin, V., Rizzuto, R., Bassetto, F., De Caro, R. and Vettor, R. 2014. Human white adipocytes express the cold receptor TRPM8 which activation induces UCP1 expression, mitochondrial activation and heat production. Mol Cell Endocrinol **383**(1-2): 137-146.

Rothman, K. J. 1990. No adjustments are needed for multiple comparisons. Epidemiology **1**(1): 43-46.

Rothman, K. J. 2014. Six persistent research misconceptions. J Gen Intern Med **29**(7): 1060-1064.

Rousset, S., Alves-Guerra, M. C., Mozo, J., Miroux, B., Cassard-Doulcier, A. M., Bouillaud, F. and Ricquier, D. 2004. The biology of mitochondrial uncoupling proteins. Diabetes **53 Suppl 1**: S130-135.

Satyanarayana, A., Klarmann, K. D., Gavrilova, O. and Keller, J. R. 2012. Ablation of the transcriptional regulator Id1 enhances energy expenditure, increases insulin sensitivity, and protects against age and diet induced insulin resistance, and hepatosteatosis. FASEB journal **26**(1): 309-323.

Saunders, T. J., Palombella, A., McGuire, K. A., Janiszewski, P. M., Despres, J. P. and Ross, R. 2012. Acute exercise increases adiponectin levels in abdominally obese men. J Nutr Metab **2012**: 148729.

Seale, P., Kajimura, S., Yang, W., Chin, S., Rohas, L. M., Uldry, M., Tavernier, G., Langin, D. and Spiegelman, B. M. 2007. Transcriptional control of brown fat determination by PRDM16. Cell Metabolism **6**(1): 38-54.

Shabalina, I. G., Hoeks, J., Kramarova, T. V., Schrauwen, P., Cannon, B. and Nedergaard, J. 2010. Cold tolerance of UCP1-ablated mice: a skeletal muscle mitochondria switch toward lipid oxidation with marked UCP3 up-regulation not associated with increased basal, fatty acid- or ROS-induced uncoupling or enhanced GDP effects. Biochimica et Biophysica Acta **1797**(6-7): 968-980.

Shore, A., Emes, R. D., Wessely, F., Kemp, P., Cillo, C., D'Armiento, M., Hoggard, N. and Lomax, M. A. 2012. A comparative approach to understanding tissue-specific expression of uncoupling protein 1 expression in adipose tissue. Frontiers in genetics **3**: 304.

Streijger, F., Pluk, H., Oerlemans, F., Beckers, G., Bianco, A. C., Ribeiro, A. O., Wieringa, B. and Van der Zee, C. E. E. M. 2009. Mice lacking brain-type creatine kinase activity show defective thermoregulation. Physiology & Behavior **97** 76–86.

Stuempfle, K. J., Hoffman, M. D. and Hew-Butler, T. 2013. Association of gastrointestinal distress in ultramarathoners with race diet. Int J Sport Nutr Exerc Metab **23**(2): 103-109.

Tajino, K., Hosokawa, H., Maegawa, S., Matsumura, K., Dhaka, A. and Kobayashi, S. 2011. Cooling-Sensitive TRPM8 Is Thermostat of Skin Temperature against Cooling. PLOSONE **6** (3): e17504.

Tajino, K., Matsumura, K., Kosada, K., Shibakusa, T., Inoue, K., Fushiki, T., Hosokawa, H. and Kobayashi, S. 2007. Application of menthol to the skin of whole trunk in mice induces autonomic and behavioral heat-gain responses. Am J Physiol Regul Integr Comp Physiol **293**(5): R2128-2135.

Topp, R., Winchester, L., Mink, A. M., Kaufman, J. S. and Jacks, D. E. 2011. Comparison of the effects of ice and 3.5% menthol gel on blood flow and muscle strength of the lower arm. J Sport Rehabil **20**(3): 355-366.

Tseng, Y. H., Kokkotou, E., Schulz, T. J., Huang, T. L., Winnay, J. N., Taniguchi, C. M., Tran, T. T., Suzuki, R., Espinoza, D. O., Yamamoto, Y., Ahrens, M. J., Dudley, A. T., Norris, A. W., Kulkarni, R. N. and Kahn, C. R. 2008. New role of bone morphogenetic protein 7 in brown adipogenesis and energy expenditure. Nature **454**(7207): 1000-1004.

Valente, A., Carrillo, A. E., Tzatzarakis, M. N., Vakonaki, E., Tsatsakis, A. M., Kenny, G. P., Koutedakis, Y., Jamurtas, A. Z. and A.D., F. 2015. The absorption and metabolism of a single L-menthol oral versus skin administration: effects on thermogenesis and metabolic rate. Food and Chemical Toxicology **in press**.

Valente, A., Jamurtas, A. Z., Koutedakis, Y. and Flouris, A. D. 2014. Molecular pathways linking non-shivering thermogenesis and obesity: focusing on brown adipose tissue development. Biol Rev Camb Philos Soc **90**(1): 77-88.

van der Lans, A. A., Hoeks, J., Brans, B., Vijgen, G. H., Visser, M. G., Vosselman, M. J., Hansen, J., Jorgensen, J. A., Wu, J., Mottaghy, F. M., Schrauwen, P. and van Marken Lichtenbelt, W. D. 2013. Cold acclimation recruits human brown fat and increases nonshivering thermogenesis. The Journal of clinical investigation **123**(8): 3395-3403.

van Marken Lichtenbelt, W. D. and Schrauwen, P. 2011. Implications of nonshivering thermogenesis for energy balance regulation in humans. American Journal of Physiology - Regulatory, Integrative and Comparative Physiology **301**(2): R285-296.

van Marken Lichtenbelt, W. D., Vanhommerig, J. W., Smulders, N. M., Drossaerts, J. M., Kemerink, G. J., Bouvy, N. D., Schrauwen, P. and Teule, G. J. 2009. Cold-activated brown adipose tissue in healthy men. N Engl J Med **360**(15): 1500-1508.

Vaughan, R. A., Gannon, N. P., Barberena, M. A., Garcia-Smith, R., Bisoffi, M., Mermier, C. M., Conn, C. A. and Trujillo, K. A. 2014. Characterization of the metabolic effects of irisin on skeletal muscle in vitro. Diabetes Obes Metab **16**(8): 711-718.

Vijgen, G. H., Bouvy, N. D., Teule, G. J., Brans, B., Schrauwen, P. and van Marken Lichtenbelt, W. D. 2011. Brown adipose tissue in morbidly obese subjects. PLoS One **6**(2): e17247.

Vila-Bedmar, R., Garcia-Guerra, L., Nieto-Vazquez, I., Mayor, F., Jr., Lorenzo, M., Murga, C. and Fernandez-Veledo, S. 2012. GRK2 contribution to the regulation of energy expenditure and brown fat function. FASEB Journal **26**(8): 3503-3514.

Virtanen, K. A., Lidell, M. E., Orava, J., Heglind, M., Westergren, R., Niemi, T., Taittonen, M., Laine, J., Savisto, N. J., Enerback, S. and Nuutila, P. 2009. Functional brown adipose tissue in healthy adults. N Engl J Med **360**(15): 1518-1525.

Vosselman, M. J., van der Lans, A. A., Brans, B., Wierts, R., van Baak, M. A., Schrauwen, P. and van Marken Lichtenbelt, W. D. 2012. Systemic beta-adrenergic stimulation of thermogenesis is not accompanied by brown adipose tissue activity in humans. Diabetes **61**(12): 3106-3113.

Walden, T. B., Hansen, I. R., Timmons, J. A., Cannon, B. and Nedergaard, J. 2012. Recruited vs. nonrecruited molecular signatures of brown, "brite," and white adipose tissues. American Journal of Physiology - Endocrinology and Metabolism **302**(1): E19-31.

Wang, H. and Woolf, C. J. 2005. Pain TRPs. Neuron **46**(1): 9-12.

Wargent, E. T., O'Dowd, J. F., Zaibi, M. S., Gao, D., Bing, C., Trayhurn, P., Cawthorne, M. A., Arch, J. R. and Stocker, C. J. 2013. Contrasts between the effects of zinc-alpha2-glycoprotein, a putative beta3/2-adrenoceptor agonist and the beta3/2-adrenoceptor agonist BRL35135 in C57Bl/6 (ob/ob) mice. The Journal of endocrinology **216**(2): 157-168.

Wells, T., Davies, J. R., Guschina, I. A., Ball, D. J., Davies, J. S., Davies, V. J., Evans, B. A. and Votruba, M. 2012. Opa3, a novel regulator of mitochondrial function, controls thermogenesis and abdominal fat mass in a mouse model for Costeff syndrome. Human molecular genetics **21**(22): 4836-4844.

Wieseler, B. and McGauran, N. 2010. Reporting a Systematic Review. CHEST **137**(5): 1240 – 1246.

Wijers, S. L., Schrauwen, P., Saris, W. H. and van Marken Lichtenbelt, W. D. 2008. Human skeletal muscle mitochondrial uncoupling is associated with cold induced adaptive thermogenesis. PLoS One **3**(3): e1777.

World Health Organization 2010Population-based prevention strategies for childhood obesity. Geneva, Switzerland.

World Health Organization 2010WHO Global Infobase.

Wright, C. E., Bowen, W. P., Grattan, T. J. and Morice, A. H. 1998. Identification of the L-menthol binding site in guinea-pig lung membranes. Br J Pharmacol **123**(3): 481-486.

Xiao, X. Q., Williams, S. M., Grayson, B. E., Glavas, M. M., Cowley, M. A., Smith, M. S. and Grove, K. L. 2007. Excess Weight Gain during the Early Postnatal Period Is Associated with Permanent Reprogramming of Brown Adipose Tissue Adaptive Thermogenesis. Endocrinology **148**(9): 4150–4159.

Yamashita, H., Wang, Z., Wang, Y., Segawa, M., Kusudo, T. and Kontani, Y. 2008. Induction of fatty acid-binding protein 3 in brown adipose tissue correlates with increased demand for adaptive thermogenesis in rodents. Biochemical and Biophysical Research Communications **377**(2): 632-635.

Yoneshiro, T., Aita, S., Matsushita, M., Kayahara, T., Kameya, T., Kawai, Y., Iwanaga, T. and Saito, M. 2013. Recruited brown adipose tissue as an

antiobesity agent in humans. The Journal of clinical investigation **123**(8): 3404-3408.
Yosipovitch, G., Szolar, C., Hui, X. Y. and Maibach, H. 1996. Effect of topically applied menthol on thermal, pain and itch sensations and biophysical properties of the skin. Arch Dermatol Res **288**(5-6): 245-248.
Zhang, L., Liu, P. F., Zhu, W. L., Cai, J. H. and Wang, Z. K. 2012. Variations in thermal physiology and energetics of the tree shrew (Tupaia belangeri) in response to cold acclimation. J Comp Physiol B **182**(1): 167-176.
Zhang, X. Y., Jing, B. B. and Wang, D. H. 2009. Cold exposure does not decrease serum leptin concentration, but increases energy intake and thermogenic capacity in pregnant Brandt's voles (Lasiopodomysbrandtii). Zoology **112**: 206–216.
Zhang, X. Y., Li, Y. L. and Wang, D. H. 2008. Large litter size increases maternal energy intake but has no eVect on UCP1 content and serum-leptin concentrations in lactating Brandt's voles (Lasiopodomys brandtii). Journal of Comparative Physiology B **178**: 637–645.
Zhao, Z. J. and Wang, D. H. 2009. Plasticity in the Physiological Energetics of Mongolian Gerbils Is Associated with Diet Quality. Phy.siological and Biochemical Zoology **82**(5): 504-505l505.
Zhu, H., Pollock, N. K., Kotak, I., Gutin, B., Wang, X., Bhagatwala, J., Parikh, S., Harshfield, G. A. and Dong, Y. 2014. Dietary sodium, adiposity, and inflammation in healthy adolescents. Pediatrics **133**(3): e635-642.

CHAPTER 7

Annexes – Ethical approvals for human experiments

University of Thessaly
Department of Physical Education and Sport Science

IInternal Ethics Committee

Trikala: 28/6/2012
Protocol Number.: 601

Application for approval of research entitled: Acute effect of dietary and skin TRPM8 stimulation on thermoregulation and metabolism in adult males and females.

Scientist responsible – supervisor: Dr. Andreas D. Flouris, Dr. Athanasios Jamurtas

Main researcher – student: Angelica Valente

Institution & Department: FAME Laboratory, Centre for Research and Technology Thessaly, Department of Physical Education and Sport Science, University of Thessaly.

The proposed research relates to a:

Research grant ☐ Postgraduate thesis ■ Undergraduate thesis ☐ Independent research ☐

Contact phone: +30 2431 063 190
Contact email: aflouris@cereteth.gr

The Internal Ethics Committee (IEC) of the Department of PE and Sport Science (DPESS), University of Thessaly, examined the proposal in its 2-5/20-6-2012 meeting and approves the implementation of the proposed research.

The Chair of the IEC – DPESS

Athanasios Tsiokanos, PhD

University of Thessaly
Department of Physical Education and Sport Science

Internal Ethics Committee

Trikala: 28 / June / 2012
Protocol Number.: 602

Application for approval of research entitled: Effect of chronic dietary and skin TRPM8 stimulation on body composition and white adipose tissue phenotype in adult males

Scientist responsible – supervisor: Dr. Andreas D. Flouris, Dr. Athanasios Jamurtas

Main researcher – student: Angelica Valente

Institution & Department: FAME Laboratory, Centre for Research and Technology Thessaly; Department of Physical Education and Sport Science, University of Thessaly

The proposed research relates to a:

Research grant ☐ Postgraduate thesis ■ Undergraduate thesis ☐ Independent research ☐

Contact phone: +30 2431 063 190
Contact email: aflouris@cereteth.gr

The Internal Ethics Committee (IEC) of the Department of PE and Sport Science (DPESS), University of Thessaly, examined the proposal in its 2-6/20-6-2012 meeting and approves the implementation of the proposed research.

The Chair of the IEC – DPESS

Athanasios Tsiokanos, PhD